Univ.-Prof. Dipl.-Ing. Dr. Gerald Badurek

Diplomarbeit

Magnetic Resonance based Polymer Gel Dosimetry

ausgeführt am

Zentrum für biomedizinische Technik und Physik
der Medizinischen Universität Wien

und

Atominstitut der Österreichischen Universitäten
der Technischen Universität Wien

unter der Anleitung von
ao. Univ.Prof. Dr. Andreas Berg
Univ.-Prof. Dipl.-Ing. Dr. techn. Gerald Badurek

durch
Michael Wieland
Radingerstraße 7/1/100
A-1020 Wien

Wien, Februar 2010

Acknowledgements

I would like to the following persons for their professional help and support:

Prof. Dr. Andreas Berg introduced me to magnetic resonance imaging and polymer gel dosimetry. This work would not have been possible without his help, patience and scientific input. I am especially thankful that he was available even on weekend evenings when problems at the MR tomographs occurred during long measurement sessions.

Dr. Christian Bayreder teached me the preparation technique of normoxic polymer gels and its little but important “secrets”.

At the general hospital of Vienna Prof. Dr. Dietmar Georg was willing to allow access to linear accelerators and the ^{60}Co calibration unit. DI Gabriele Kragl spent two long evenings with me to operate the linear accelerators and perform the necessary absolute dosimetry measurements.

Dr. Werner Schmidt supervised my collaboration with DI Lena Siebert at the “Donauspital” Vienna and encouraged us to present parts of this work at the ÖGRO 2009 conference.

Special thanks have to be given to DI Lena Siebert for many hours and days operating the linear accelerator, performing absolute dosimetry measurements and helping with the IMRT-irradiation and its analysis.

I would like to extend my gratitude to my parents and brother for their endless, unconditional love and my friends for their persistent moral support. Robert Farthofer and Laurids Schimka shared with me many hours of hard learning and preparation for exams. My friend and work colleague at ÖAMTC Martin Maier helped me out whenever he could to make it possible for me to work and study. Eleni Boutsika was so kind to proofread the manuscript. For over two years she supported me in our relationship. I am thankful that she accepted the fact that working and studying sometimes leaves only little time for a private life.

Finally I would like to thank Univ.-Prof. Dr. Gerald Badurek for the supervision of this thesis.

Abstract

This work deals with normoxic polymer gels used as dosimetric verification tool in radiotherapy. Magnetic resonance imaging is used as read-out technique to generate 2D and 3D images of complex dose distributions.

The intention of this work was to investigate properties of MAGIC polymer gels crucial to radiotherapy dosimetry. These properties are precision, accuracy, dependence on radiation quality, dose rate, storage and handling conditions. The results showed that the dose response is independent of radiation quality and independent of dose rate up to 2.5 Gy/min in the investigated range. It was discovered that non-linearity in dose response can be avoided with extended storage time between production and irradiation of the gels. The work also includes the first investigation of the influence of systematic constituent variation on the limits of spatial resolution and edge enhancement at sub-millimeter scale. The gathered data verified the assumption that the edge enhancement effect can be reduced with increased gelatin concentration. The final part of the work is the verification of an IMRT treatment plan with polymer gel dosimetry and a head phantom.

Contents

1 Introduction

The aim of radiation therapy is the precise irradiation of tumor tissue in the human body while sparing the surrounding organs. The development and refinement of techniques such as Intensity Modulated Radiation Therapy (IMRT), brachytherapy, stereotactic surgery, proton or heavy ion therapy allow for an ever improving accuracy to fulfill these requirements. These techniques can produce complex three dimensional irradiation geometries with steep dose gradients. The planning of a radiotherapy treatment is performed with computer programs that utilize special algorithms to calculate the dose distribution in a patient. In spite of considerable improvements of these algorithms and computing power the dosimetric verification of treatment plans is still mandatory. The traditional methods for this purpose are ion chamber dosimetry (Attix 1986) and silver halide film dosimetry (Dogan et al 2002). Nevertheless they are not well suited for the verification of the complex three dimensional irradiation geometries and steep dose gradients produced by the modern therapy techniques. Both are not tissue equivalent and cannot directly record three dimensional dose distributions.

Magnetic resonance imaging based polymer gel dosimetry (MRPD) offers the opportunity to directly record complex three dimensional dose distributions with high spatial resolution. Polymer gels consist of monomers that polymerize when irradiated. Gelatin is added to spatially stabilize the dose response. The degree of polymerization changes MR-properties such as the relaxation time T2 and therefore allows for 2D- or 3D-MR imaging. The original gel formulation (Maryanski et al 1993) was very sensitive to O_2-presence. Oxygen solved in the gels inhibits the dose response and therefore gels had to be prepared under inert gas atmosphere. Another drawback of these gels was the use of the toxic and carcinogen acrylic acid as monomer source. In 2001, Fong et al introduced the normoxic MAGIC (**M**ethacrylic and **A**scorbic Acid in **G**elatine **i**nitiated by **C**opper) gels. Ascorbic acid and copper bind the remaining oxygen in the gels and therefore these gels can be prepared at normal room atmosphere. Methacrylic acid is far less toxic than acrylic acid and can be handled without special care.

The intention of this work was the investigation of properties of the MAGIC formulation BangKit™, that are important to decide if MAGIC gels can be used as dosimetric system for the verification of modern radiotherapy treatment plans. The investigated features in this work are dependence on radiation quality, dose rate, storage time, storage temperature, precision and accuracy of MAGIC gels.

Another aspect of the work is represented by the achievable spatial resolution in MRPD. We used the DMTF (Dose Modulation Transfer Function) concept (Berg et al 2004) and dedicated MR-micro-imaging equipment.

An unsolved problem of polymer gels is the so called ‘edge enhancement effect’. At steep dose gradients monomers get depleted in high dose regions causing a migration of

monomers from low dose regions into monomer depleted areas. The result is an over modulation at the borders of high and low dose regions.

Spatial resolution and edge enhancement were systematically investigated for varying gel formulations and different doses. Finally an existing IMRT plan for a head and neck tumor was chosen to demonstrate the potential of MAGIC polymer gel as clinical dosimeter.

2 Theory

2.1 Radiotherapy and Dosimetry

The aim of radiotherapy is the irradiation of cancerous tissue in the human body while sparing the surrounding healthy tissue. The development of modern techniques such as intensity modulated radiotherapy (IMRT), brachytherapy, stereotactic surgery, proton and ion therapy, allow for ever more precise irradiations. Accurate treatment of tumors is achieved with complex irradiation geometries that produce steep dose gradients at the edges of the tumor target volume. Radiation therapies are planned individually with computer programs that apply special dose calculation algorithms (Bortfeld 2006). The accuracy of those programs has been improved substantially. Nevertheless the verification of the delivered dose with one or several dosimetric devices is still mandatory (Mayles et al 2007).

2.1.1 Dosimetric Principles (ICRU 1980, 1998; Attix 1986)

Ionizing radiation is divided into the two categories: directly and indirectly ionizing radiation. (1) Charged particles (electrons, protons & ions) that transfer their energy through Coulomb-interactions directly to matter are directly ionizing. (2) Indirectly ionizing particles are uncharged (photons of any energy or neutrons). They deliver their energy to matter in a two step process, by transferring their energy to charged particles, which then in turn deposit energy as above.

The most important quantity for ionizing radiation in medicine is the absorbed dose D which is defined as $D=d\bar{\varepsilon}/dm$, the mean energy imparted by ionizing radiation to a mass m of the volume V. The unit of absorbed dose is Gray: [Gy] = [J/kg]. The imparted energy, ε, is defined as the difference between the radiant energy entering and the radiant energy leaving the volume V, including conversions of mass and energy:

$$\varepsilon = (R_{in})_u - (R_{out})_u + (R_{in})_c - (R_{out})_c + \Sigma Q$$

$(R)_u$ … radiant energy of all uncharged particles
$(R)_c$ … radiant energy of all charged particles
ΣQ … net energy derived from the change of rest mass energy in V
(positive for m -> E, negative for E-> m)

The dose rate $\dot{D}$ is defined as absorbed dose dD in a time interval dt:

$$\dot{D} = \frac{dD}{dt} \left[\frac{Gy}{s}\right]$$

Dose is measured with a radiation dosimeter. A dosimeter should give a reading proportional to the absorbed dose. Therefore a dosimeter must be able to measure a physical effect that is a function of the absorbed dose. The dosimeter together with its read-out modality is referred to as dosimetric system.

2.1.2 Dosimetry in Radiotherapy (Podgorasak et al 2003)

In radiotherapy it is important to be able to estimate the exact absorbed dose to tissue with considerable certainty. To be useful in radiotherapy a dosimeter should exhibit several desirable characteristics. These are:

- High accuracy and precision
- Independence of dose rate
- Independence of radiation quality
- Directional independence
- High spatial resolution
- Tissue equivalence
- Convenient application
- Possible absolute dose determination

Accuracy and Precision

Results of a measurement are always afflicted with uncertainty. There are two different types of standard uncertainties. Type A standard uncertainties are of stochastic nature. Stochastic errors can be assessed by statistical analysis of repeated measurements. If a quantity x is measured N times it is estimated as the arithmetic mean value $\bar{x}$.

$$\bar{x} = \frac{1}{N}\sum_{i=1}^{N} x_i$$

The average uncertainty of a single measurement is defined as the standard deviation σ_x from the arithmetic mean value $\bar{x}$.

$$\sigma_x = \sqrt{\frac{1}{(N-1)}\sum_{i=1}^{N}(x_i - \bar{x})^2}$$

The type A standard uncertainty u_A is defined as the standard deviation of the mean value.

$$u_A = \sigma_{\bar{x}} = \frac{1}{\sqrt{N}}\sigma_x = \sqrt{\frac{1}{N(N-1)}\sum_{i=1}^{N}(x_i - \bar{x})^2}$$

Type B standard uncertainties represent systematic errors that include influences of the measuring process. They cannot be derived with statistical methods. They have to be

estimated by scientific judgment or “intelligent guesses”. The combined uncertainty u_C of a dosimetric quantity is derived as quadratic sum of type A and type B uncertainties.

$$u_C = \sqrt{u_A^2 + u_B^2}$$

In radiotherapy the measurement uncertainties are often expressed in terms of accuracy and precision. Accuracy is an expression for the proximity of the measured value to the real value of a quantity. It is determined by the collective error of all steps of a measurement procedure and is characterized as uncertainty. Precision is an estimate of the reproducibility of measurements under the same condition. High precision is therefore equivalent to a small standard deviation of a measured quantity (DeDeene 2006).

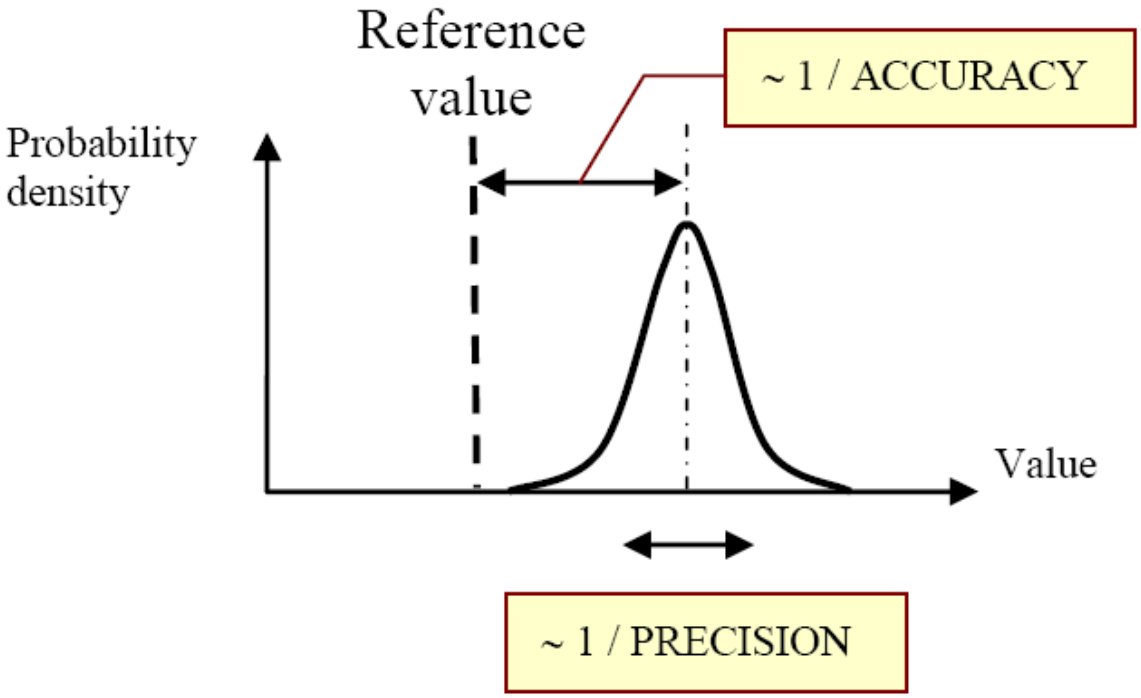

Figure 2.01 (DeDeene 2006): Precision and Accuracy.

Energy and Dose Rate Dependence

Radiotherapy techniques such as IMRT make use of several different beams of varying shape that involve changing dose rates over the volumes of interest. Furthermore the applied therapeutic beams are not monoenergetic (DeWagter 2004). Therefore a dosimeter reading should be independent of beam energy and dose rate.

Spatial Resolution and Directional Dependence

The recent developments in radiotherapy made it possible to confine applied doses mainly to tumor tissue with increasing precision. The resulting steep dose gradients at the edges of the tumor have to be verified to avoid overexposure of healthy tissue or underexposure of cancerous tissue. This can only be achieved with high spatial resolution dosimeters (Berg et al 2001). In IMRT the confinement of dose is realized with multiple beams from different

angles. This dynamical approach demands for directional independent and integrating dosimeters.

Tissue Equivalence

Absorbed dose is strongly depending on the composition of matter at the point of interest and therefore tissue equivalence (in atomic composition) is a desired property. Furthermore, it should be possible to integrate the dosimeter in a (part of a) phantom.

Absolute Dosimetry

A dosimeter should allow for absolute dosimetry via calibration curve obtained by irradiation of the dosimeter to known doses (DeWagter 2004). The gold standard in dosimetry has long been and still is the ionization chamber. It is the dosimeter recommended by the IAEA for beam calibrations in therapeutic applications. While it is a reliable instrument for the evaluation of dose under straightforward conditions it shows several disadvantages for the dosimetry of modern radiotherapy techniques. An ionization chamber is a single point dosimeter. Three-dimensional dosimetry can only be done with repeated measurements. It has a rather big sensitive volume which limits the spatial resolution (Gustavsson et al 2003).

A standard method for the verification of an IMRT plans involves ionization chamber and film dosimetry. Absolute dosimetry at a reference point in the irradiated volume is performed with an ionization chamber. Relative film dosimetry is used to verify the distribution in chosen planes of the volume (Ting and Davis 2001). A stack of films can be used to gain a quasi 3D dose map of the volume. The dose response of silver halide films is depending on the energy of the radiation. They contain several high-Z components which results in different photon interaction probabilities compared to human tissue (Hendee et al 2005). Film dosimetry verification of IMRT treatments in the present time are performed with GafChromic™ films (www.gafchromic.com, USA). They are tissue equivalent, energy and dose rate independent and don't need dark room development. Both film dosimetry systems exhibit directional dependence (Suchowerska et al 2001) and only come in standard sizes. For quasi 3D dosimetry the slices of the film stacks also have to be positioned correctly for evaluation. Although gel dosimetry has not become a widely used technique in radiotherapy dosimetry, it is still believed that it can become an important part of it. Gel dosimetry is still the only method capable of direct and integrating 3D-dose verification. Especially the complex dose distributions in IMRT demand for a volumetric verification (Schreiner 2009). The gels are tissue equivalent and in combination with MRI can offer sub-millimeter spatial resolution (Berg et al 2001, Berg et al 2004, Bayreder et al 2008).

2.2 Basics of Polymer Gel Dosimeters

2.2.1 History (Baldock 2009)

The idea to combine polymer gels with radiosensitive chemicals to record dose and dose distribution was first proposed in the 1950s (Andrews et al 1957), but at that time no sufficiently accurate read-out technique was available. This changed with the development of MRI and the idea was taken up again in the 1980s. Then, MRI was used to detect changes in gels containing Fricke solution (Gore et al 1984). In a Fricke ferrous sulfate dosimeter (Fricke and Morse 1927) radiation induces a conversion of ferrous ions (Fe2+) into ferric ions (Fe3+). Experiments showed that the gel matrix can stabilize the spatial distribution of Fe2+ and Fe3+ ions (i.e. information about the dose distribution) only for a short time. After a few minutes diffusion causes a blurring of the dose distribution and makes the method inapplicable for clinical dosimetry (Schulz et al 1990).

Table 2.01 (Jirasek 2006): Common polymer gels

	Anoxic/Normoxic	Acrylamide	Methacrylic acid	N,N' Methylene bis acrylamide	N-vinylpyrrolidone	Ascorbic acid	Copper Sulfate	THPC	THPS
PAG	A	x							
nPAG	N	x							x
PAGAT	N	x						x	
MAGIC/BANGKit™	N		x			x	x		
nMAG	N		x						x
MAGAT	N		x					x	
VIPAR	A			x	x				

In 1990 Schulz and Gore reported the use of gels containing acrylic monomers to circumvent the problem of dose distribution blurring. The first systematic investigation of such polymer gels was described by Maryanski et al. in 1993: These gels were composed of water, gelatin and acrylic monomers and were called PAG (**P**oly**a**crylamide **g**el). Upon irradiation radicals are formed by the radiolysis of water and initiate polymerization of the monomers. It was shown that polymerization correlates with applied dose. The growing of the polymer chains reduces their mobility and corresponds to the decrease of the MR relaxation times T1 and T2. Maryanski et al. also reported a linear dependence of the relaxation rate R2=1/T2 on the

applied dose. The introduction of polymer gels overcame the decisive problem of spatial dose distribution blurring at the expense of labor and time intensive manufacturing of the new dosimeters. The presence of oxygen in the gels inhibits the polymerization reaction (Hepworth et al 1999). Hence the dosimeters had to be prepared at hypoxic conditions in a glove box flushed with an inert gas such as nitrogen.

In 2001 Fong et al. presented a new gel formulation relatively insensitive to oxygen termed MAGIC (**M**ethacrylic and **A**scorbic Acid in **G**elatin **I**nitiated by **C**opper). Ascorbic acid is added as oxygen scavenger and copper sulfate acts as catalyst improving the scavenging rate (Taqui Kahn and Martell 1967). MAGIC gels can be prepared at normal room atmosphere. Other normoxic polymer gels contain THPC (**T**etrakis-**H**ydroxy-methyl-**P**hosphonium-**C**hloride) as oxygen scavenger (DeDeene et al 2002).

Since the first days of polymer gel dosimetry many gel formulations were proposed and existing ones modified. Some of the more intensively investigated polymer gels and their contents are listed in table 2.01.

2.2.2 Detection Principle of normoxic Polymer Gels (DeDeene et al 2002)

The constituents of the normoxic polymer gel BANGKit™ (MGS research Inc., Guilford, USA) used in this work are water (80%), gelatin (14%), methacrylic acid (monomers, 6%), ascorbic acid (2mM) and copper sulfate (10µM). The fundamental detection principle of all radiosensitive gels is the radiation induced formation of polymer chains. Radiolysis generates water radicals:

$$H_2O \rightarrow 2R^*$$

The water radicals R* initiate polymerization by reaction with monomer molecules M. Together they form monomer radicals RM*. These monomer radicals can react with further monomer molecules to form polymer radicals RM_n^* of the length n:

$$R^* + M_n \rightarrow RM_n^*$$

The polymerization process can be inhibited and stopped by mutual termination of radicals (A) or disproportionation (B) where a hydrogen atom is transferred from one polymer radical to another.

(A)

$$R^* + R^* \rightarrow RR$$
$$R^* + RM_n^* \rightarrow RR + M_n$$
$$RM_n^* + RM_m^* \rightarrow RR + M_{n+m}$$

(B)

$$RM_n^* + RM_m^* \rightarrow RR + M_n + M_m$$

Radical termination is additionally caused by the presence of dioxygen O_2. Peroxides created during irradiation also react with the formed radicals. This reaction occurs at a higher rate than polymerization and therefore polymer chain growth is inhibited. The problem of inhibition was solved with the introduction of normoxic polymer gels by Fong et al in 2001. Ascorbic acid (AscA) added to the solution during preparation is acting as oxygen scavenger. The oxidation of ascorbic acid is catalyzed in the presence of copper:

$$AscA + O_2 + Cu^{2+} \rightarrow AscA\text{-}O_2\text{-}Cu\text{-}Complex$$

2.3 MR Imaging in Polymer Gel Dosimetry

For the basic principles of nuclear magnetic resonance imaging the reader is referred to specialized literature (e.g. Haacke et al 2001). Only the MRI sequences and methods used for this work will be discussed in this section.

The radiation induced polymerization in polymer gels changes the spin-spin (transversal) relaxation rate within them (Maryanski et al 1993). This effect is used when applying T2 parameter selective imaging sequences. Other MRI contrasts such as the spin-lattice (longitudinal) relaxation rate R1 (=1/T1), magnetization transfer (Lepage et al 2002) and chemical shift (Murphy et al 2000) can also be utilized. Most works concentrate on T2-weighted imaging sequences because the dose response effect on T2 (R2) is more pronounced than for the other parameters (Berg et al 2004, DeDeene 2004).

2.3.1 The Carr-Purcell-Meiboom-Gill (CPMG) Sequence

The CPMG sequence is a multiple spin echo sequence. In a spin echo sequence a 90° excitation radio frequency pulse is followed by one or several 180° refocusing pulses. After the spins are aligned by the 90° pulse they dephase. When a 180° refocusing pulse is applied after the time TE/2 the spins rephase at the echo time TE with reduced intensity. The signal at TE is detected.

2.3.2 Parameter selective R2-Imaging

For n echoes the signal reappears at the times n·TE while decaying exponentially. After the n^{th} echo the signal has the intensity:

$$I_n = I_0 e^{-\frac{TE_n}{T_2}} = I_0 e^{-R_2 \cdot TE_n}$$

The exponential decay can be used to gain the relaxation time T2 or the relaxation rate R2. If only two echoes are recorded R2 can be calculated with:

$$R_2 = \frac{lnS_1 - lnS_1}{TE_2 - TE_1}$$

This principle can be extended to more than 2 echoes. An exponential fit over the different echo times can be applied for each pixel in the image. The result of this procedure is a T2-map-image.

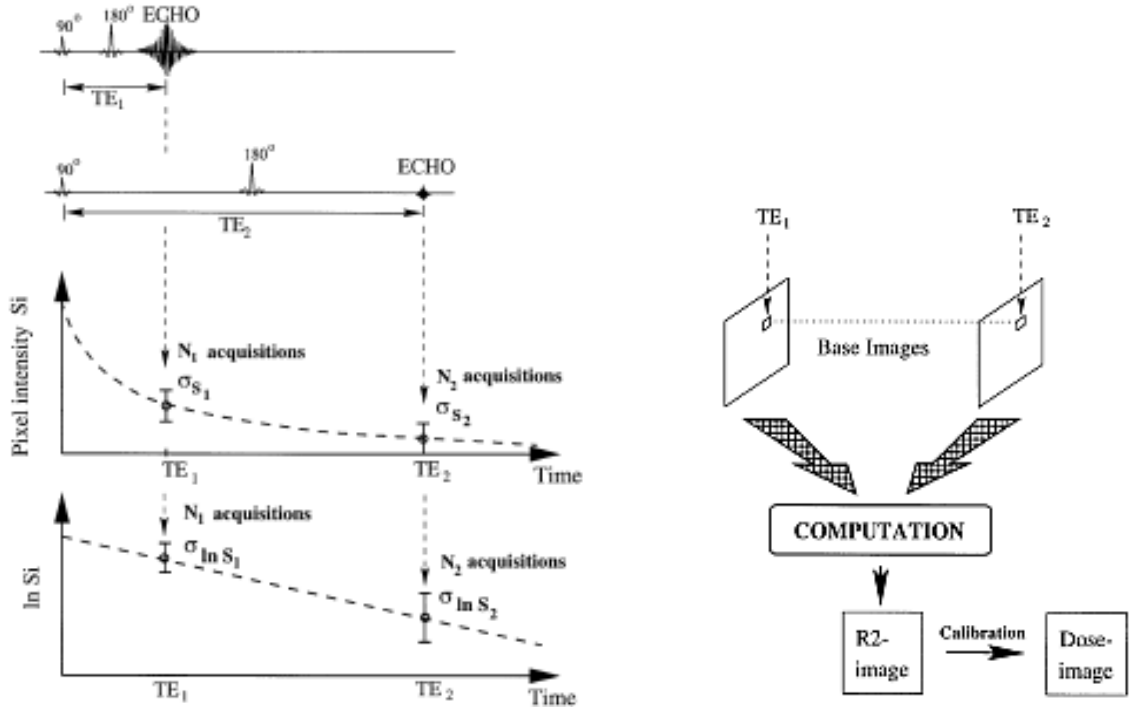

Figure 2.02 (DeDeene et al 1998): Spin-Echo image acquisition with 2 images.

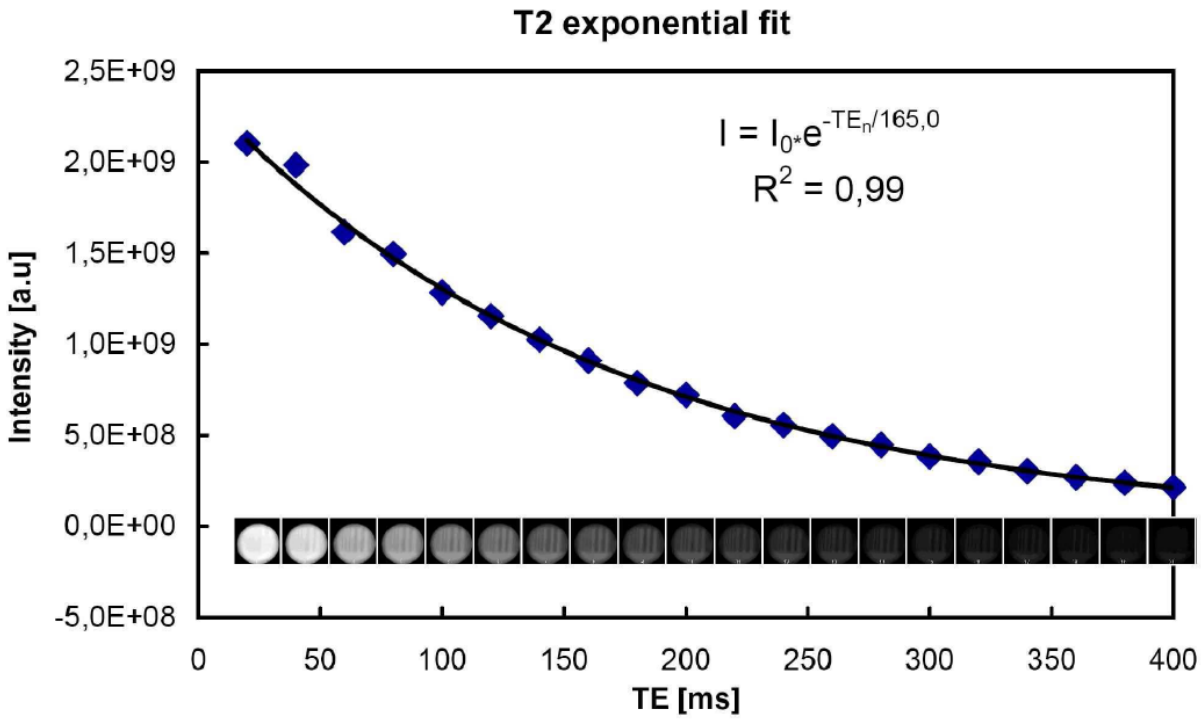

Figure 2.03 (Bayreder 2009): Spin-Echo image acquisition with 20 images.

2.4 Properties of Polymer Gel Dosimetry

For the application in radiotherapy polymer gel dosimeters have several advantages over conventional dosimetric methods. Gel dosimeters offer true 3D dosimetry and integration of dose within the dosimeter. Their densities and electron densities are almost equivalent to water and soft tissue (Venning et al 2005). This guarantees identical radiological properties (photon absorption and scattering probabilities). The radiation characteristic equivalence has been investigated for many gel compositions and radiation energies from a few keV up to the therapeutical MeV range. The photon interaction probabilities of water and MAGIC gels can differ up to 5% below 100keV. Energies applied in radiotherapy are higher than 100keV and the differences are less than 1% (Venning et al 2005).

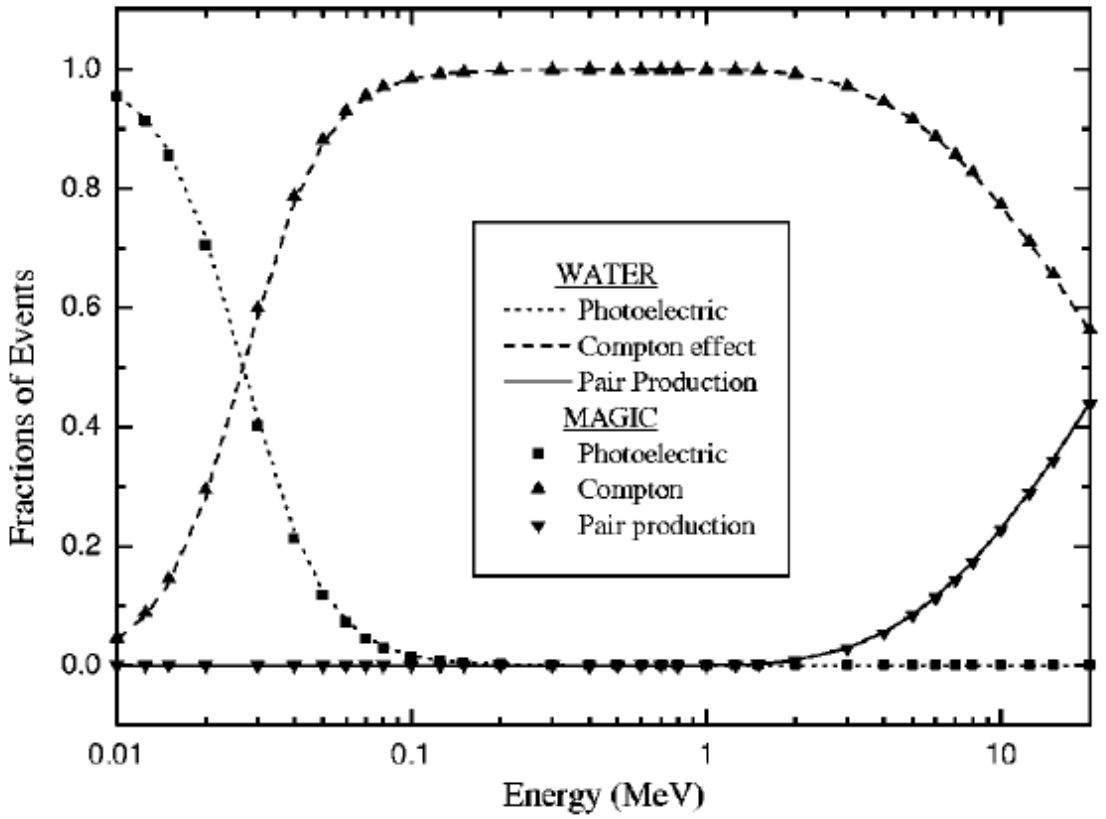

Figure 2.04 (Venning et al 2005): Fractional photon interaction probabilities for water and MAGIC.

A detailed review of the deviations from water equivalence of a wide range of polymer gel formulations can be found in Sellakumar et al. (2007).

A fact of concern during the early days of polymer gel dosimetry was the toxicity of the acrylamide based gels. The gels had to be prepared carefully and disposed into toxic waste. This problem was solved with the introduction of MAGIC gels based on methacrylic acid. The oral lethal dose LD50 in rats is 2260mg/kg for methacrylic acid in comparison to only 124mg/kg for acrylamide (Fong et al 2001).

The problem of toxicity reoccurs for MAGAT gels with the use of THPC (THPC-$LD50_{oral}$ in rats = 850mg/kg) as oxygen scavenger (www.chemdat.de, 2009).

2.4.1 Dose Response, Sensitivity and Linearity

The dose response of a polymer gel depends on many factors. The most important ones will be discussed in this section.

Ideally a dosimeter has a high sensitivity which corresponds with a better ability to distinguish between small differences in dose. In MRPD the sensitivity of a gel dosimeter equates to the steepness of the slope of the dose response curve in a R2-dose plot: dR2/dD [s-1*G-1]. All gels exhibit an offset reading $R2_0$ (intercept), with $R2_0$ = R2 (D=0Gy).

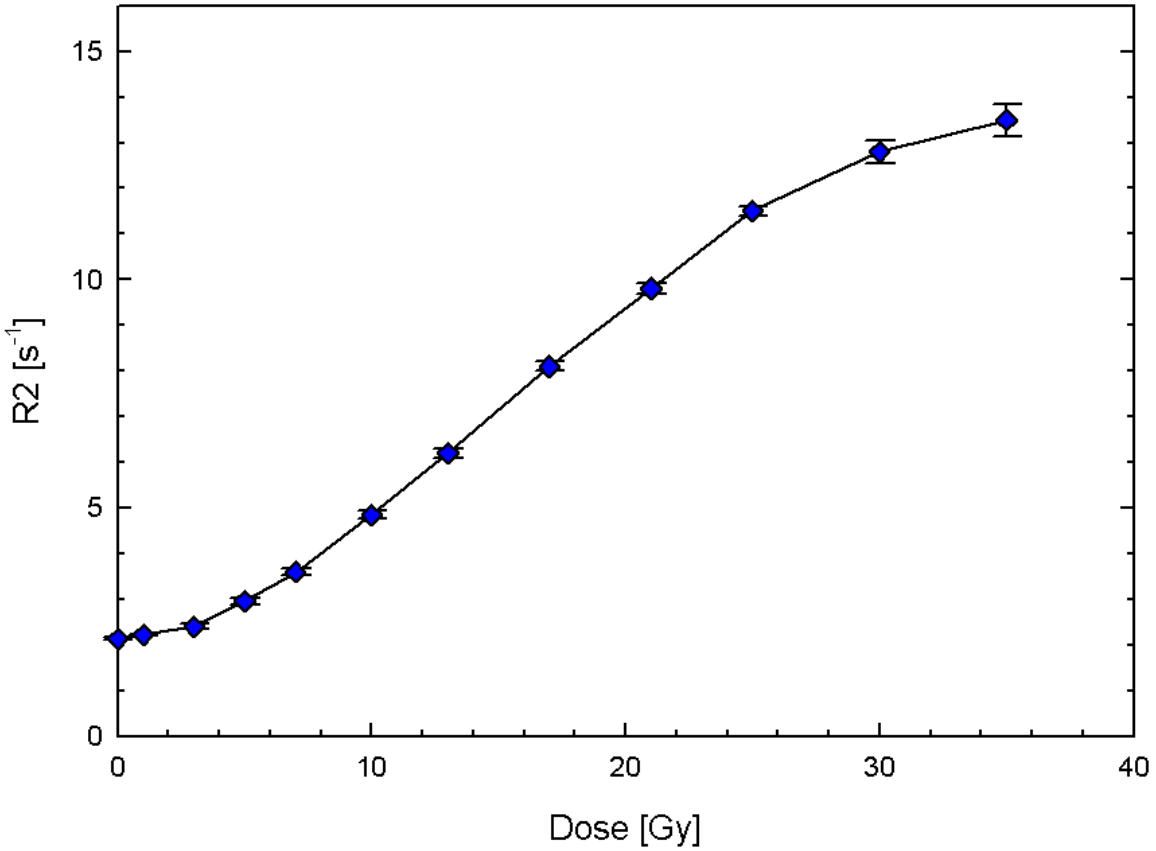

Figure 2.05: Example dose-R2-response with spline interpolation: Reduced dose response in the low dose region and saturation in the high dose region.

A dosimeter should also exhibit a linear dependence of the reading on the absorbed dose over a wide range. Linearity allows for simple absolute dosimetry calibration curves and the comparison of the sensitivity for different gel formulations. Non-linear calibration curves can be applied, but loss in dose resolution is expected in non-linear regions with reduced sensitivity of the dose response (DeDeene 2004b). Real gel dosimeters often show non-linearities in low and high dose regions (Maryanski et al 1993).

For high doses all monomers in a gel dosimeter are consumed by the process of polymerization and the reading of the dosimeter is saturated. Non-linearities in the low dose regime in hypoxic gel dosimeters may be attributed to polymerization inhibition by oxygen (DeDeene 2000). The same reason might be relevant for normoxic polymer gels, if not all present oxygen is scavenged by the added anti-oxidant or oxygen is diffusing into the phantom after preparation.

2.4.2 Dose Uncertainty and Dose Resolution (Baldock et al 2001)

The determination of dose with MRI-R2-maps is a procedure with several steps: Gel preparation, storage and handling, irradiation, parameter selective MRI, subsequent evaluation of R2 values and - in the case of absolute dosimetry - a generation of a dose-R2 calibration curve. R2 values are determined in MR-pictures as mean value in a region of interest (ROI). σ_{R2} is associated to the standard deviation of the mean value in the ROI.

Dose Uncertainty

Each step in the procedure is influencing the uncertainty of the dose determination. According to the Gaussian error, propagation the standard uncertainty of dose is a function of the type A and type B uncertainties of R2 and the dose-R2 calibration curve:

$$u_c^2(D) = \left[\frac{\partial D}{\partial R_2}\right]^2 \left[u_A^2(R_{2)} + u_B^2(R_{2)}\right]$$

With careful experimental design type B uncertainties can be discarded. With the assumption that the uncertainty originating from the calibration fit curve is much smaller than the uncertainty in R2 the dose uncertainty can be written as:

$$u_c(D) = \left[\frac{\partial D}{\partial R_2}\right] u(R_2)$$

To determine the dose uncertainty to a specific level of confidence (ISO 1995), it is multiplied with a coverage factor k_p to gain the expanded dose uncertainty U_p:

$$U_p(D) = k_p u_c(D) = k_p \left[\frac{\partial D}{\partial R_2}\right] u(R_2)$$

The coverage factor may be used in connection to the t-distribution in order to define a level of confidence:

Level of confidence	kp
52%	1/√2
68%	1
95%	1,96

Dose Resolution (Baldock et al 2001)

Two important characteristics of a polymer gel dosimeter in terms of uncertainty are accuracy and precision (see section 2.1.2). In 2001 Baldock et al proposed the concept of dose resolution as an alternative for the determination of the intrinsic precision. It can be regarded as lower limit of precision because dose resolution does not cover stochastic variations in chemical concentration, dose delivery or the calibration procedure (DeDeene Y 2006).

It can be assumed that a R2-value determined as mean value in a ROI is the most probable of a normal probability distribution with a standard deviation σ_{R2}. If the dose is estimated via a dose-R2 calibration curve, a dose value will also be the most probable of a normal probability distribution (see figure 2.06).

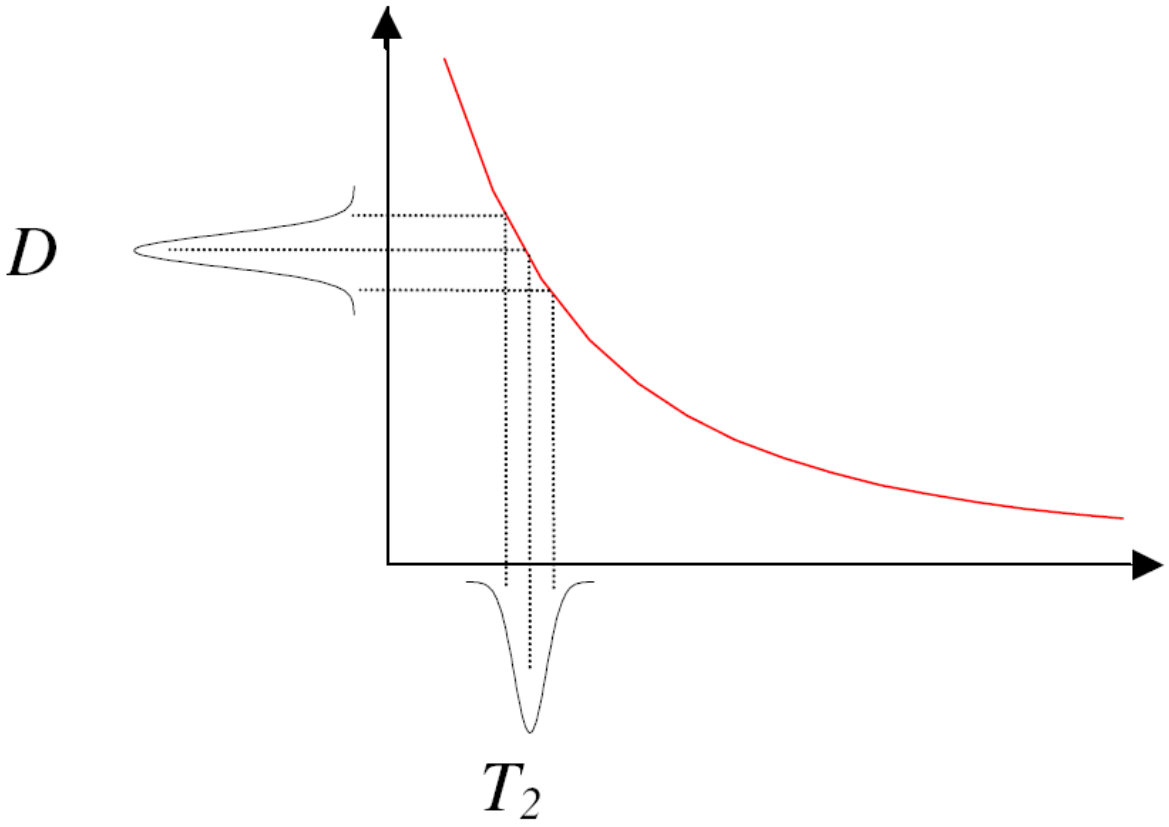

Figure 2.06 (Baldock et al 2001): Transformation of a normal probability distributed R2-value into a normal probability distributed dose-value via calibration curve.

If two dose values D_1 and D_2 have the standard deviations σ_{D1} and σ_{D2}, the sampling distribution resulting from the difference of the two populations is given by:

$$\sigma_{diff} = \sqrt{\sigma_{D1}^2 + \sigma_{D2}^2}$$

Then the dose resolution is the minimal separation of the dose distributions at which their most probable values are different, with a given level of confidence:

$$D_{\Delta}^{p} = k_p \sigma_{diff}$$

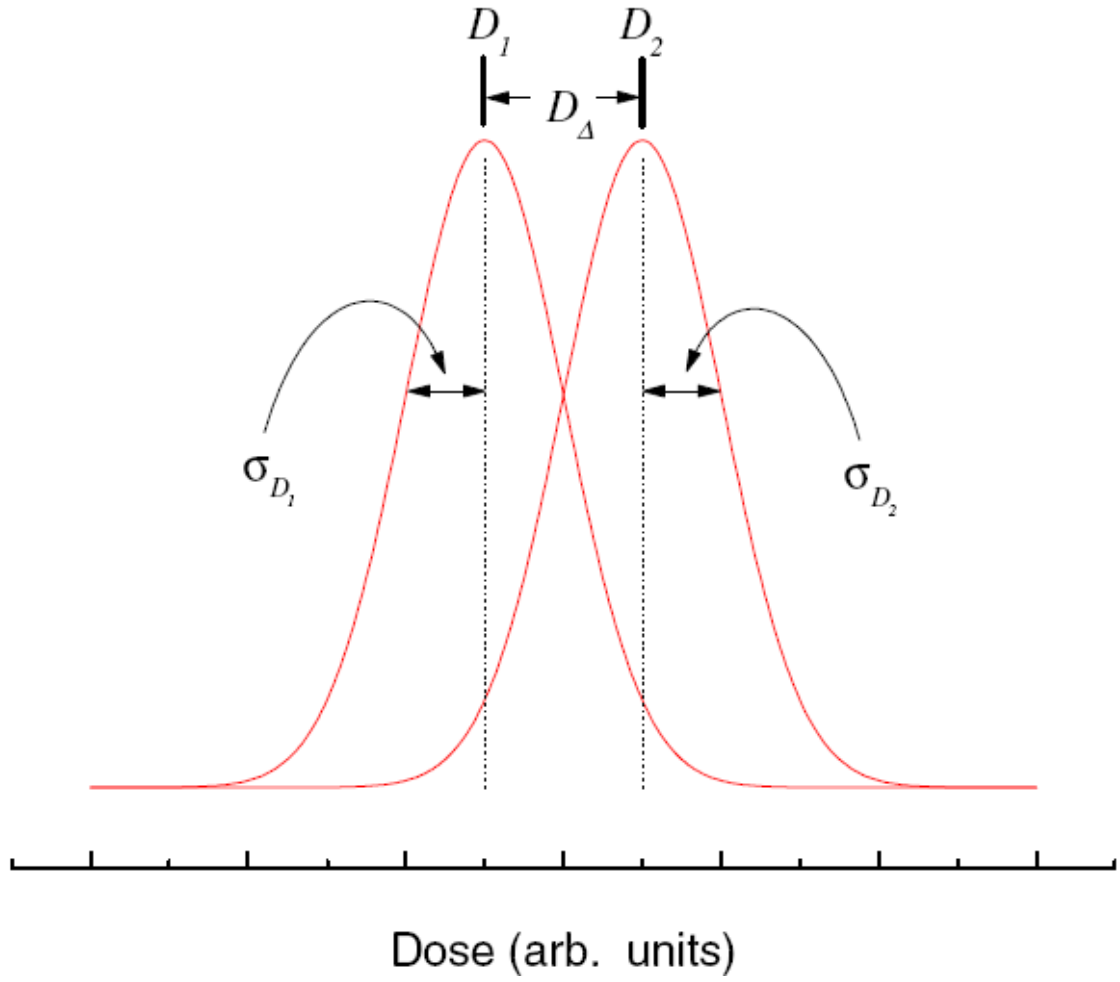

Figure 2.07 (Baldock et al 2001): The concept of dose resolution as detectable difference of the dose distributions D_1 and D_2 with their standard uncertainties σ_{D1} and σ_{D2}.

For two neighboring dose values $\sigma_1 \approx \sigma_2 = \sigma_D$ is a good approximation and therefore:

$$D_{\Delta}^{p} = k_p \sqrt{2} \sigma_D$$

DeDeene Y (2004b) extended the concept with the parameter of relative dose resolution which includes the active dose range of the dosimeter:

$$D_{\Delta\%}^{p} = \frac{D_{\Delta}^{p}}{D_{max} - D_{min}}$$

In the case of a linear R2-dose response a calibration curve has the form:

$$R_2 = R_0 + \alpha D$$

Using the formula for the Gaussian error propagation σ_D can be written as (Crescenti et al 2007):

$$\sigma_D = \frac{D}{\alpha}\sqrt{\sigma_\alpha^2 + \left(\frac{\sigma_{R2}}{D}\right)^2 + \left(\frac{\sigma_{R0}}{D}\right)^2}$$

The dominating factor in this equation is σ_{R2} (Baldock et al 1999) and therefore:

$$D_\Delta^p = k_p\sqrt{2}\,\frac{\sigma_{R2}}{\alpha}$$

2.4.3 Gel Formulation

The formulation and the proportion of ingredients of a polymer gel dosimeter are the major factors for its dose response. The influence of systematic variation of polymer gel constituents on the dose response has been investigated for several gel formulations. For MAGIC-gels this has been done and reported by Fong et al (2001), DeDeene et al (2002), Scheib et al (2004) and Luci et al (2007). Murakami Y et al (2007) analyzed the dose response for varying concentrations of ascorbic acid and copper sulfate especially for the BANGKit™ formulation.

Gelatin is serving as matrix for the growing polymer chains in the gels. An increased amount of gelatin is generally increasing $R2_0$ because it leads to stiffer gels (McAuley 2006). Further, a variation in gelatin is influencing sensitivity (Luci et al 2007), dose resolution (Luci et al 2007), monomer/polymer diffusion and temporal stability of the gels (McAuley 2006). The fact that gelatin is also actively taking part in the polymerization process is still not fully understood and was topic of recent papers (Hayashi S et al 2009).

An increase in monomer concentration typically increases the dose value where the polymerization effect is going into saturation. Some groups found that sensitivity, $R2_0$ and σ_{R2} will increase (Fong et al 2001, Luci et al 2007) and others that the response is changing from linear to bi-exponential (Scheib et al 2004).

The consequences for varying amounts of Cu^{2+} and AscA are somewhat more complicated. Good linearity is achieved with the basic BANGKit™ concentrations AC1-5 (1mM of ascorbic acid, 5µM of copper sulfate). If both levels are doubled or tripled (AC2-10, AC3-15) the dose range increases on the cost of sensitivity decrease and R20 increase. Aberrations from this fixed ratio or even higher concentrations (AC4-20,…) have negative effects on linearity (Murakami Y et al 2007).

2.4.4 Temporal Stability

In 2000 DeDeene et al described two factors influencing the temporal stability of the dose response. After manufacturing, the gelation process is going on for days and maybe even weeks. This is affecting the entire gel and after irradiation $R2_0$ is increasing while the slope of the dose response is not changing.

A second post-irradiation longtime instability is caused by long living radicals in the gels. These radicals keep consuming monomers for several hours up to days after irradiation which is altering the slope of the dose response.

For the BANGKit™ formulation Murakami et al (2007) found that the dose response is stable three days after irradiation.

2.4.5 Spatial Stability – Diffusion and Edge Enhancement

Long living macro radicals produced during irradiation affect not only the temporal but also the spatial stability. During and after irradiation monomers can diffuse from low dose regions to high dose regions where monomers are depleted (DeDeene et al 2002b). In the high dose region the monomers react with long living macro radicals. This causes dose overshoots (edge enhancements) in regions of steep dose gradients. It has been shown that edge enhancement is dose and time dependent (DeDeene 2004b). Diffusivity can be reduced with an increase in gelatin concentration. The increase in gelatin concentration leads to higher viscosity and therefore enhancing spatial stability up to higher doses (DeDeene et al 2000).

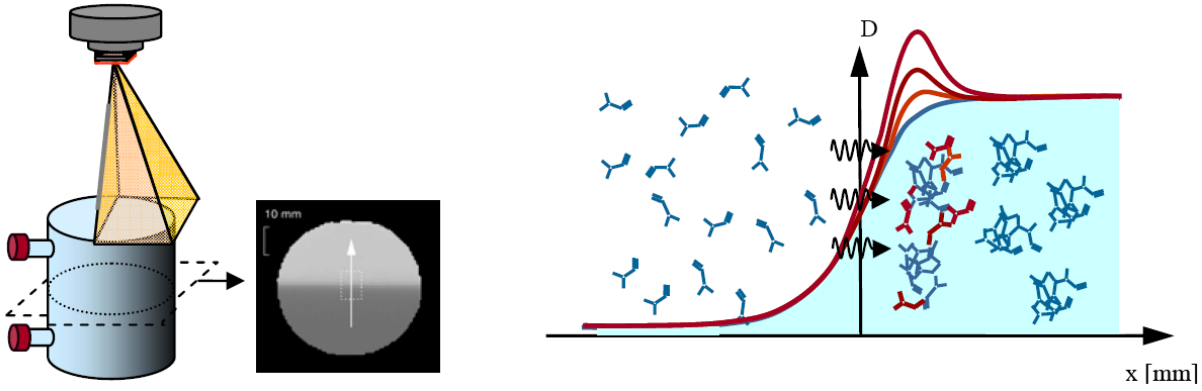

Figure 2.08 (DeDeene 2006): Edge enhancement due to monomer depletion and long living macro radicals. Edge enhancement is increasing with post irradiation time.

2.4.6 Dose Rate Dependence

Polymerization propagation and termination, involving the loss of water radicals, is proportional to the radical concentration. In contrast, the creation of radicals is independent on its concentration. Therefore a higher radical concentration due to a higher dose rate increases the radical consumption and dose rate dependence can be expected. Dose rate

dependence was reported for PAG and MAGAT gels (McAuley 2006, DeDeene et al 2006). For the BANGKit™ formulation only minor dose rate dependence was found below the saturation region (Bayreder 2009). In another publication dose rate dependence was shown for dose rates above 2,7Gy/min (Murakami et al 2007).

2.4.7 Energy and LET Dependence

No significant difference of dose response to varying photon energies has been found for MAGIC gels (DeDeene et al 2006). The response to high LET (**L**inear **E**nergy **T**ransfer) radiation (i.e. neutrons, protons, carbon ions, etc.) is different to the response to photons and electrons. Delta ray emission along the tracks of incident particles saturates the dosimeter and is causing under-response (Jirasek 2006). Delta rays are fast electrons knocked out of atoms orbits by high energy particles that can themselves ionize further atoms. Comparing neutron irradiation (<E>=7MeV) with ^{60}Co-irradiation Berg et al (2009) observed a reduction in sensitivity by 63% (factor: 0.37). For 68MeV protons, it has been found, that the dose is underestimated in the Bragg peak region by 20% compared to ionization chamber measurements (Berg et al 2005). Sensitivity of the gel response is also strongly reduced for carbon-ion irradiated gels compared to photon irradiated gels (Ramm et al 2004).

2.4.8 Dependence on Temperature

Temperature variation during production, irradiation and scanning of polymer gels can have strong influence on the polymer gel dose response. Different storage conditions and cooling rates after production and their influence on dose response, were investigated by DeDeene et al 2007. They reported differences in dose up to more than 60% for gels stored at room temperature and stored in a fridge. Different container volumes might cause different cooling rates and therefore different dose response.

The temperature during irradiation is important for the dose response of the gels. Reaction kinetics, particle movement and gel viscosity are influenced by the temperature (DeDeene 2004b). Sensitivity decreases significantly with increasing temperature.

The polymerization process itself is an exothermic process that generates heat. For MAGAT gels (6% to 9% Methacrylic acid) a temperature increase of approximately 10°C within the gels has been reported (Sedaghat M et al 2009). The temperature increase was reported to be more pronounced for higher dose rate and larger volumes. This can be a problem, if big phantoms with a volume of several liters are calibrated with small calibration vials with volumes of 10 to 150ml.

The dependence of the dose response on the ambient temperature upon scanning is even more pronounced. Dipole-dipole interactions are less efficient with increasing particle movement, due to increasing temperature and therefore T2 times are increasing (DeDeene et al 2006).

Another temperature related error - in specific cases - might be introduced by measurement times longer than 40 minutes. RF intensive measurement sequences could lead to significant heating. This effect would be more pronounced for phantom diameters comparable to resonant wavelength of the system (26cm for 3 Tesla). RF absorption is more efficient then and temperature increases especially at the edges of phantoms. Temperature increases of 1.5°C within 80 minutes of measurement were observed for FSE-(**F**ast **S**pin **E**cho)-sequences (Liney et al 2009).

If two gel dosimeters are to be compared they should be from the same batch, filled in equivalent phantoms, experience the same temperature history, irradiated at the same temperature and finally scanned at the same temperature.

2.4.9 Spatial Resolution - DMTF Concept (Berg et al 2004)

Radiotherapy applications such as brachytherapy, γ-knife, stereotactic surgery and IMRT involve steep dose gradients. A correct dosimetry of these techniques is demanding for a dosimeter with high spatial resolution. The concept of modulation transfer function (MTF) is widely used as tool for the investigation of resolving power of imaging systems (Evans 1981). A periodic pattern of structures (e.g.: lines) with decreasing width and distance is representing a spectrum of spatial frequencies. Spatial frequency is the inverse of the distance between two structures (a full period).

$$f = \frac{1}{\Delta x} \; [mm^{-1}]$$

In an image, the periodic structures are represented as modulation of pixel values. Ideally the modulation equals one but it decreases with increasing spatial frequencies.
The concept was adapted as DMTF (dose-modulation transfer function) for dosimetric imaging systems by Berg et al (2004). DMTF is defined as the ratio of dose output contrast (DOC) to dose input contrast (DIC):

$$DMTF = \frac{DOC}{DIC}$$

With the maximum and minimum amplitudes written as $D_{i\,max}$ and $D_{i\,min}$, DIC and DOC at the spatial frequency f are defined as:

$$DIC_{(f)} = \frac{D_{i\,\max(f)} - D_{i\,\min(f)}}{D_{i\,\max(f)} + D_{i\,\min(f)}}$$

$$DOC_{(f)} = \frac{D_{o\,\max(f)} - D_{o\,\min(f)}}{D_{o\,\max(f)} + D_{o\,\min(f)}}$$

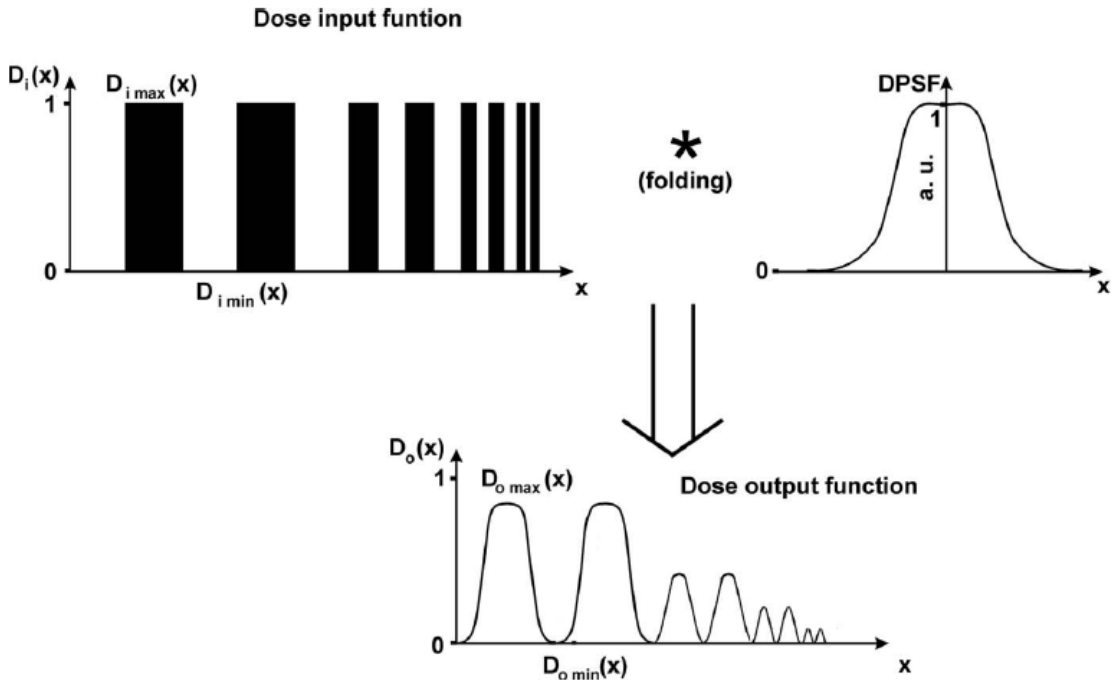

Figure 2.09 (Bayreder et al 2008): Dose input folded with a dose point spread function resulting in a dose output function.

The limit of resolution can be defined as the spatial frequency where the modulation is 50% or larger:

$$DMTF \geq 0.5$$

Noise present in real images can be considered by an additional criterion named dose modulation to noise ratio (DMNR). The dose modulation (DM) must be stronger than the present noise:

$$DMNR = \frac{DM}{Noise}$$

If noise is estimated as the standard deviation in a region of interest in a dose map and the confidence level for detecting a dose modulation is set to p = 68%, the criterion can be written as:

$$DMNR \geq \sqrt{2}$$

Therefore the minimum dose modulation necessary for detection is $DM_{min} = \sqrt{2}\sigma$.

Dose modulation can be generated with an absorber grid placed in between radiation source and dosimeter. Dose input ratio is in fact an unknown parameter, but can be calculated theoretically with Monte Carlo simulations. It can also be approximated by assuming that small spatial frequencies (large structures) are transferred without demodulation (DMTF = 1).

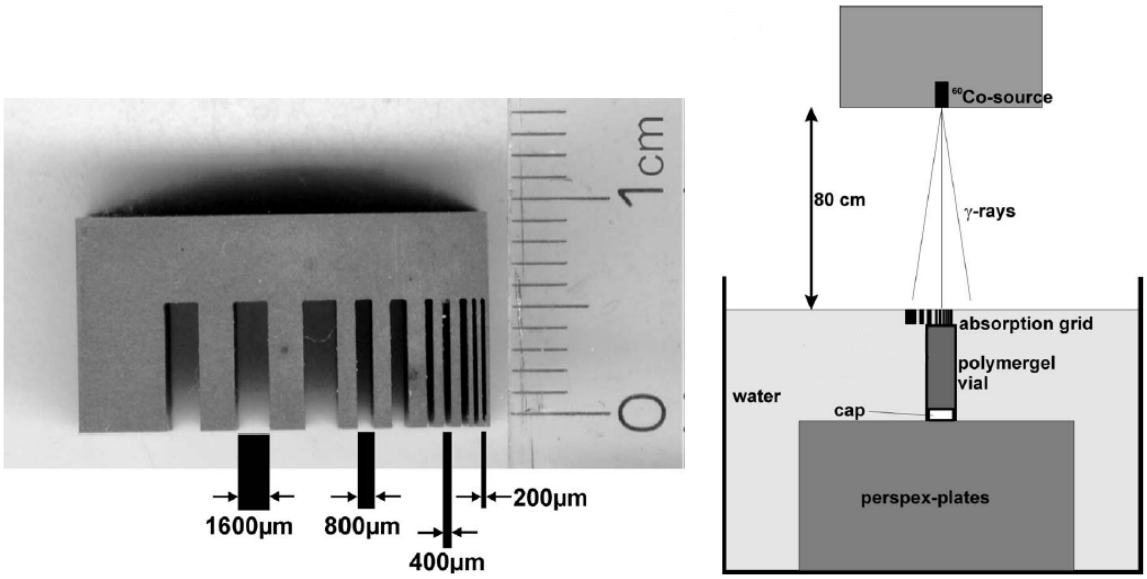

Figures 2.10 and 2.11 (Bayreder et al 2008): Grid absorber for the generation of a dose modulation and irradiation set-up with grid absorber.

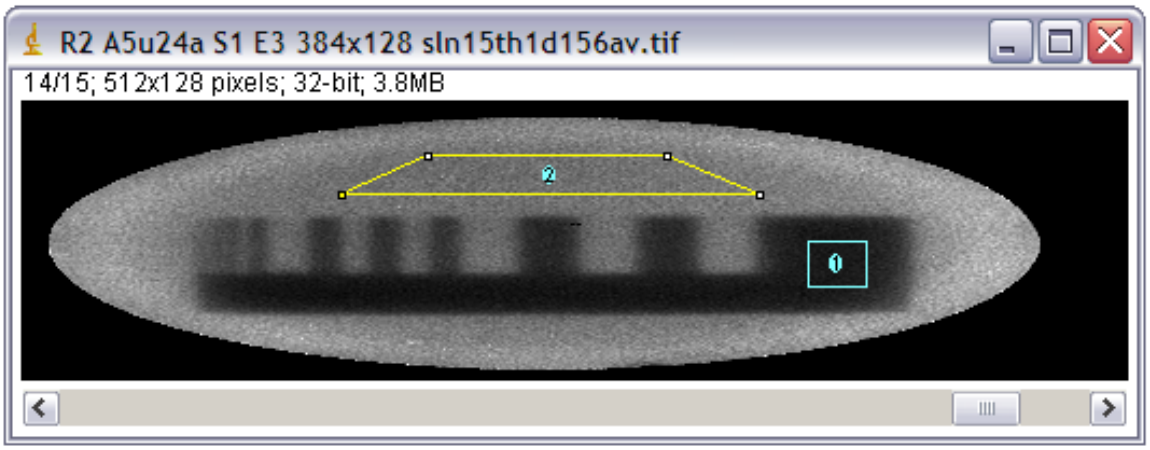

Figure 2.12: Irradiated gel with ROIs in the areas of maximum and minimum dose. Dose input modulation can be approximated as the ratio of the R2 values in the ROIs which represents dose modulation at the minimal spatial frequency.

3 Materials and methods

3.1 MAGIC Polymer Gels

3.1.1 Composition

MAGIC (**M**ethacrylic and **A**scorbic Acid in **G**elatin **i**nitiated by **C**opper) polymer gels (Fong et al 2001) belong to the class of normoxic dosimeters, which can be prepared at standard atmosphere oxygen pressure in a laboratory without special equipment. The ingredients of the MAGIC gels are deionized water ("Destilliertes Wasser", Freiberg KHGmbH/Germany), gelatin ("Gelatin from porcine skin, Type A, 300bloom", Sigma Aldrich/Germany), methacrylic acid (99%, Sigma Aldrich/Germany), Cupric sulfate Pentahydrate (99%, Fluka/Germany) and Ascorbic acid (99%, Acros/Belgium). The composition of 1l of the MAGIC type polymer gel is listed in table 3.01.

Table 3.01: Composition of 1 liter MAGIC (BANGKit™) polymer gel

Deionized water (H_2O)	80% (w/w)	800g
Gelatin 300bloom ($C_{17}H_{32}N_5O_6$)	14% (w/w)	140g
Methacrylic acid ($C_4H_6O_2$)	6% (w/w)	60g
Cupric sulfate Pentahydrate ($CuSO_4x5H_2O$)	10µM	0,025g
Ascorbic acid (C6H8O6)	2mM	0,3522g

The main principle of a polymer gel dosimeter is the irradiation induced polymerization of monomer molecules (Methacrylic Acid).The rate of polymerization is depending on the absorbed dose. Reduced mobility of the growing polymer chains causes an increase of the transverse NMR relaxation rate (R2=1/T2). Free O_2 molecules suppress polymerization by capturing the water radicals necessary for initialization of the polymer chain reaction (Maryanski et al 1993). Therefore, Ascorbic Acid is added as an oxygen scavenger. Together with the copper it traps the oxygen molecules within the monomer gelatin water mixture in a metallo-organic complex (Fong et al 2001).

3.1.2 Preparation

All gel fabrications followed the preparation instructions for the commercially available "Dry BANGKit™" polymer gel dosimeter (MGS Reasearch, Inc/USA).

The Methacrylic acid is added to the deionized water in a glass container and the solution is mixed by hand with a glass rod for 5 minutes. Then, the gelatin is poured into the solution, while the resulting compound is slowly stirred with the glass stick until the gelatin has

swelled from soaking. The glass container is placed in a water bath at 55°C until a clear solution without visible air bubbles is achieved. Ascorbic acid and the cupric sulfate, both dissolved in 30ml of deionized water, are added and the gel is mixed using a high speed propelling mixer for five minutes. Then again the glass container is heated in the water bath to 55°C. The temperature is held for 30 to 50 minutes to remove air from the solution. The time needed is depending on the gel volume and the preparation tank. The gelatin solution is then poured in containers and all gels are stored in a refrigerator at 8°C, until the day before irradiation, to prevent spontaneous thermal and light induced polymerization. The dose response of polymer gel dosimeters is strongly depending on temperature at the time of irradiation (DeDeene et al 2006). Therefore the gels have to be placed into room temperature environment (at localization of measurement) 24 hours before irradiation.

3.1.3 Gel Containers

a) Standard container

High-resolution measurements using a micro gradient system and sensitive coils (inner bore diameter: 35mm) demand for small and thin walled gel containers, with excellent oxygen barrier qualities, to prevent oxygen permeation. Cylindrical Barex 210 (Hildering's Emballagebedrijf BV/Netherlands) containers were used and Saran™ (foil put on top of the container openings. The foil was pushed into the opening and additional gel was poured on top of it before closing the container with its cap. This was done to ensure complete filling of the containers without remaining air bubbles and to prevent oxygen permeation into the vial via the container cap. Both Barex and Saran are excellent oxygen diffusion barriers (Bayreder 2009).

b) Container for IMRT-irradiations

The 3D-visualization capabilities for clinical radiation therapy on tumors were to be investigated. An existing Intensity-Modulated Radio Therapy (IMRT) plan for a head tumor at SMZ-Ost/Vienna was applied to MAGIC gels. The Polyethylene-High-density (PE-HD) container (3.6 l volume, cylindrical form, diameter: 20cm) was shaped approximately like a head. The oxygen diffusion through PE-HD is not negligible and therefore the volume from within 1cm of the container walls has to be excluded from analysis due to oxygen contamination of the gel. The container was almost entirely filled with polymer gel and a saran foil was put on top of the gel as well. The rest of the volume was filled with a monomer free gelatin water solution, to avoid an oxygen reservoir in the closed container.

Before gel preparation, all containers were filled with an oxygen-scavenging solution, for at least 24 hours, to remove oxygen adsorbed to the container walls (Bayreder 2009). The density of both container materials is close to the density of water and therefore the radiation pathway trough the container walls is almost equivalent to that of water (Ibbott et al 2002).

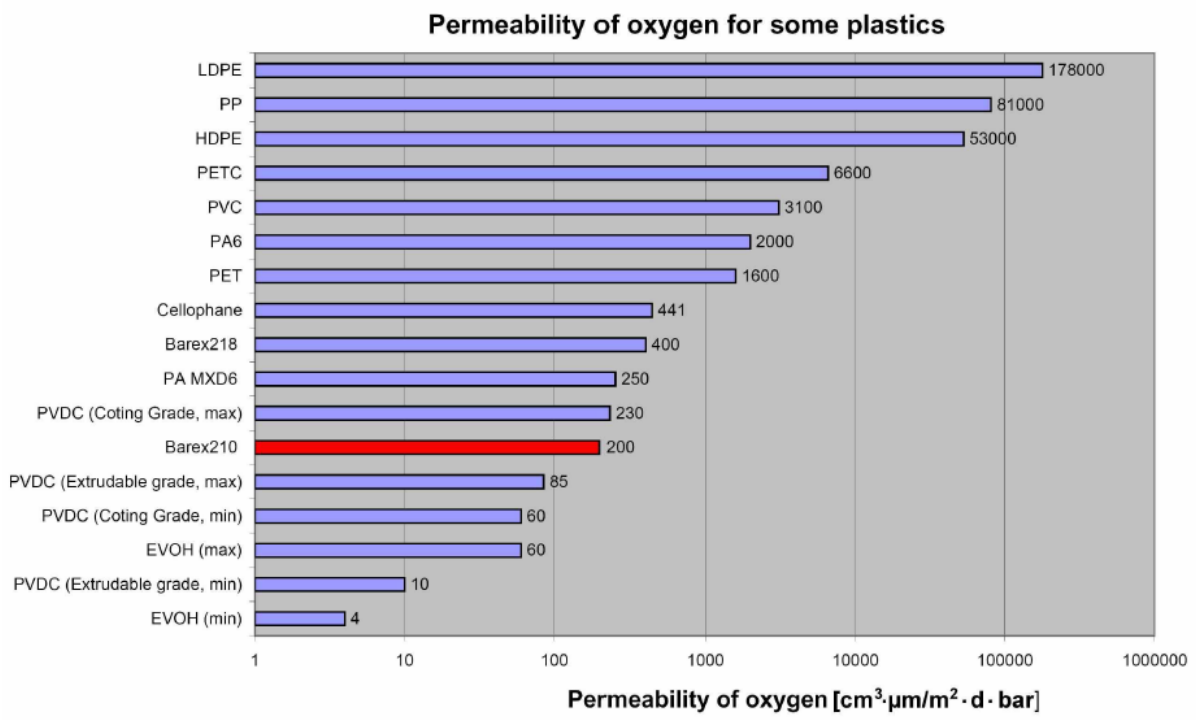

Figure 3.01 (Bayreder 2009): Permeability of oxygen for some plastics.

3.2 MRI Equipment and Image Analysis

3.2.1 MRI Scanner

All measurements were performed at the MR Centre of Excellence at the Medical University of Vienna on a Bruker Medspec 30/80. The scanner was installed in 1996 as research unit for (medical) imaging, in vivo spectroscopy and fMRI. The permanent magnetic field of 3 Tesla is generated with a superconductive Niobium-Titanium magnet (inner bore diameter: 55cm). The Bruker software package ParaVision 2.1.1 was used for imaging.

Figure 3.02: Bruker Medspec 30/80 with actively shielded micro-imaging gradient system BGA-12

3.2.2 Standard Imaging Equipment

The system incorporated patient gradient system (S550) can deliver gradient strengths up to 45mT/m. All standard resolution measurements were performed using this gradient system together with the Bruker knee coil 1P T9127 (inner diameter: 20cm). The IMRT images were

taken with the Bruker head coil 1P T5020 (inner diameter: 25cm) for size reasons. In order to reduce the error in measurements due to coil non-uniformity the quasi uniform volume of the coils was determined with separate analyses. All samples measured with the knee or head coil were stored in the MR scanner room at least 12 hours prior to measurement to obtain room air temperature equilibrium and temperature was controlled before each measurement (between 20.5°C and 21.5°C).

3.2.3 Micro Imaging Equipment

All high resolution measurements were performed using the actively shielded micro-imaging gradient system BGA-12 with a maximum gradient strength of 200mT/m (further specifications see table 3.02) and a birdcage resonator with an inner diameter of 35mm. The whole system can be slid into the MR scanner. To reduce vibrations, it is fixated to the inner bore with threaded screw (Berg et al 2001). Due to the small volume of the gradient system and temperature adaptation reasons (water temperature of gradient water cooling: 14°C), all samples were put into the gradient system at least 12 hours before measurement, to guarantee constant temperature at the time of measurement (approximate air temperature in the coil: 17°C).

Table 3.02 (Pfleger 2007): Bruker Biospec micro-imaging gradient system BGA-12 specifications

Inner diameter	120 mm
Maximum Intensity of current I_{max}	100 A
Maximum Voltage	150 V
Gradient strength at I_{max}	200 mT/m

3.2.4 MRI Measurements and Image Analysis

The protocol parameters for all measurements are listed in table 3.03. All images were gathered with parameter selective T2 multi-slice multi-echo (MSME) sequences. The sequences consist of 10 or 20 equidistant echoes (35ms to 350ms or 20ms to 400ms). For the high resolution images the chosen matrix was rectangular, instead of quadratic, to reduce the measurement time down to 14.5 hours. The number of phase encoding steps (matrix size Mtx_y), which determines measurement time, was set to lower values. The frequency encoding matrix Mtx_x was set to higher values, which results in higher spatial resolution at the same field of view (FOV). The raw data was converted to T2 images with ParaVision 2.1.1. The image data sets were then transferred from the Bruker work station to a personal computer and all image analysis was performed with the software ImageJ (Abramoff et al 2004).

Table 3.03: Measurement parameters

Protocol	IMRT	Standard resolution	High resolution
Method	MSME	MSME	MSME
FOV [cm^2]	20x20	15x15	3x3
Matrix [px^2]	128x128	128x128	384x128
Resolution [$mm/px]^2$	1.56x1.56	1.17x1.17	0.078x0.234
TR [s]	25.51	5	6.39
TE [ms]	20	20	20
Number of echoes	20	20	20
Bandwidth [kHz]	50	50	50
Slice thickness [mm]	3	3	1
Slice distance [mm]	3	6	1
Number of slices	50	10	15
Averages	4	4 to 16	56 to 64

3.3 MAGIC Quality Assurance (QA)

Polymer gel dosimetry is a three step process. The gels have to be manufactured, irradiated and finally scanned. The radiation induced polymerization causes a change of the MR-relaxation-rate (R2) in the gels proportional to the absorbed dose. The dose response of the gels is sensitive to the variation of ambient conditions and variation of parameters during manufacturing and irradiation. The resulting R2-map is also influenced by parameters of the scanning procedure and conditions during scanning.

Table 3.04 (DeDeene 2004, 2004b, 2006): Parameters that (may) influence the R2-dose response

- Composition (gelatin, monomer, oxygen scavenger concentrations)
- Temperature history (temperature during production, storage, irradiation and scanning)
- mixing conditions
- Container size, volume and shape
- Stability and accuracy of dose delivery system
- Dose rate and radiation quality
- Time intervals during production, irradiation and scanning
- Choice of MR sequence and parameters
- Positioning accuracy at irradiation and scanning

These parameters do not only influence the dose response but also the dose uncertainty and the spatial resolution of the gels. The investigation and analysis of these influences is crucial for the development of reliable polymer gel dosimeters for modern radiation therapy.

3.3.1 Calibration Data and Sensitivity of the Dose Response

For the calibration of the polymer gel dose response a set of 5 to 10 gels from the same batch was irradiated to known doses (0 to 50Gy). The exact number of irradiated gels and range of the applied doses varied with the different experiments. An important characteristic of the dose response is the sensitivity. It is defined as the slope of the linear part of the resulting dose-R2-curve ($k=\Delta R2/\Delta D$). Ideally the dose response is linear over the whole dose range.

3.3.2 Irradiation Set-Ups

The various experiments were performed under three different experimental set-ups at two different locations. In the further text they are called Set-up A (Linear Accelerator, Medical University of Vienna), Set-up B (^{60}Co-unit, Medical University of Vienna) and Set-up C (Linear Accelerator, SMZ-Ost Vienna).

Irradiation Set-up A (Linear Accelerator, Medical University of Vienna)

The first investigations of dose rate and energy dependence of the gel dosimeters were realized with this set-up. The gels were irradiated at the Department of Radiation Oncology at the Medical University of Vienna using a standard radiation unit for cancer treatment Clinac 2100, Varian*)*. The gels were placed in a 40x40x39cm^3 polystyrene tank (Med-Tec, MT150, US) filled with distilled water. The SSD (**S**ource **S**urface **D**istance) was 100cm and the gels were positioned in the beam center in the region of the dose maximum, with the depth depending on the radiation quality. The gels were irradiated in a 10x10cm^2 field one by one, with the bottom end pointing to the source. The dose maximum was 5mm away from the bottom part of the container within the gel.

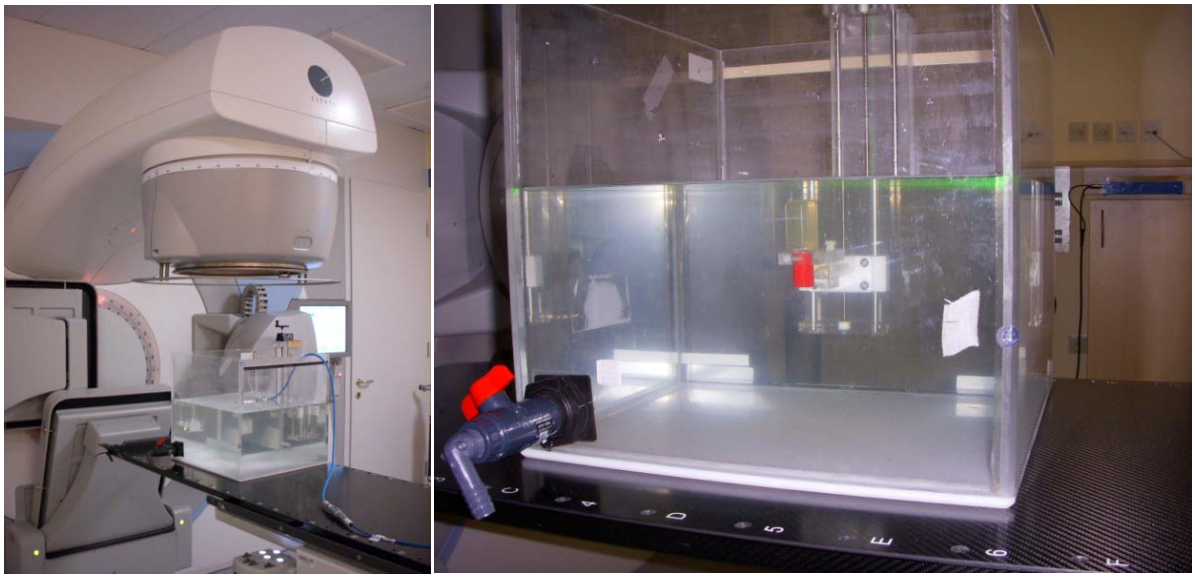

Figure 3.03: Irradiations at the Linear Accelerator of the Medical University of Vienna. **Left:** Accelerator gantry and water phantom. **Right:** Water phantom with a gel container positioned at depth of irradiation.

Absolute dosimetry measurements were performed based on calibrated ionization chambers by staff members (Thanks to DI Gabriele Kragl and Prof. Dr. Dietmar Georg). Photon dosimetry was done with a Farmer type chamber (0.6cm^3, type 30003/0319, PTW Freiburg, Germany) and electron dosimetry with a Roos chamber (0,35cm^3, type 34001/0333, PTW Freiburg, Germany). Both ionization chambers were connected to an electrometer (UNIDOS 1, PTW, Freiburg, Germany). The Linac was calibrated to deliver 0.1Gy with 100 Monitor Units (MU) at the reference depth. The dose was verified and the dose rate in relation to the MU rate was estimated at the depth of the dose maximum for all different beam energies. The measurements were repeated three times. According to the MU controlled delivery system, all gel irradiations were performed under stable conditions.

Irradiation Set-up B (^{60}Co-unit, Medical University of Vienna)

Gels irradiated under this set-up were positioned in a 40x40x39cm^3 polystyrene tank (Med-Tec, MT150, US) filled with distilled water with a ^{60}Co-beam (15x15cm^2 field size) from an external treatment unit (Theratron, Elite 780, Theratronics, Canada). The gel dosimeters

were fixated in a custom made gel container holder upside down just below the water surface. The SSD was 80cm for all experiments. The gel container holder was manufactured in the technical laboratory of the Oncology Department according to plans of the author.

Before each irradiation session absolute dosimetry was performed using a calibrated Farmer type ionization chamber (0.6cm^3, type 30006/0319, PTW Freiburg, Germany) and an electrometer (UNIDOS 1, PTW, Freiburg, Germany). The dose rate was verified at a depth of around 6mm at the maximum of the dose depth curve. This was done for all points in the radiation field where polymer gels were positioned during the experiment to minimize errors due to field inhomogeneities. The field uniformity for the 15x15cm^2 irradiation field was better than 4%.

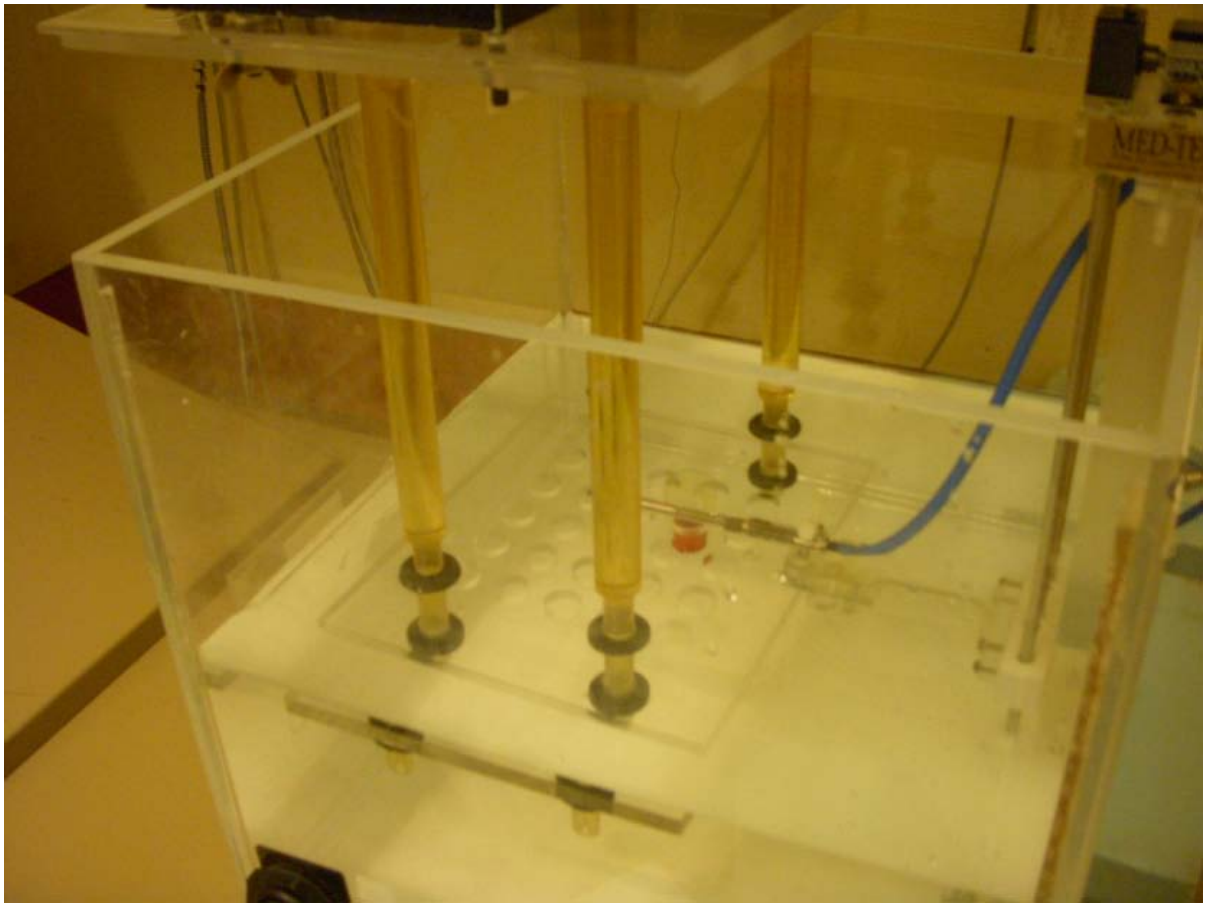

Figure 3.04: Irradiations with ^{60}Co at the Medical University of Vienna. One gel container is placed in the custom made polymer gel phantom holder.

Irradiation Set-up C (Linear Accelerator, SMZ-Ost Wien)

Further experiments were realized at the department of Radiation Oncology at the SMZ-Ost (**S**ozial**m**edizinisches **Z**entrum Ost) with a standard radiation unit for cancer treatment (Oncor, Siemens, Germany). The gels were placed upside down in the gel container holder originally designed for the ^{60}Co-unit at the Medical University of Vienna. The gels were irradiated all together in a 30x30cm^2 field (field homogeneity +/-1%). SSD and depth of irradiation varied with the different experiments.

Absolute dosimetry for photon and electron beams was performed in the same fashion as in irradiation Set-up A by a staff member (thanks DI Lena Siebert).

3.3.3 Dosimetric Precision and Accuracy

Two important characteristics of any dosimeter are its accuracy and precision. If a gel dosimeter is regarded as a black box only dose input and the R2 output are of concern. Both parameters are influenced by several independent parameters, where most of them can be eliminated with careful experimental design (DeDeene 2006). This can be nearly achieved if all gel samples used for the determination of precision and accuracy are made from the same batch and identical containers. Furthermore the gels should be irradiated and scanned simultaneously and otherwise treated equally. Under these conditions the remaining influences are mainly: dose delivery stability, variation in dose response between gels and inherent MR-precision (MacDougall et al 2002). The gel dosimeter precision can then be defined as variation in relaxation rate results, expressed as coefficient in variation (CV= $\sigma[R2]/\mu[R2]$) within one batch of gels irradiated to the same dose (MacDougall et al 2002). Accuracy is defined as the difference between the absorbed dose measured by gel, using a calibration curve, compared to the reference dose, measured by a calibrated ionization chamber (MacDougall et al 2002). Accuracy is expressed as percentage of the "true" dose.

For the evaluation of the gel's feasibility as dosimeter in radiation, therapy precision and accuracy should be specified for dose values throughout the whole dynamic range. Investigation of precision and accuracy was performed with a batch of 25 gels fabricated from one batch and irradiated 7 days later under irradiation set-up C. After preparation the gels were put in a fridge to solidify. 48h before irradiation they were transferred to the Linac control room to reach room temperature. Ten gels were used for a calibration curve. They were irradiated one by one in the beam center with known doses (0 to 34 Gy), verified with calibrated ionization chamber measurements. In addition 15 gels were irradiated at three different dose values (5, 16 and 28 Gy), five gels simultaneously for each dose in order to investigate precision. One gel was positioned in the beam center. The other four were placed at the corners of the innermost square positions (within an area of $10x10cm^2$) of the gel container holder originally designed for the ^{60}Co treatment unit at the Medical University of Vienna. Absolute dosimetry measurements showed that the uniformity within the irradiation field of $30x30cm^2$ was in the range of +/-1%. Precision was determined as the standard deviation of the mean value of the 5 gels (Bayreder et al 2006). The same 15 gels used for the assessment of precision were used for the determination of accuracy. The calibration curve was applied to convert the R2-values of these gels to absorbed dose. Then the deviations of these values to the actual applied dose (verified with calibration chamber) were calculated. Accuracy was determined for three dose values (5, 16 and 28Gy) as main value of the deviations to the reference dose value (MacDougall et al 2002).

3.3.4 Energy and Dose Rate Dependence

Energy and dose rate dependence of the polymer gel response have been investigated for many gel formulations, including methacrylic based gels (for example in DeDeene et al 2006). For MAGIC gels the situation is different though. The influence of dose rate variation on MAGIC gels was only reported in two publications (Bayreder 2009, Murakami et al 2007) and no data at all exists for the dependence on radiation beam quality (Literature research 02.12.2009). The analysis of energy dependence within this diploma work was performed at two different locations. The first series was irradiated at the Department of Radiation Oncology at the Medical University under irradiation set-up A. All gels were made from the same batch and irradiated 5 days after preparation. They were stored in a fridge and transferred to the Oncology Department 12h before irradiation to reach room temperature. The gels were divided into four subsets and irradiated with two different electron and photon energies to doses from 0 to 35Gy. They were irradiated on the same day and treated under the same conditions (including storage, transport and temperature history). Irradiation parameters are listed in table 3.05. All gels were scanned in one session 16 days after irradiation.

Table 3.05: Irradiation specifications for the investigation of energy dependence (AKH Vienna)

Radiation Beam Quality	x6MV	x18MV	e6MeV	e20MeV
Dose Rate [cGy/min]	505	461	436	439
Depth of irradiation (at dose maximum) [cm]	1.5	3	1.4	4.7

The gels of the second series were irradiated at the department of Radiation Oncology at the SMZ-Ost under irradiation set-up C. All gels of this series were made from the same batch and treated equally. Two subsets of the batch were used for the evaluation of the radiation beam quality dependence of the dose response. One set was irradiated with electrons and the other one with photons. Dose rate dependence was investigated with a third subset irradiated with photons and a differing dose rate. The Linac software does not allow manual manipulation of the dose rate and therefore exact matching was not possible. Instead the distance of the phantom was changed to utilize the $1/r^2$-law for radiation.

Table 3.06: Irradiation specifications for the investigation of energy dependence (SMZO Vienna)

Radiation Beam Quality	x6MV	x6MV	e7MeV
Dose Rate [cGy/min]	159	245	290
Depth of irradiation [cm]	7.5	7.5	1.5

The gels were irradiated 37 days after preparation to doses from 0 to 30Gy. All gels were stored in a fridge and placed together in the Linac control room 48h before irradiation. Irradiation parameters are listed in table 3.06. The gels were irradiated at the reference depth according to the quality assurance protocol of the department. Both subsets were scanned together 6 days after irradiation.

3.3.5 Storage Temperature Dependence

Temperature can have a strong impact upon the polymer gel dose response. Several works have been published on the variation of dose response for different temperatures during irradiation or scanning (e. g. DeDeene et al 2006). Results from another publication (DeDeene et al 2007) also showed influence of cooling rate on the dose response. All these works analyzed gels of the types PAG, PAGAT and MAGAT. One work presented data for MAGIC gels of the BANGKit™-type (Murakami et al 2007), but only for temperature variation at the time of irradiation. The data showed strong evidence for a temperature dependent dose response similar to the other gel formulations. The code of practice in house is to store gels in a fridge until the time of irradiation. For practical reasons it was investigated if gels could be stored at room temperature at least for a few days without a significant change in dose response. Therefore a batch of gels was divided into two sub groups after preparation. One set was stored in a fridge at 6°C, the other set was stored at room temperature (approx. 22°C). All gels were irradiated 4 days after preparation under irradiation set-up B. They were then placed in the MR-room and scanned 16 days after irradiation.

3.3.6 Non-Linearity in the Low Dose Regime

During the investigations on the dose rate and radiation beam quality two batches of gels (identical formulation) were prepared. One batch was not needed and therefore not irradiated 4 days after preparation with the gels of the other batch. Instead, this batch was stored sealed in a box at room temperature (approx 22°C, air condition controlled) and irradiated 40 days later, during another experiment. A comparison of the dose response between the two batches both irradiated with ^{60}Co beam showed significant differences. The gels irradiated 40 days after preparation showed a linear dose response in the low dose region, whereas the gels irradiated 4 days after preparation exhibited a non-linear response. The fact that both batches were made on the same day and under the same conditions raised the suspicion that the crucial difference was the storage time. Hence a new batch was prepared and divided into two subsets. The gels were transferred and stored at room temperature (approx 22°C, air condition controlled) at the location of irradiation. One set was irradiated 6 days and the other set 37 days after preparation under irradiation set-up C (0 to 34Gy). The first subset was scanned 8 days after irradiation the second subset 6 days after irradiation.

3.3.7 Spatial Resolution and Edge Enhancement

The ideal dosimeter for modern day radiotherapy applications with steep dose gradients has a very high spatial resolution. We therefore wished to investigate the inherent spatial resolution of the polymer gel dose response with the alternative DMTF concept (Berg et al 2004). We approached this concept using a specially fabricated tungsten-carbide (additions: 9% Co, 0.2% TiC, 0.4% Ta(Nb)C) absorber grid (Bayreder et al 2008). The grid is designed with periodic slits (a/2: 1600, 800, 400, 200µm). Unfortunately one 400µm grid blade is missing and the last 200µm grid blade is partly broken.
Soon after the introduction of polymer gel dosimetry, edge enhancement effects (dose overshoots) were observed near high dose gradients (Maryanski et al 1994). This negative effect is believed to be a consequence of monomer and multimer diffusivity (Vergote et al 2004). Here the systematic investigation of edge enhancement was realized as analysis of the dose response around an ideally rectangular dose shape. Therefore, a cubical brass absorber was placed on top of the gels with one edge positioned above the middle of the gel container covering one half of the gel.

All gels were irradiated with a ^{60}Co beam under set-up B. The gels were positioned in a water phantom upside down directly below the surface with the absorbers placed on the container. Analysis of edge enhancement and spatial resolution were performed in the dose maximum (depth of 6mm) at varying doses (12, 24 and 50Gy) for different monomer and gelatin concentrations. Nine batches of gels with different combinations of gelatin and monomer concentration were produced. Each batch was designated with a corresponding combination of characters and numbers (table 3.07).

The gels were scanned with the micro imaging equipment four to ten days after irradiation.

Table 3.07: Gel formulations for the investigation of edge enhancement and spatial resolution

		Methacrylic Acid [%]		
		4	**6**	**8**
Gelatin [%]	**10**	g10-m4	g10-m6	g10-m8
	14	g14-m4	g14-m6	g14-m8
	18	g18-m4	g18-m6	g18-m8

3.3.8 Influence of gelatin and monomer concentration on the dose response

Differing concentrations of monomers and gelatin influence the dose response of the gel dosimeters (Luci et al 2007). Therefore a minimum of 8 gels of each batch, produced for the

analysis of spatial resolution and edge enhancement, were used to record a calibration curve (0 to 50Gy). All gels of the same batch were irradiated together with the gels for edge enhancement and spatial resolution analysis, but without absorber (for set up see 3.7.7). Each batch was scanned as a whole with the knee coil to analyze their general dose response.

3.4 IMRT

For the evaluation of MRPD as method of dosimetry for an actual cancer treatment an IMRT plan for a patient at the SMZ-Ost was selected. The plan ("step and shoot"-IMRT, 4 gantry angles, 26 segments) for the treatment of a cranial tumor was chosen for its steep dose gradients, close to risk organs. Before gel production the PE-HD-container, that served as head phantom (see 3.1.3), was filled with water and a CT image was taken. This image was transferred to the irradiation planning system (Corvus, NOMOS Corporation, Sewickley, USA). The irradiation plan was then recalculated for the phantom geometry and also modified to place the 100% dose region close to the center of the container. Its original dose values were multiplied by ten (tumor volume dose: 20Gy) to fit the applied doses into the sensitive range of the polymer gel (5 to 35 Gy) for a single session irradiation.

Five liters of MAGIC gel were produced and filled into the PE-HD-container and 9 Barex-containers. All gels were treated equally from production to scanning. They were irradiated under set-up C. The 9 gels in the Barex-containers were irradiated doses from 0 to 25 Gray (1.6Gy/min) to generate a calibration curve for the gel in the head phantom. The doses were verified with a calibrated ionization chamber. Head phantom and calibration gels were scanned together.

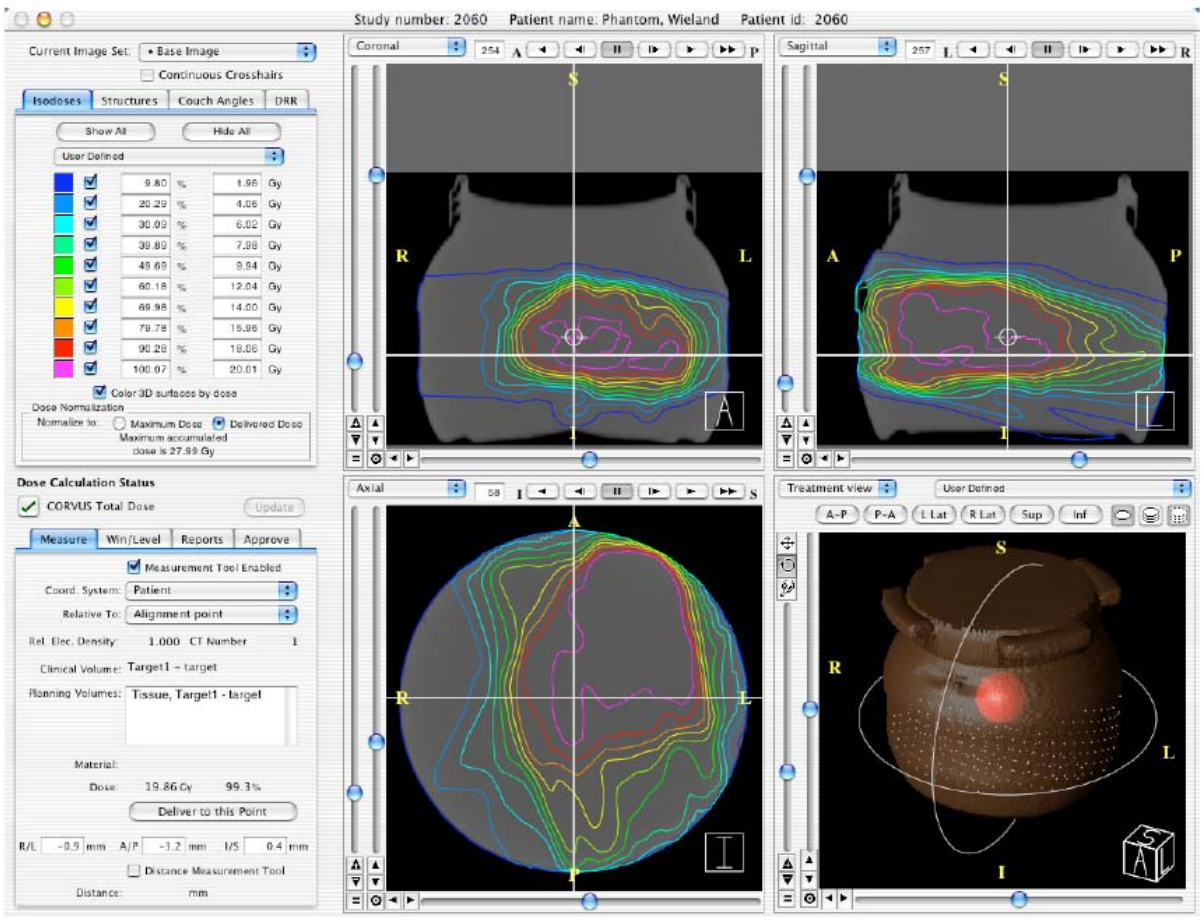

Figure 3.06: Corvus (NOMOS Corporation, Sewickley, USA) IMRT planning software. Isodose lines within the phantom for exemplary slices in sagittal, coronal and axial direction.

4. Results and Discussion

4.1 MAGIC Quality Assurance

4.1.1 Precision and Accuracy

From a batch of 25 gels 10 were irradiated one by one at the Sozialmedizinisches Zentrum Ost (SMZO) Vienna at a clinical linear accelerator (Linac) with increasing doses to generate a calibration curve (0, 1, 3, 5, 8, 12, 16, 22, 28, 34Gy). Precision and accuracy were investigated at three different dose values (5, 16, 28Gy) with five gels irradiated together at each dose value. All gels were scanned with a clinical knee-coil.

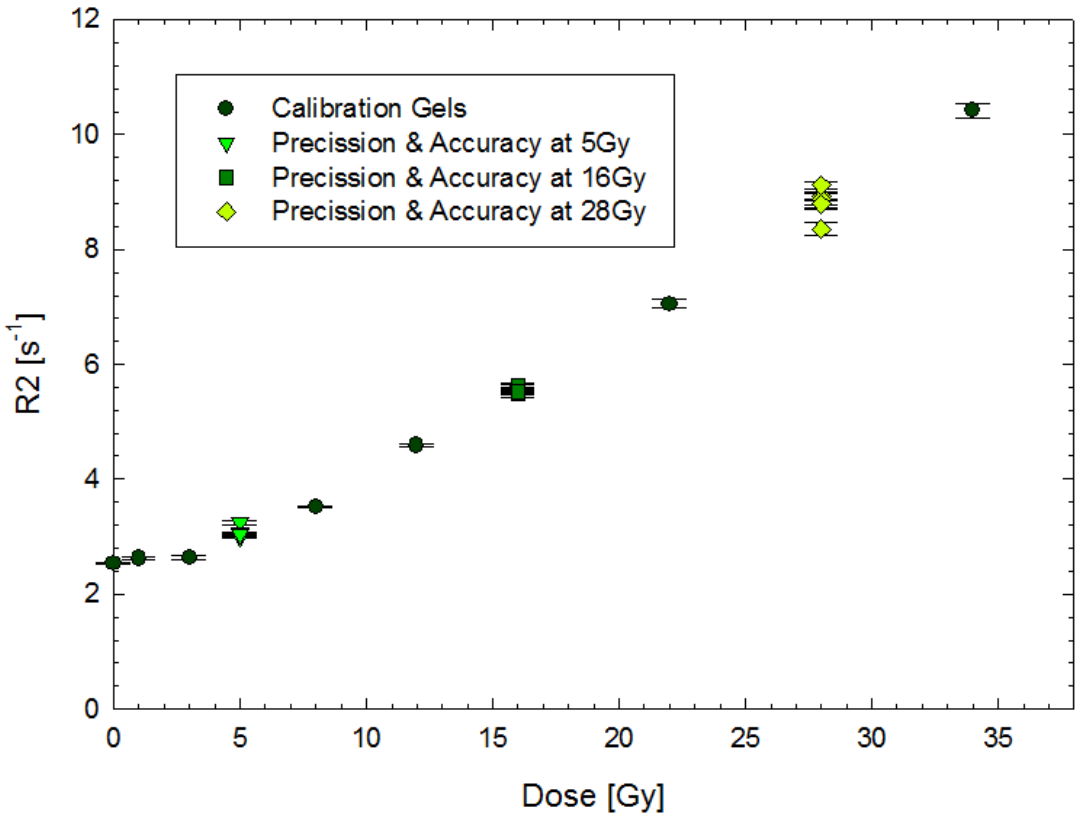

Figure 4.01: Relaxation rates R2 of the calibration gels and the gels used for the estimation of precision and accuracy at 5, 16 and 28Gy.

Over the whole dose range a calibration curve can be fitted with a polynomial function of third order (figure 4.02). From 3 to 34Gy a linear fit calibration curve can be used (figure 4.03). Compared to sets of gels manufactured and irradiated six to twelve month earlier sensitivity is reduced by a factor of 2 (compare to graphs in section 4.1.4). The reason is unknown. Manufacturing, irradiation and measurements of gels were performed in the same way for all gel batches throughout the whole work. A possible reason would be less efficient oxygen scavenging due to less extensive mixing of the gel solution for this particular

batch. Mixing time and intensity were not reduced on purpose, but mistakes, in time stopping for example, are imaginable.

The results for precision and accuracy are listed in table 4.01. Precision does not change with the choice of the fitting curve, since it is estimated as standard deviation of the R2-values over the 5 gels at each dose. High precision is achieved for the middle of the dose range. Low and high dose region precision are reduced from around 1% and 1.5% down to about 3.2% due to one outlier each. The fact that all values but one are very close together could be a sign of misplacement of the gel vial in depth during irradiation, rather than an inherent reduced precision compared to the middle dose range.

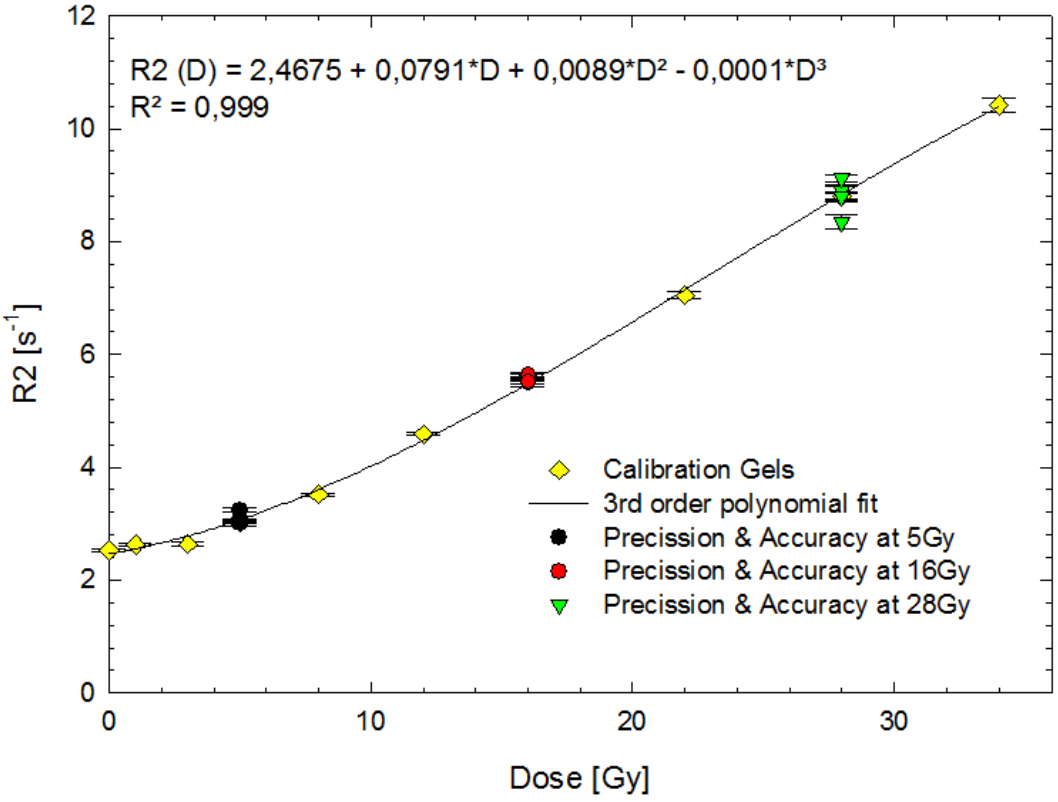

Figure 4.02: Third order polynomial fitted calibration curve over the whole dose range.

For the estimation of accuracy the dose-values of the five gels at each dose, are calculated using the R2-values and the calibration curve. Accuracy is the arithmetic mean of the deviations of the calculated dose values from the “real” applied dose verified by ionization chamber. For the linear fit accuracy at 5Gy is poor. This is a result of the nonlinear dose response in the low dose region and the resulting deviations of the fit in that region. In middle and high dose regions the accuracy is satisfying. For the polynomial fit accuracy is very high in the low and middle dose region and less satisfying at high doses. The results for precision and accuracy are in good agreement with values given in literature (Bayreder 2009).

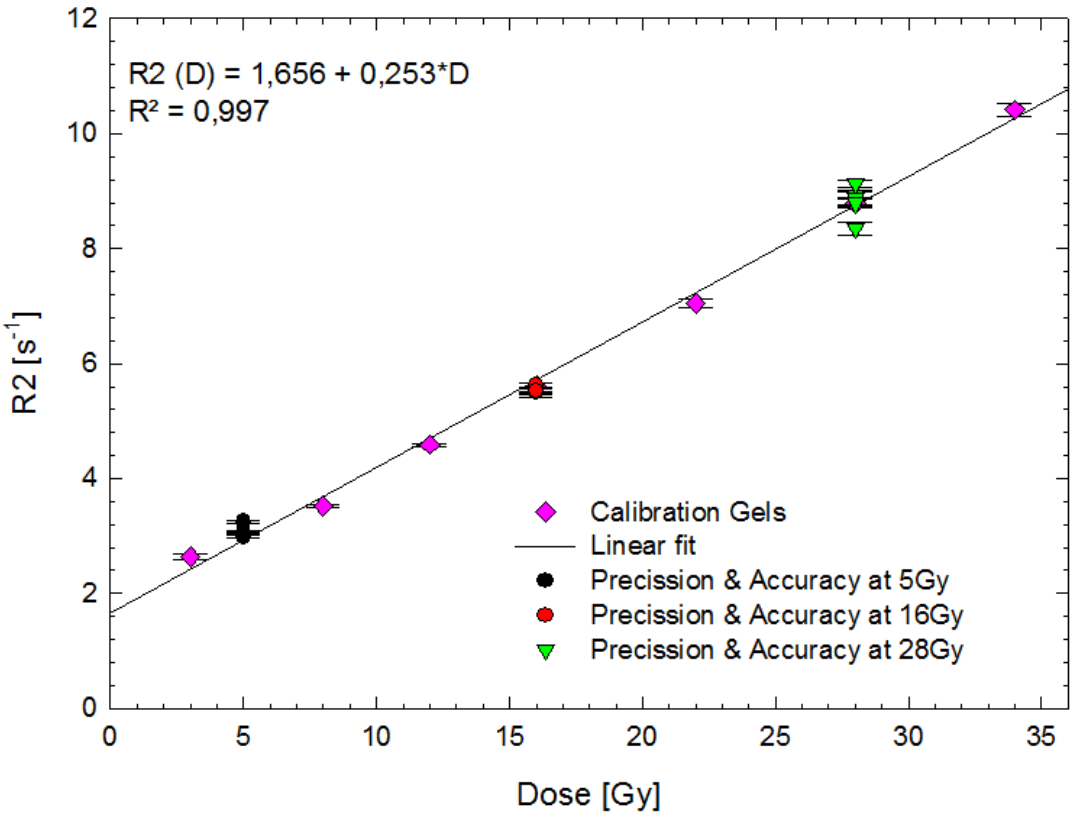

Figure 4.03: Calibration and precision data using linear fitting from 3 to 34Gy.

Table 4.01: Precision and accuracy at three different dose values

	Linear Fit			3rd Order Polynomial Fit		
	5 Gy	**16 Gy**	**28 Gy**	**5 Gy**	**16 Gy**	**28 Gy**
Precision	3.22%	0.88%	3.23%	3.22%	0.88%	3.23%
Accuracy	11.89%	3.89%	1.02%	0.36%	1.17%	6.79%

The estimation of precision and accuracy is a very time consuming process, even if it is only performed for selected dose values. An alternative concept of intrinsic precision is the dose resolution proposed by Baldock et al (2001):

$$D_{\Delta}^{p} = k_p \sqrt{2} \sigma_D$$

Dose resolution only depends on the dose uncertainty and the level of confidence p. The dose uncertainty σ_D for a linear dose-R2-calibration is calculated using the Gaussian law of error propagation:

$$\sigma_D = \frac{D}{\alpha}\sqrt{\sigma_\alpha^2 + \left(\frac{\sigma_{R2}}{D}\right)^2 + \left(\frac{\sigma_{R0}}{D}\right)^2}$$

The relevant parameters of the linear fit $R2 = \alpha D + R_0$ are given in table 4.02. In table 4.03 some representative values of dose uncertainty and dose resolution are presented for the linear fit (3 to 34Gy).

Table 4.02: Linear fit parameters with uncertainties

$\alpha \pm \sigma_\alpha$	$R_0 \pm \sigma_{RO}$
0.2531 ± 0.0056 (2.2%)	1.6562 ± 0.1070 (6.4%)

Table 4.03: Dose uncertainty and dose resolution for the linear fit at chosen dose values

		5 Gy	16 Gy	28 Gy
Dose Uncertainty	**σ_D/D**	8.84%	3.61%	2.95%
Dose Resolution	**$D_\Delta^{95\%}$**	24.51%	10.00%	8.17%
Dose Resolution	**$D_\Delta^{68\%}$**	12.50%	5.10%	4.17%
Dose Resolution	**$D_\Delta^{52\%}$**	8.84%	3.61%	2.95%

Results are worse compared to those of other gel formulations presented in literature (Bayreder 2009, Baldock et al 2001). Dose uncertainty and dose resolution are inversely proportional to the sensitivity of the dose response. The particular batch of gels used for the estimation of dose resolution, exhibited a reduced sensitivity (factor 2) compared to other gel batches of the same composition. Possible reasons are discussed above. Gels presented in other works show sensitivity three times as high (Bayreder 2009) to five times as high (Murakami et al 2007) compared to this batch. If sensitivity is larger by these factors, the dose resolution is also improved by these factors, if the associated error is not changing.

In radiotherapy the dose delivered to a patient is not allowed to deviate more than 5% from the prescribed value (Brahme 1984). Therefore uncertainty of a dosimeter reading, used to monitor dose delivery, has to have an uncertainty significantly less than 5%. This criterion is matched by MAGIC polymer gels in the dose range from 10Gy to at least 34Gy (figure 4.04) using linear fits.

Radiotherapy is planned with dedicated computer dose calculation software, that has to be verified with reference dose measurements. Planned and actual dose should not deviate more than 2% (ICRU 1987). A dosimeter should be able to detect differences of that magnitude, i.e. dose resolution of a dosimeter should be 2% or less. This criterion could not be matched with MAGIC gels of this set (see figure 4.05).

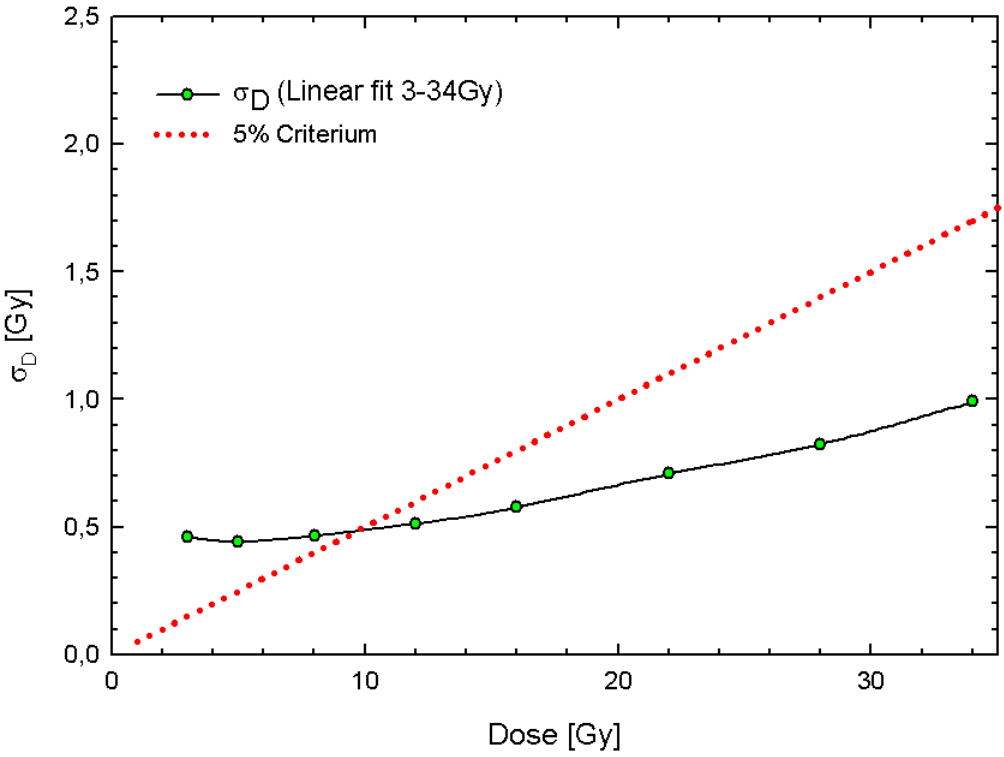

Figure 4.04: Dose Uncertainty for the linear fit (3-34Gy)

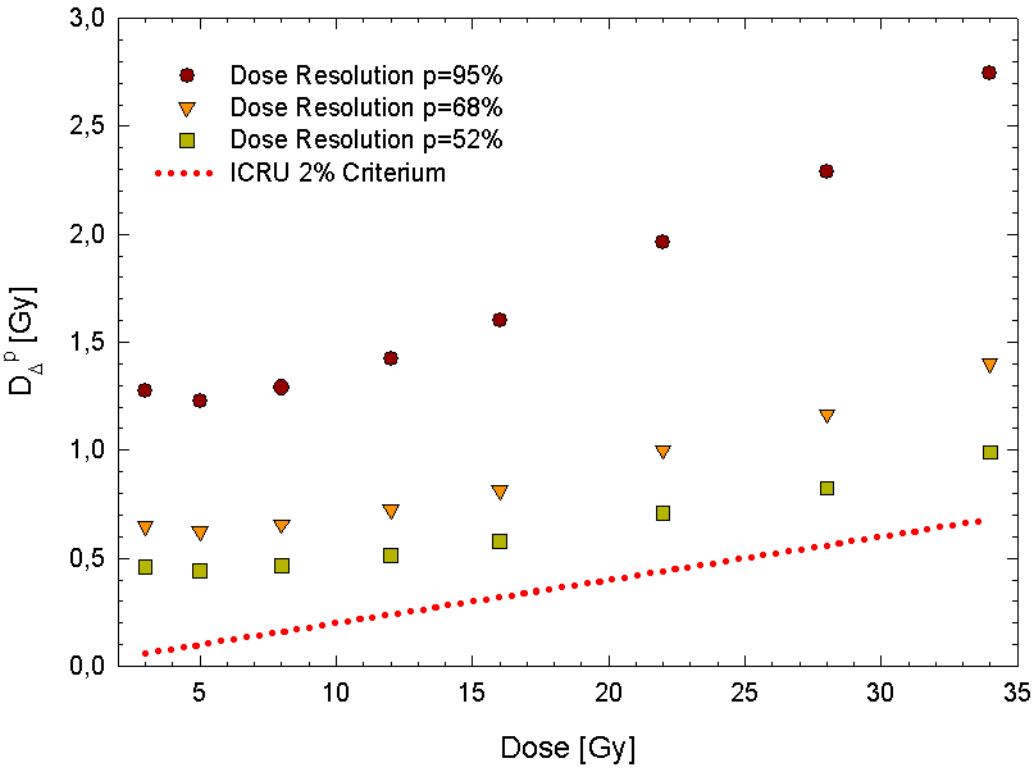

Figure 4.05: Dose Resolution for MAGIC gels (linear fit from 3 to 34Gy) for different levels of confidence compared to the ICRU 2% recommendation.

4.1.2 Energy dependence

4.1.2.1 Irradiations at the General Hospital Vienna (AKH Wien)

The first set of gels for the investigation of energy dependence was irradiated at the Medical University of Vienna/AKH. Dose-R2-curves for gel subsets irradiated with 1.2 MeV (^{60}Co), 6MV and 18MV photons, 6MeV and 20MeV electrons are shown in figures 4.06 and 4.07. All subsets were made from the same batch, got irradiated the same day (4 days post production) and finally measured on the same day (4 days post irradiation). The ^{60}Co-irradiations were performed with the Theratron calibration unit (irradiation set-up B). Gels were irradiated according to Monitor Units (MU). The Linac was calibrated to deliver 1Gy to reference depth and under reference conditions with 100MU. For practical reasons gels were not irradiated at depth of reference. The relation of measured MU to applied dose was determined with calibrated ionization chambers (see chapter 3.3.2). Due to a calculation error in the absolute dose calculation the gels haven't been irradiated to the same doses. The calculation errors were discovered after irradiation and could be corrected for.

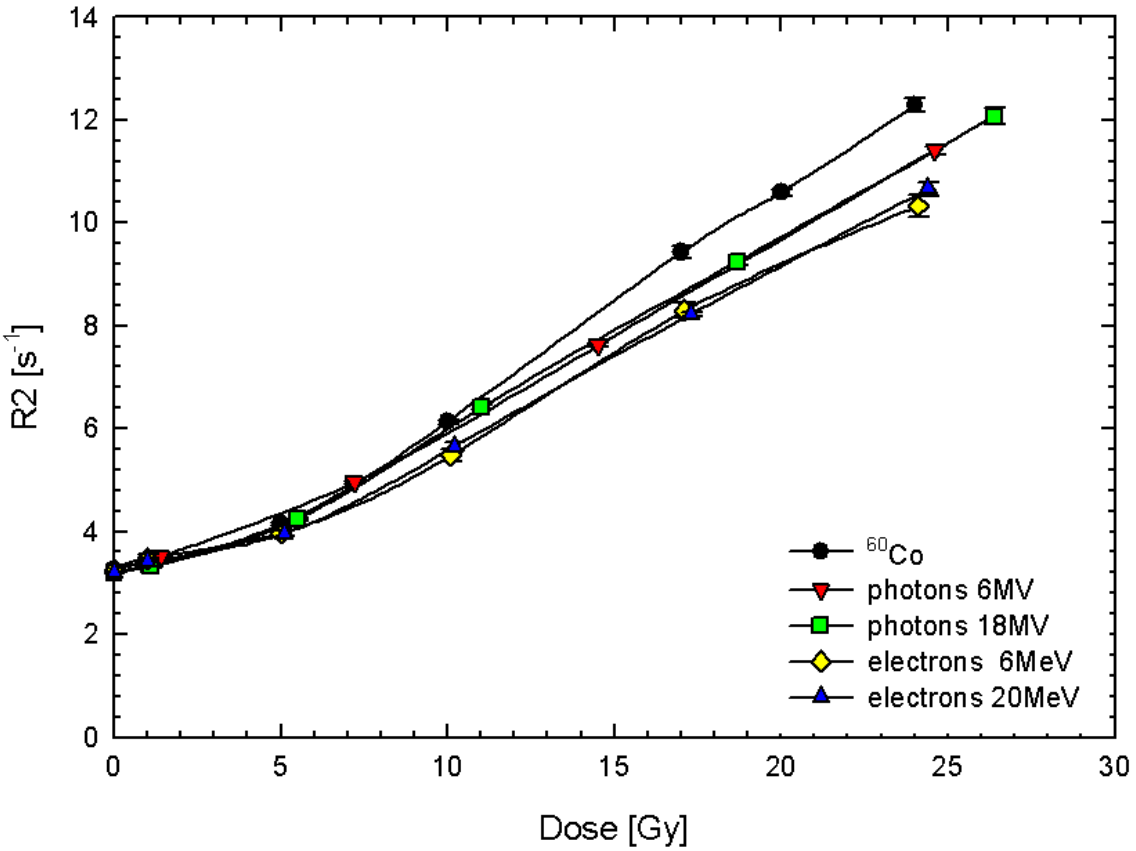

Figure 4.06: Dose-R2-curves for various photon and electron energies (irradiations at AKH Vienna).

The three irradiation modalities (^{60}Co, Linac photons and Linac electrons) were executed under different set-ups. The total uncertainty of the delivered dose to the relevant position in the polymer gel is determined as combined uncertainty of several influencing factors

(table 4.04). The dose to water in a phantom is estimated with a calibrated ionization chamber. Calibration, environmental conditions during measurement, establishment of reference conditions add up to a combined uncertainty for dose to water (IAEA, 2000). The output of the Linac is not completely stable. The influence of mispositioning of the gels in the water phantom and the mispositioning of the MR-read-out slice are depending on the steepness of the dose depth curve. The approximate percentage errors for a deviation of 1mm to 2mm are given in table 4.04. The uncertainties for the delivered dose are added as error bars for the x-coordinate in figure 4.07.

Table 4.04: Combined uncertainty for the delivered dose to the polymer gel

	^{60}Co	Photons	Electrons
Estimation of dose to water with a calibrated ionization chamber	0.9%	1.5%	2.1%
Variation of Linac Output	1.0%	1.0%	1.0%
Error for gel position	0.5%	0.5%	3.0%
Error for the postion of the read out slice	0.5%	0.5%	3.0%
Combined Uncertainty	1.5%	1.9%	4.8%

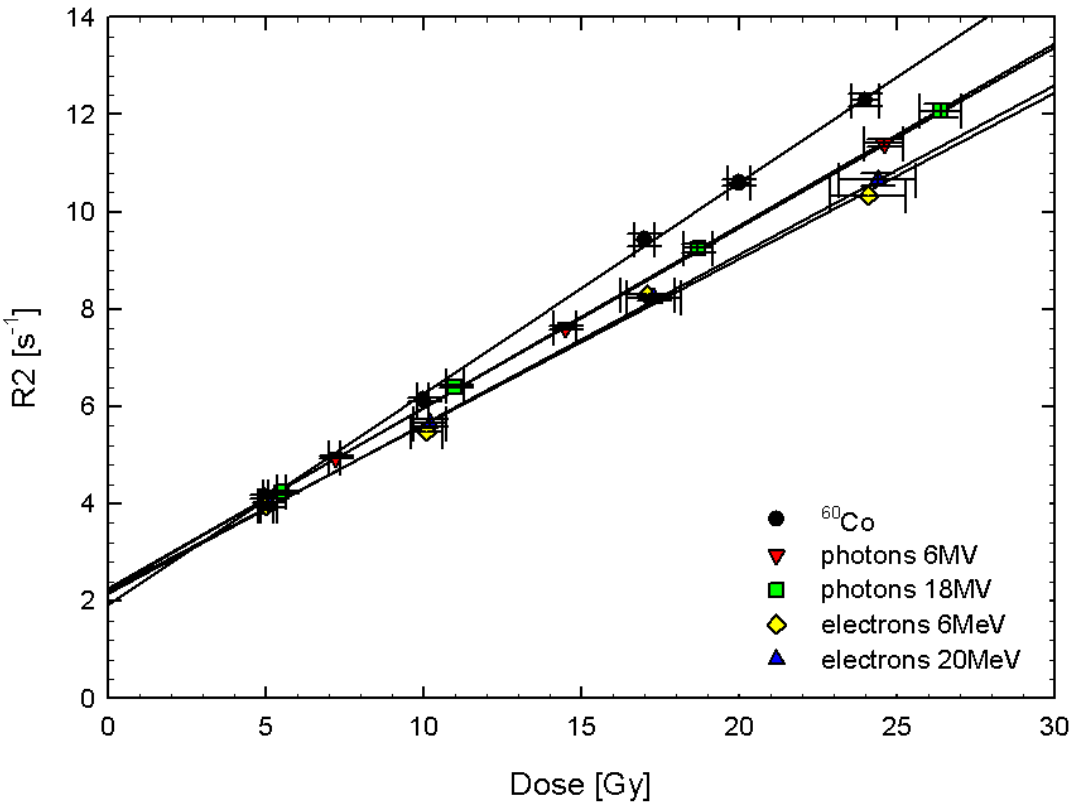

Figure 4.07: Linear fits (5 to 30Gy) of the dose-R2-curves for various photon and electron energies (irradiations at AKH Vienna).

The large differences (about 10%) between ^{60}Co-photon response and Linac-photons response could be a dose rate effect. Dose rates were 0.9Gy/min for the ^{60}Co-photons, 4.6 and 5Gy/min for the Linac-photons. Murakami et al (2007) reported a 10% drop in dose response for a dose rate of 4Gy/min compared to 0.7Gy/min for the same type of MAGIC gels (BANGKit™).

No energy dependence in dose response can be seen for the two photon energies and for the two electron energies. The difference in dose response between electrons and photons is considerable but not significant due to the uncertainties in dose delivery.

4.1.2.2 Energy dependence measurements at the SMZ-Ost Vienna

Due to the problems during absolute dose determination for the first experiment a second experiment was performed at the SMZ-Ost Vienna. Two subsets of a batch of gels were irradiated with 6MV photons (2.5Gy/min) and 7MeV electrons (3Gy/min). The dose-R2-curves are shown in figure 4.08 and the linear fit parameters with their standard deviations in table 4.05.

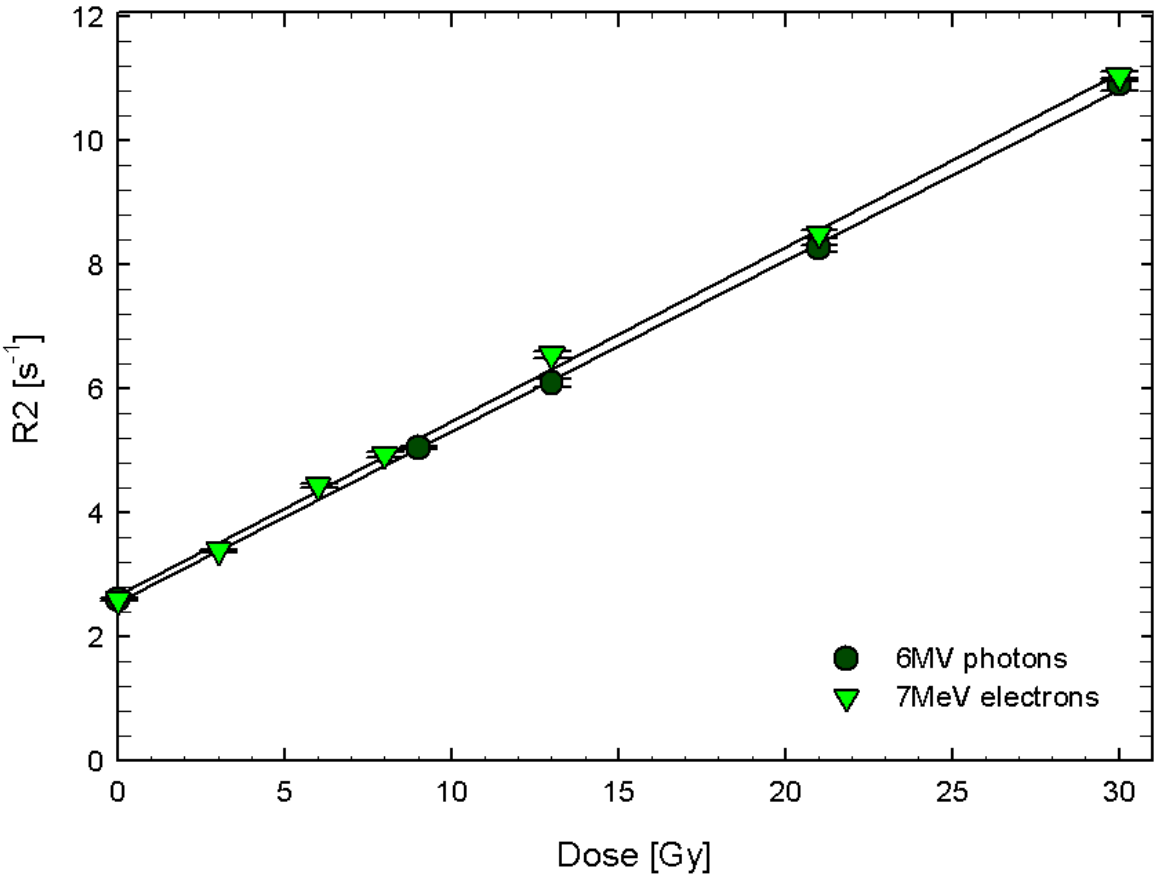

Figure 4.08: Dose-R2-curves for 6MV photons and 7MeV electrons (irradiations at SMZO Vienna).

Table 4.05: Linear fit parameters with uncertainties for photon/electron irrad. (SMZO Vienna)

	$\alpha \pm \sigma_\alpha$	$R_0 \pm \sigma_{RO}$
7 MeV electrons	0.2806 ± 0.0051 (1.8%)	2.6783 ± 0.0777 (2.9%)
6 MV photons	0.2757 ± 0.0032 (1.2%)	2.5615 ± 0.0579 (2.3%)

No significant difference is observed for the dose response to 7MeV electrons and 6MV photons. The differences of sensitivities and offsets are smaller than the standard deviation. Together with the results of the first experiment (4.1.2.1), where no difference was observed comparing pair wise different energies of photons or pair wise electron energies, the data seem to prove the assumption of negligible dependence on energy of the dose-R2-response.
In the literature only rare data is available for energy dependence of polymer gels. PAG gels and especially nPAG gels don't show dependence on radiation energy (DeDeene et al 2006). nMAG and MAGAT gels show a tendency to reduced sensitivity for lower photon energies, but the differences may be mainly attributed to the sensitivity to dose rate (Bayreder 2009). To the author's knowledge no data at all was presented for the MAGIC BANGKit™ formulation before.

4.1.3 Dose rate dependence

Dose rate dependence was investigated at the Linac at the SMZ Ost Vienna with 6MV photons. Dose rate could not be chosen arbitrarily by interface tools. We therefore made use of the $1/r^2$-law for radiation. By moving the phantom from the standard SSD (**S**ource-**S**urface **D**istance) of 100cm to the minimum SSD of 80,5cm the dose rate could be varied from 1.6Gy/min to 2.5Gy/min. The dose rates were verified with calibrated ionization chambers. Dose-R2-curves are shown in figure 4.09 and the linear fit parameters in table 4.06.

Table 4.06: Linear fit parameters with uncertainties for different dose rates

	$\alpha \pm \sigma_\alpha$	$R_0 \pm \sigma_{RO}$
1.6 Gy/min	0.2835 ± 0.0058 (2.0%)	2.6526 ± 0.1039 (3.9%)
2.5 Gy/min	0.2757 ± 0.0032 (1.2%)	2.5615 ± 0.0579 (2.3%)

In the investigated dose rate range of 1.6Gy/min to 2.5Gy/min, no significant dose rate effect is observed. Due to different reaction kinetics a variation in dose response at different dose rates could be expected. Murakami et al (2007) observed dose rate effects for rates higher than 2.7Gy/min. The reports in literature and the limited dose rate range in our experiment require more detailed investigations.

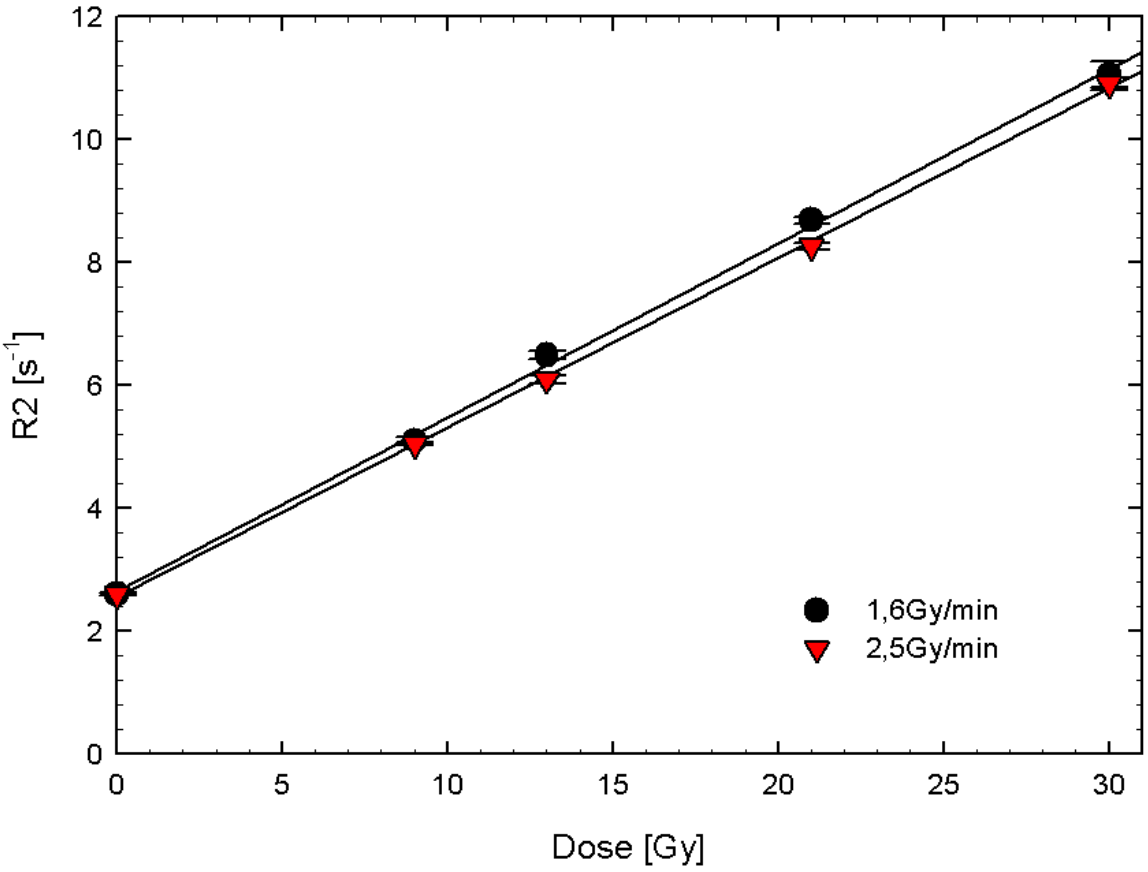

Figure 4.09: Dose-R2-curves for two different dose rates of 6MV photons

4.1.4 Storage temperature

DeDeene et al (2007) reported thermal induced pre irradiation polymerization for nMAG gels stored at room temperature in comparison to gels stored in a fridge. Pre-irradiation polymerization increased the offset of the dose-R2-response significantly and shifted the curve entirely to higher R2 values.

One set of gels was divided into two subsets. One was stored at room temperature (~22°C) for 3 days the other one was put into a fridge after manufacture and stored there for 2.5 days at approximately 9°C until a few hours before irradiation. Both subsets were transported, irradiated and measured together. The dose-R2-response curves are presented in figure 4.10. No significant difference in dose response can be seen for MAGIC gels if stored under different temperature (see table 4.07).

Table 4.07: Linear fit parameters (5 to 25Gy) with uncertainties for different storage temperatures

	$\alpha \pm \sigma_\alpha$	$R_0 \pm \sigma_{RO}$
9°C (2.5 days)	0.4336 ± 0.0072 (1.7%)	1.9260 ± 0.1299 (6.7%)
22°C (3 days)	0.4253 ± 0.0090 (2.1%)	1.8447 ± 0.1416 (7.7%)

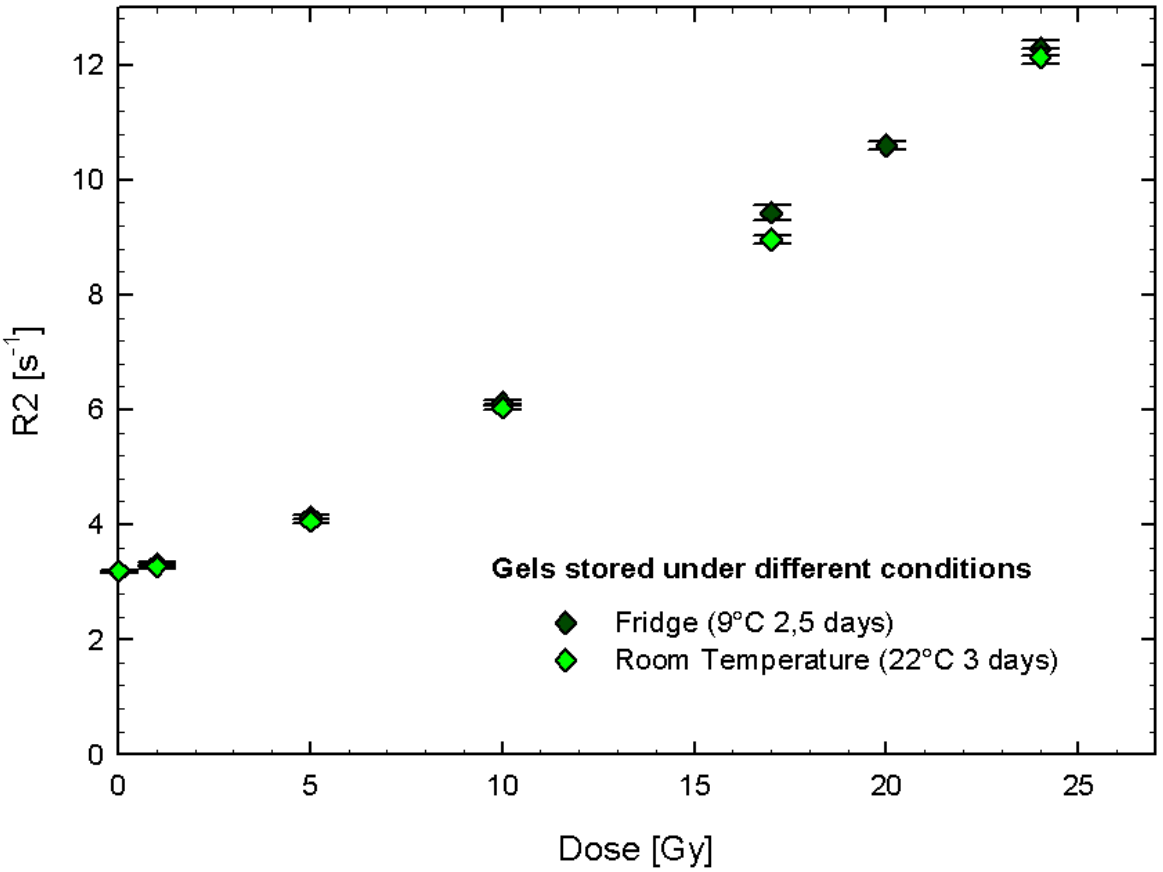

Figure 4.10 Dose-R2-curves for gels stored under different temperatures.

4.1.5 Storage time

During the first experiments for this work a batch of gels (Set A) was not needed and left un-irradiated for 41 days until it was used for another experiment. Compared to a different batch (Set B) manufactured at the same day) but irradiated 4 days after manufacture the dose response exhibited a more linear response in the low dose region and generally higher R2 values (see figure 4.11).

The difference in dose response could be a consequence of the fact that the sets A and B were not produced from the same batch of gels. Therefore a second experiment with two subsets O-a and O-b made from one batch was done to confirm the findings. The gels were treated equally during the whole process of transport and irradiation. Storage conditions and temperature during measurement were the same. Time between irradiation and measurement were almost the same (9 vs. 7 days). The major difference was the pre-irradiation storage time (6 vs. 36 days). The results can be seen in figure 4.12. They are similar to the first experiment. The sensitivity of the dose response does not change significantly (0.2616±0.0068 vs. 0.2737±0.0079), but the non-linearity in the low-dose regime disappears for the gels with the increased pre-irradiation storage time.

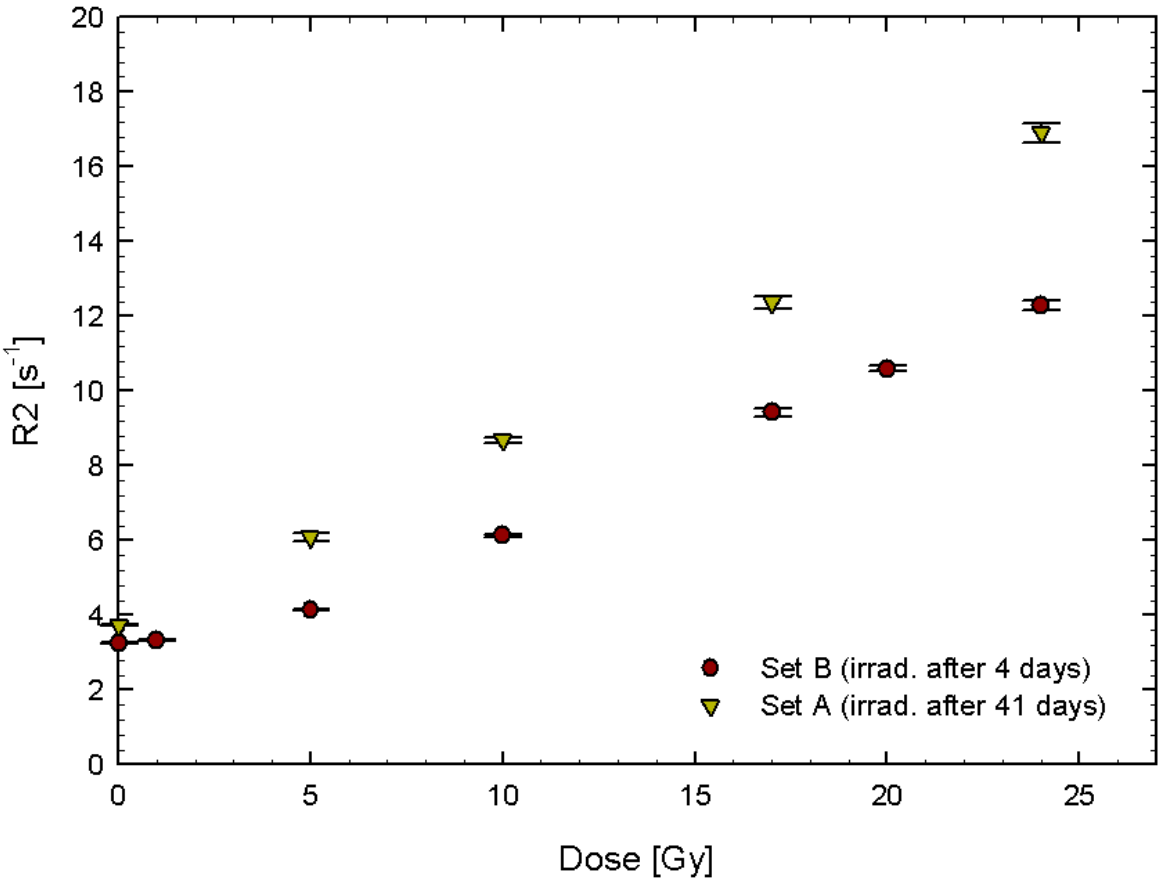

Figure 4.11: Dose response of different pre-irradiation storage times (two different sets of gels).

A possible explanation for this effect is the increased time for the scavenging of O_2 molecules, by ascorbic acid catalyzed by copper. Free O_2 molecules in the solution generate peroxides during irradiation and peroxides terminate polymer chain growth (DeDeene et al 2002):

$$RM_mOO^* + RM_n^* \rightarrow RM_mOOM_nR$$

This should be strongly pronounced in the low dose region, where the absolute number of created monomer radicals is relatively small. Until all peroxides created by O_2 molecules left in the solution are consumed by the termination reaction, polymer chain growth is inhibited and no or little change in R2 is observed. From a certain dose on all peroxides are consumed and polymer chain growth starts, resulting in increased relaxation rates R2. The less free O_2 molecules present the higher the sensitivity in the low dose region.

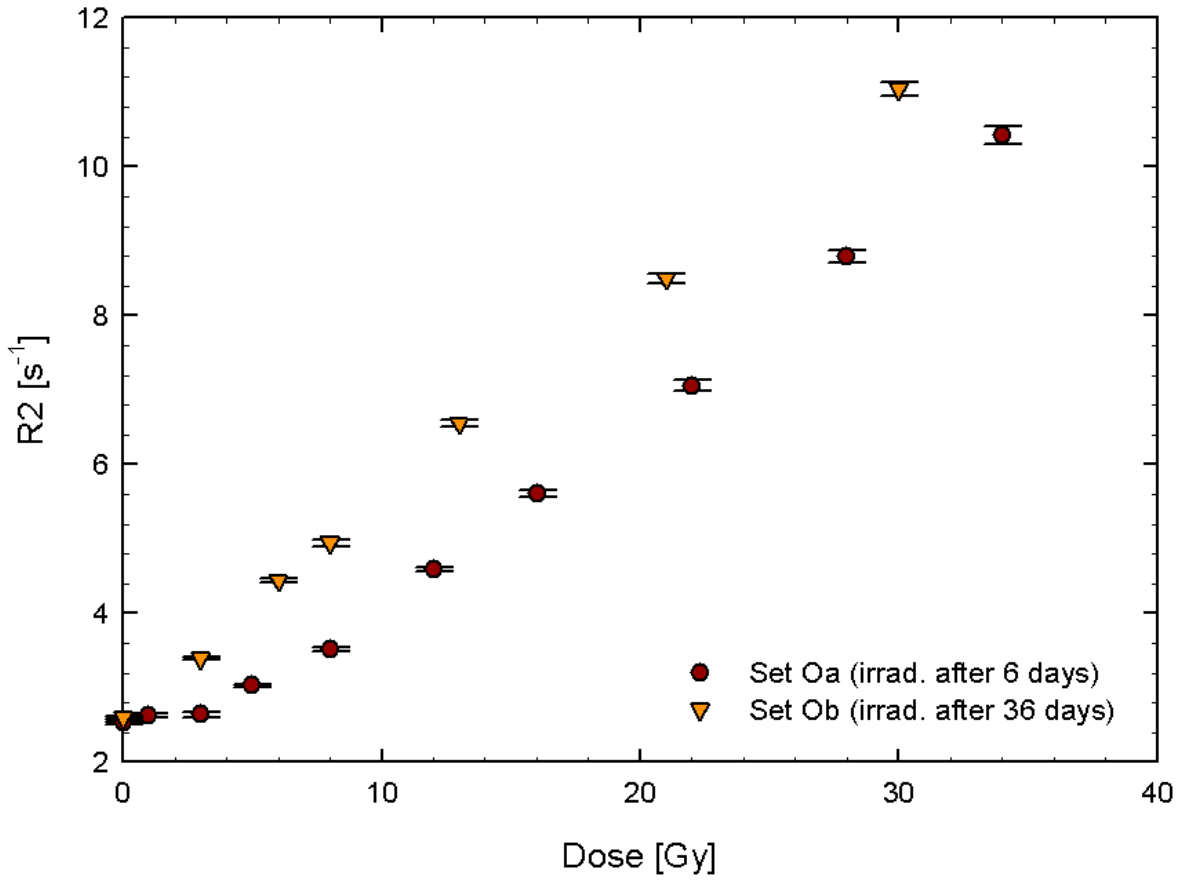

Figure 4.12: Dose response for different pre-irradiation storage times (two subsets made from one batch).

Two other publications contain data of BANGKit™ gels of the same composition. In Bayreder (2009) one batch of gels (used for the determination of precision and accuracy) shows the same non-linearity in the low dose region but no time interval between production and irradiation is given. Other batches used for a stability study with varying pre-irradiation time intervals didn't show non linearity. The dose response was fairly stable for the investigated pre-irradiation times (1 to 16 days). Murakami et al (2007) did not observe any non-linearities in the low dose region for a time interval of two days between production and irradiation of the gels.

A reason for less pronounced or absent non-linearity in the low dose region could be more effective mixing and dissolving of the oxygen scavenger. This could also be the reason for the increased sensitivity (three to five times higher) of the gels in these publications.

4.2 Spatial Resolution and Edge Enhancement

The MR-R2-maps of all gel formulations for the determination of edge enhancement and the limit of resolution were evaluated with ImageJ.

4.2.1 Spatial Resolution limits

The maximum modulation was estimated with ROIs in an area below the solid part of the absorber (minimum dose) and an area not affected by the absorber grid (maximum dose). Modulation below the grid structure was analyzed with a rectangular ROI (see figure 4.14).

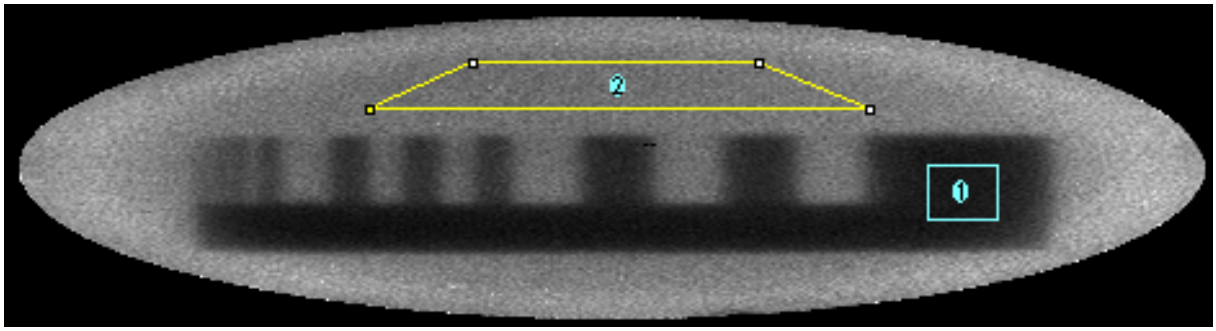

Figure 4.13: Estimation of the maximum modulation. Approximation with ROIs in an area of the gel not affected by the absorber (ROI 2, maximum dose) and below a solid part of the absorber (ROI 1, minimum dose).

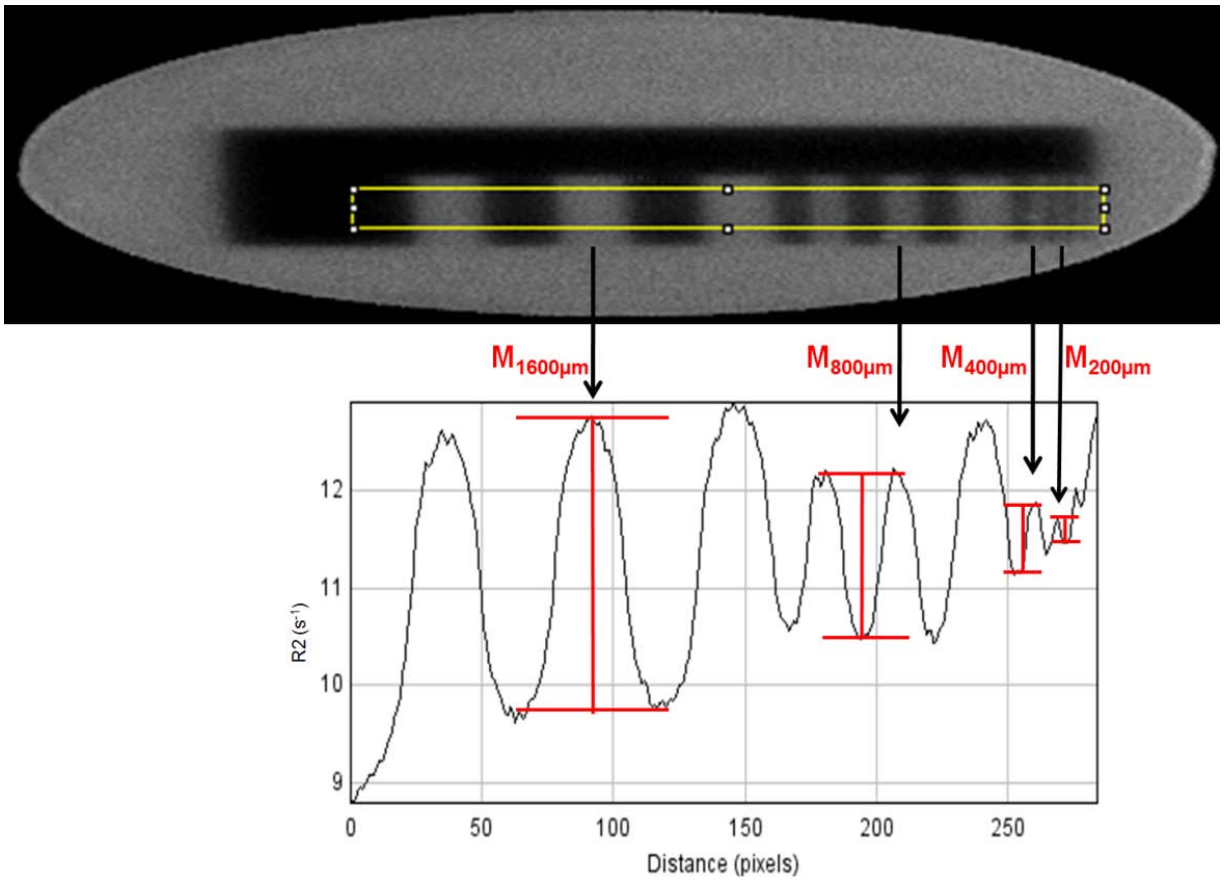

Figure 4.14: Modulation (M) under the absorber grid.

For the modulation transfer function (MTF) the modulation is plotted against the spatial frequency (inverse of the distance between two structures – a full period).
The modulation (M) must be larger than the noise (can be arbitrarily set to be twice the noise level):

$$M_{min} = 2 \cdot \sigma_{R2}$$

The noise is estimated as standard deviation of the R2 value in an ROI. We chose to use the arithmetic mean of the noise in regions of maximum and minimum dose (see figure 4.13). This approximation seems to be justified, because the absolute R2 values of the modulations $M_{200\mu m}$ and $M_{400\mu m}$ are about the same as the arithmetic mean of maximum and minimum R2 values (see figure 4.14). At present Monte Carlo (MC) Simulation is the only accurate method to determine the true actual dose (Bayreder et al 2008). No MC simulations were performed for this thesis, hence no information about the actual dose are available. Therefore the limit of spatial resolution is defined here as being half of the inverse of the interpolated spatial frequency (a half period), which features a modulation of two times the noise (see figure 4.16):

$$\Delta x = \frac{1}{2} \cdot f^{-1}[mm]$$

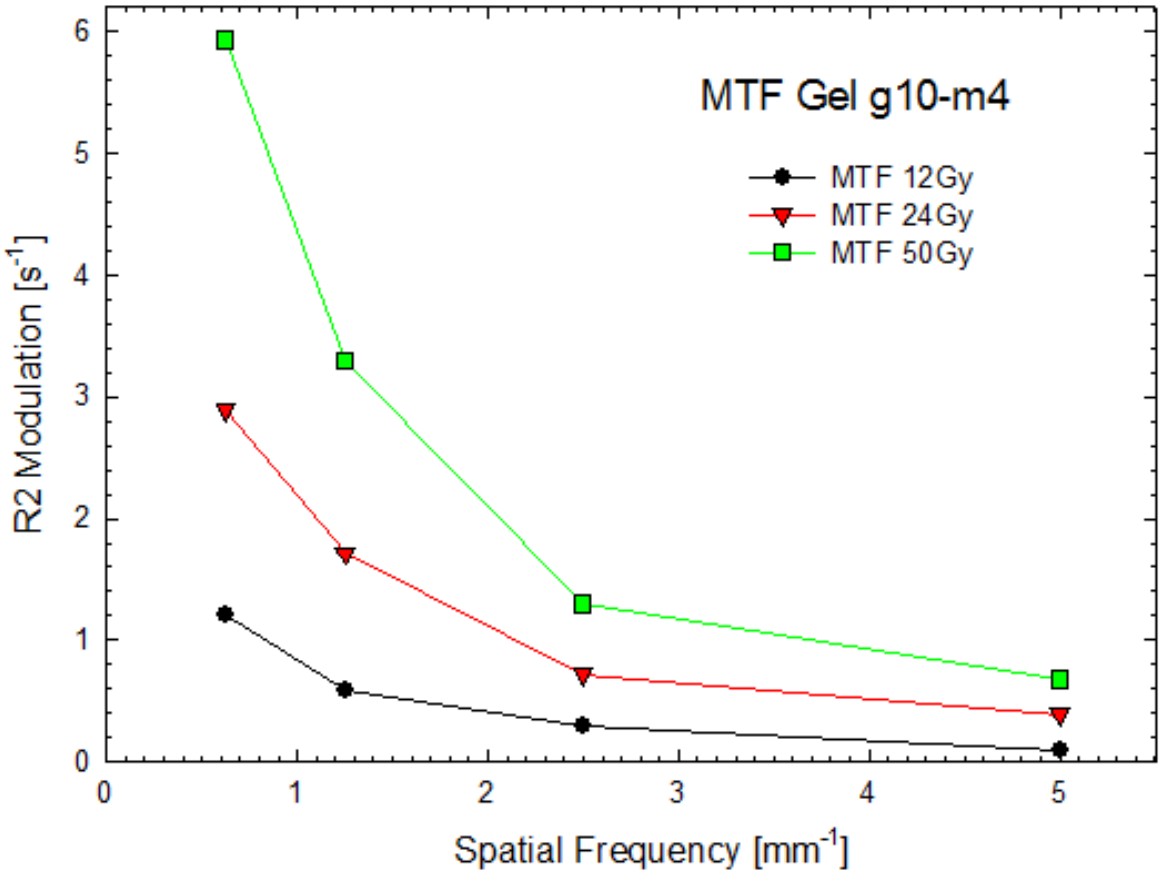

Figure 4.15: Modulation transfer function (MTF) for gel g10-m4 (10% gelatin concentration and 4% MAA concentration).

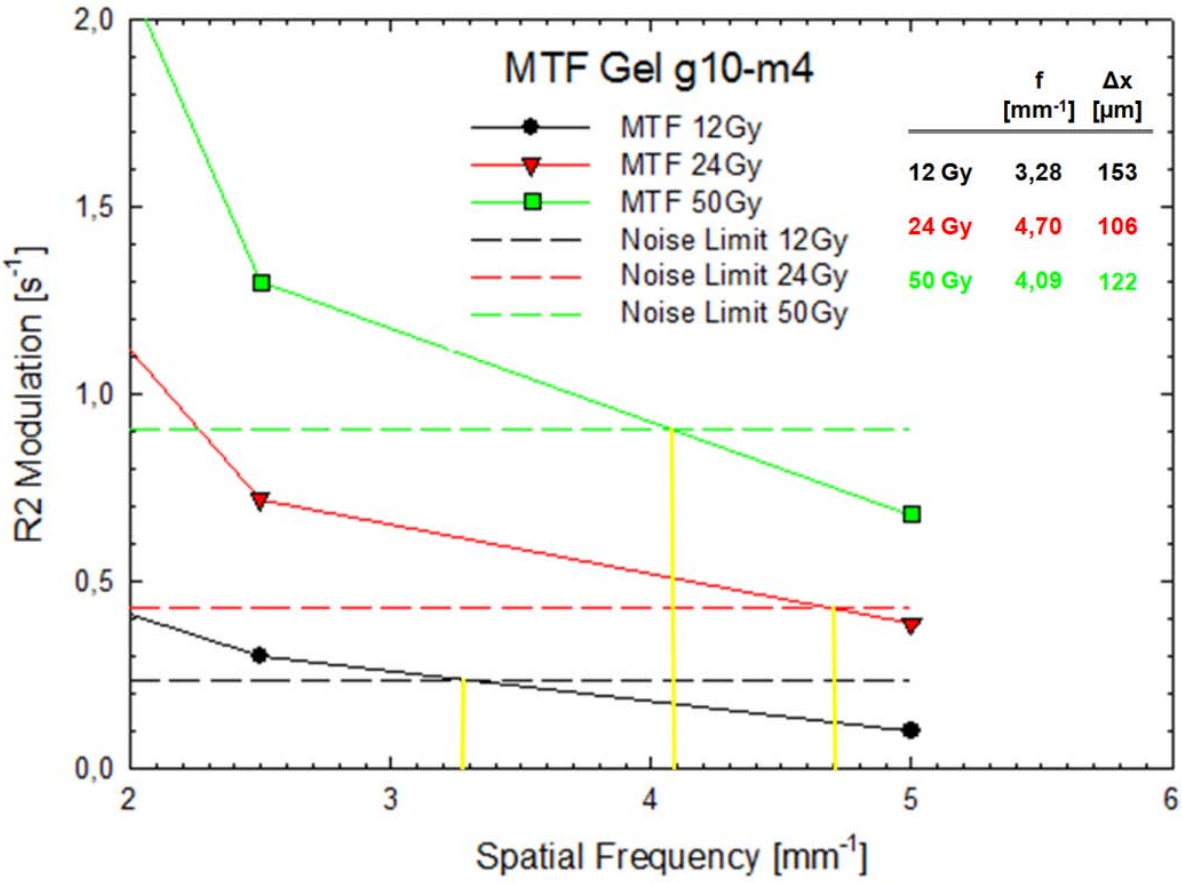

Figure 4.16: MTF and limits of spatial resolution Δx for the gel g10-m4. Note that the intersections were calculated and not determined graphically.

The results for the limits of spatial resolution are given in table 4.08.

Generally, the method of visual judgment for the estimation of R2 modulation M (see figure 4.14) is afflicted with varying uncertainties for the grid periods a/2 = 400µm and a/2 = 200µm. Even if the procedure is done with a set of fixed criteria by one person, it can't be avoided. Multiple analysis of the modulation $M_{200\mu m}$ showed variations of up to 10%. Figure 4.16 shows the determination of the spatial resolution for gel formulation g10-m4. If the modulations $M_{400\mu m}$ and $M_{200\mu m}$ for 12 Gy are varied by 10% the result for the limit of spatial resolution is also varying by ±10%.

Even with the high uncertainties one trend is noticeable from table 4.08. The spatial resolution decreases with increasing gelatin concentration. The results for gels with gelatin concentrations of 10% and 14% do not conclusively point to one gel formulation as optimum choice for high spatial resolution applications. In the dose range 12 to 24Gy, the highest spatial resolution is achieved with formulation g10-m8 (10% gelatin concentration and 8% MAA concentration), in the dose range 24 to 50Gy, it is achieved with the formulation g10-m4. Depending on the task other criteria such as precision, accuracy or (linear) dynamic range should also be considered.

Table 4.08: Spatial Resolution [µm] at 12Gy, 24Gy and 50Gy for the different gel formulations

	12 Gy Methacrylic Acid [%]				**24 Gy** Methacrylic Acid [%]		
Gelatin [%]	**4**	**6**	**8**	Gelatin [%]	**4**	**6**	**8**
10	153	185	119	**10**	106	124	109
14	183	198	199	**14**	138	149	167
18	215	402	296	**18**	183	164	177

Table 4.08 continued

	50Gy Methacrylic Acid [%]		
Gelatin [%]	**4**	**6**	**8**
10	122	151	203
14	133	188	206
18	134	162	216

4.2.2 Edge Enhancement

Edge enhancement was determined as over modulation at the border of high and low dose regions (see figure 4.17). It was not possible to place the absorber in the middle of gel container for all irradiations. Therefore, the over modulation was determined at a fixed distance from the edge with standard ROIs. R2 was measured in the maximum (minimum) of the over modulation. As base values R2 was estimated 100 pixels distant from the extreme values (see figure 4.18). Due to the time intensive measurements, not all gels could be measured with the same time interval after irradiation. They were measured at the earliest 4 days after irradiation to minimize errors introduced by ongoing post irradiation polymerization. Murakami et al (2007) found that the gels are stable 3 days after irradiation.

Similar to the investigations on spatial resolution the procedure of visual estimation of the edge enhancement is prone to rather big errors. Repeated analysis of the same image showed that the results can vary by 20%. The numbers for the high dose region (50Gy) have to be seen with caution because this dose is positioned in the non-linear region for all gel recipes. The non-linear regime is characterized by less precision, increased measurement errors and increased uncertainty for edge enhancement due to the high overmodulation. Regression analyses for the results at 12Gy and 24Gy are shown in figures 4.19 and 4.20. The regression for 24Gy is statistically not significant. The regression for 12Gy is significant and

overall the numbers support the assumption that edge enhancement is decreasing for increasing gelatin concentration.

Table 4.09: Edge enhancement in % of normal modulation. The main number is the total over modulation defined as sum of the over-modulation in high and low dose regime. In the brackets over-modulation in high and low dose regions are indicated. Due to limited amount of gel for some formulation edge enhancement could not be investigated at all dose levels for all gels.

	12 Gy		
		Methacrylic Acid [%]	
Gelatin [%]	**4**	**6**	**8**
10		32 (11/21)	
14	36 (15/21)	7 (2/5)	26 (9/17)
18		10 (9/1)	
	24 Gy		
		Methacrylic Acid [%]	
Gelatin [%]	**4**	**6**	**8**
10		16 (3/13)	
14	28 (12/16)	19 (10/9)	10 (4/6)
18		11 (1/10)	
	50Gy		
		Methacrylic Acid [%]	
Gelatin [%]	**4**	**6**	**8**
10	33 (18/15)	21 (10/11)	19 (8/10)
14	40 (19/22)	33 (8/25)	49 (22/27)
18	11 (1/10)	45 (20/25)	11 (2/9)

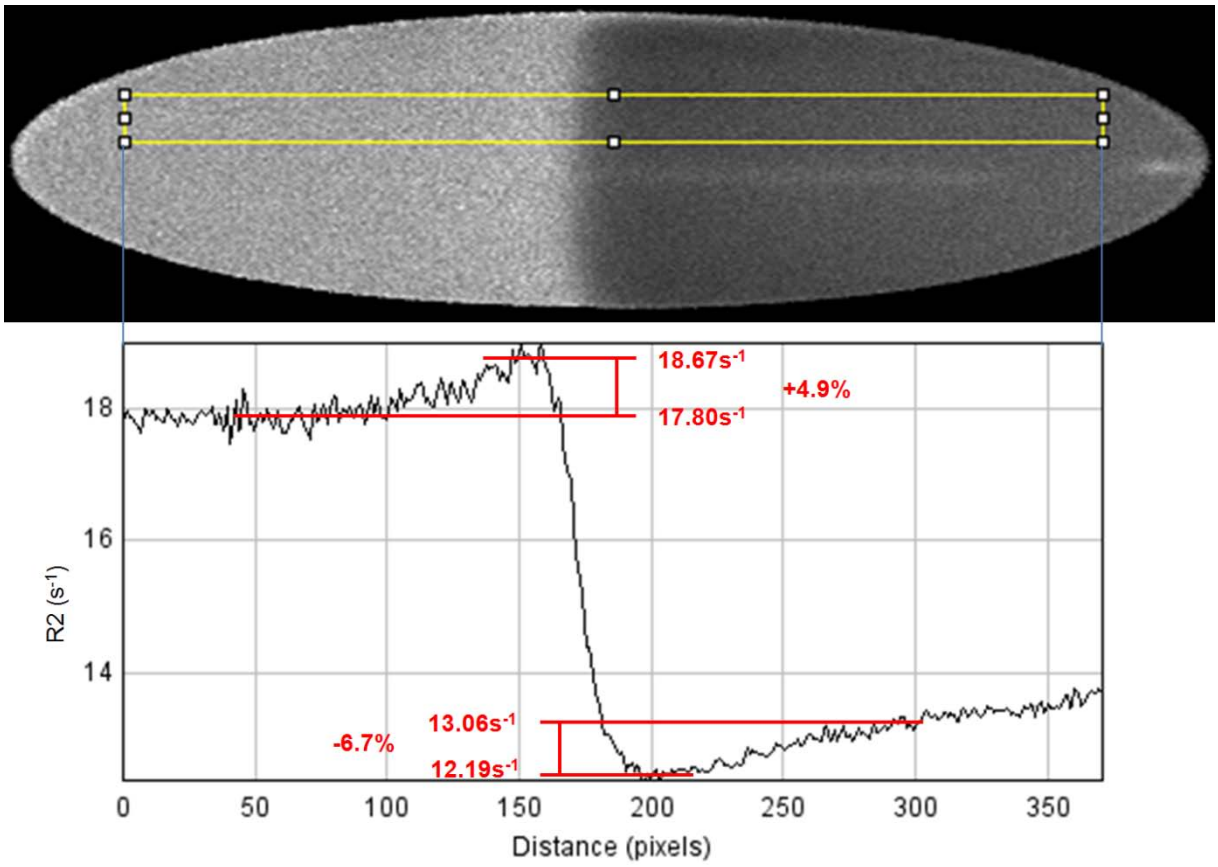

Figure 4.17: Edge Enhancement at the border of low and high dose regions. Pixel width (l-r) corresponds to 78 µm. The results for the determination of overmodulation are indicated.

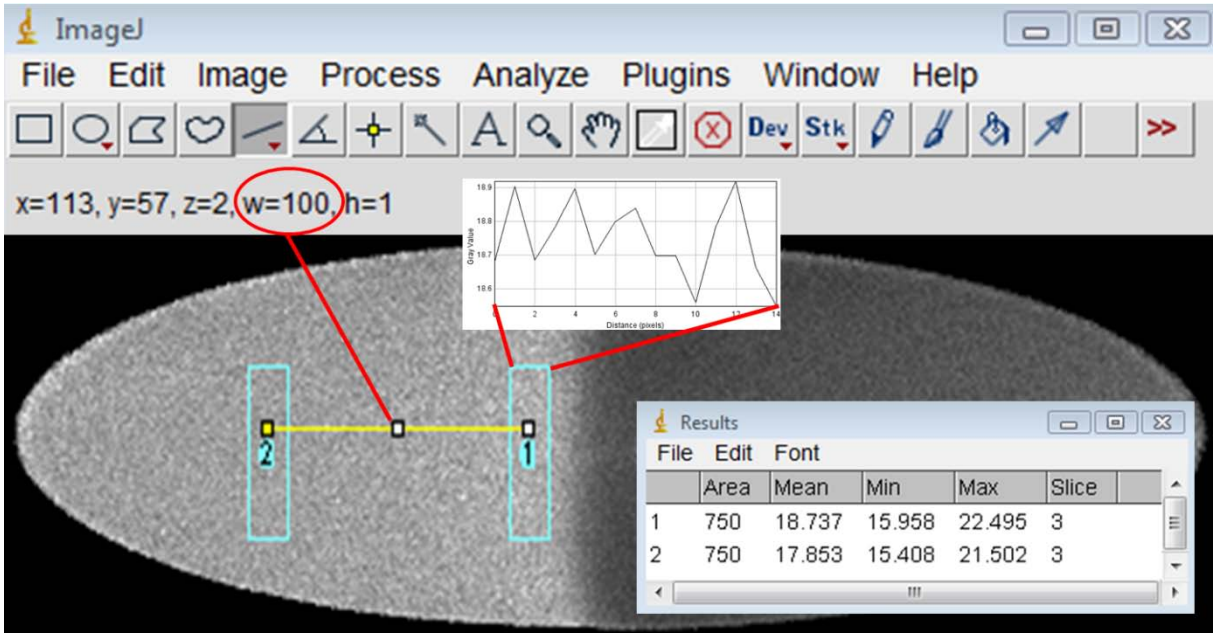

Figure 4.18: Estimation of over modulation with a standardized ROI (50x15px^2). ROI 1 (maximum value) is placed in the maximum of the over modulation. The correct position is verified with a rectangular profile. ROI 2 is set 100px (5.9mm) away from the maximum (reference base value). The procedure is then repeated for the low dose region.

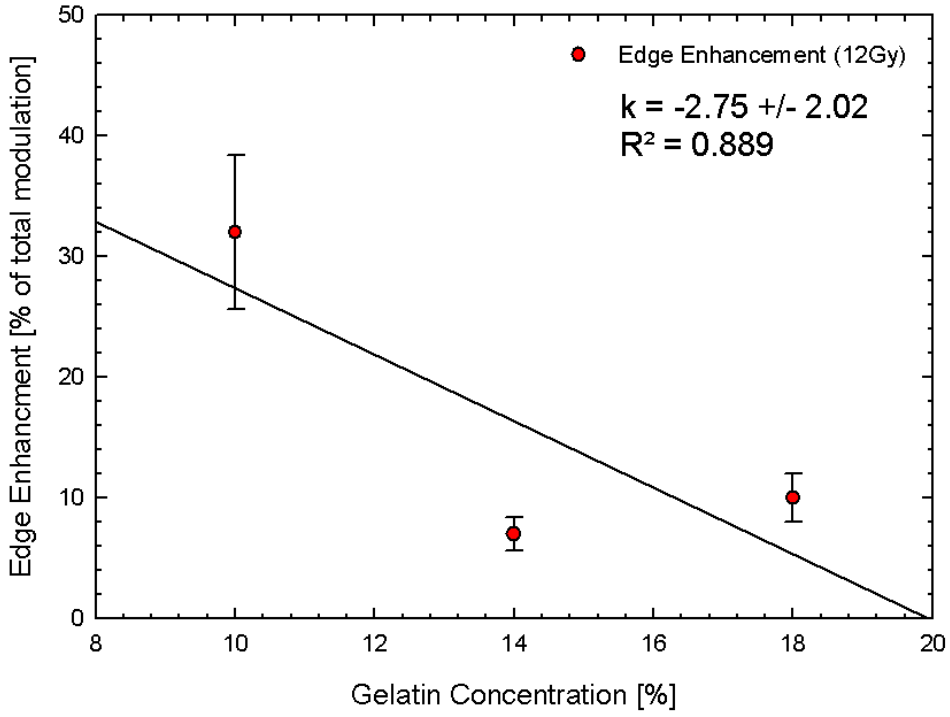

Figure 4.19: Linear regression for the dependency of the edge enhancement on gelatin concentration at 12Gy.

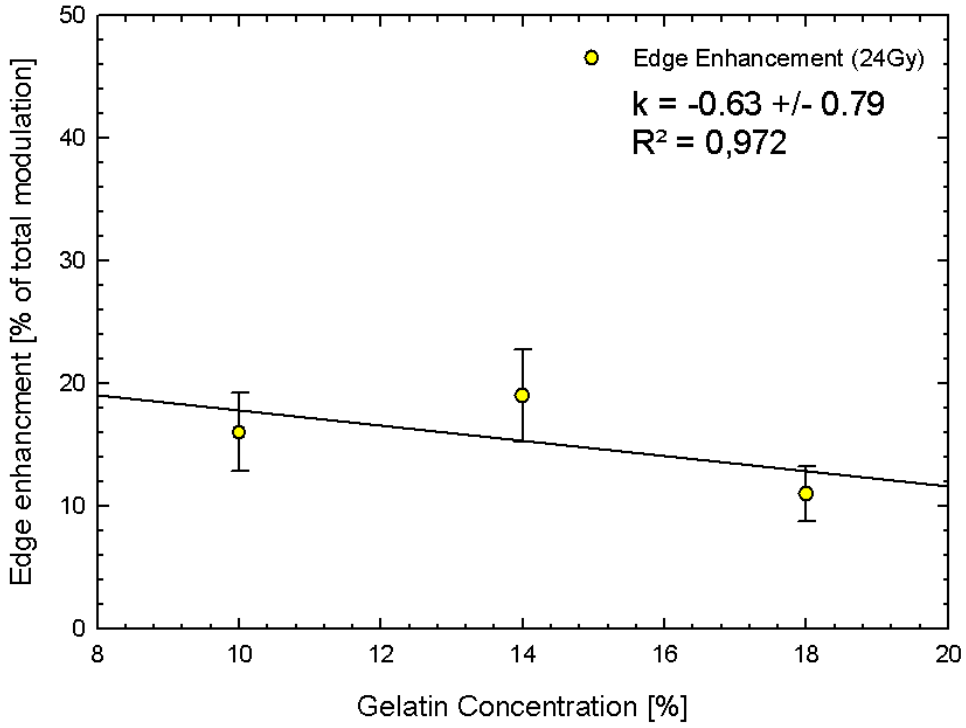

Figure 4.20: Linear regression for the dependency of edge enhancement on gelatin concentration at 24Gy.

4.3 IMRT

The IMRT-plan was executed on the phantom at the SMZO Vienna with 6MV photons from a Linac. For the purpose of absolute dosimetry 9 gels in Barex containers were irradiated to known doses (0 to 25Gy) in a water tank before IMRT irradiation. Calibration was performed with an ionization chamber. Gel in the IMRT phantom and the calibration vials were from the same batch. All gels were transported together and treated equally during the whole process from manufacture till scanning. IMRT phantom and calibration vials were scanned. The result of calibration is shown in figures 4.21 to 4.23. With the linear calibration curve the R2-images are converted into dose images. An exemplary slice with a line profile is shown in figure 4.24.

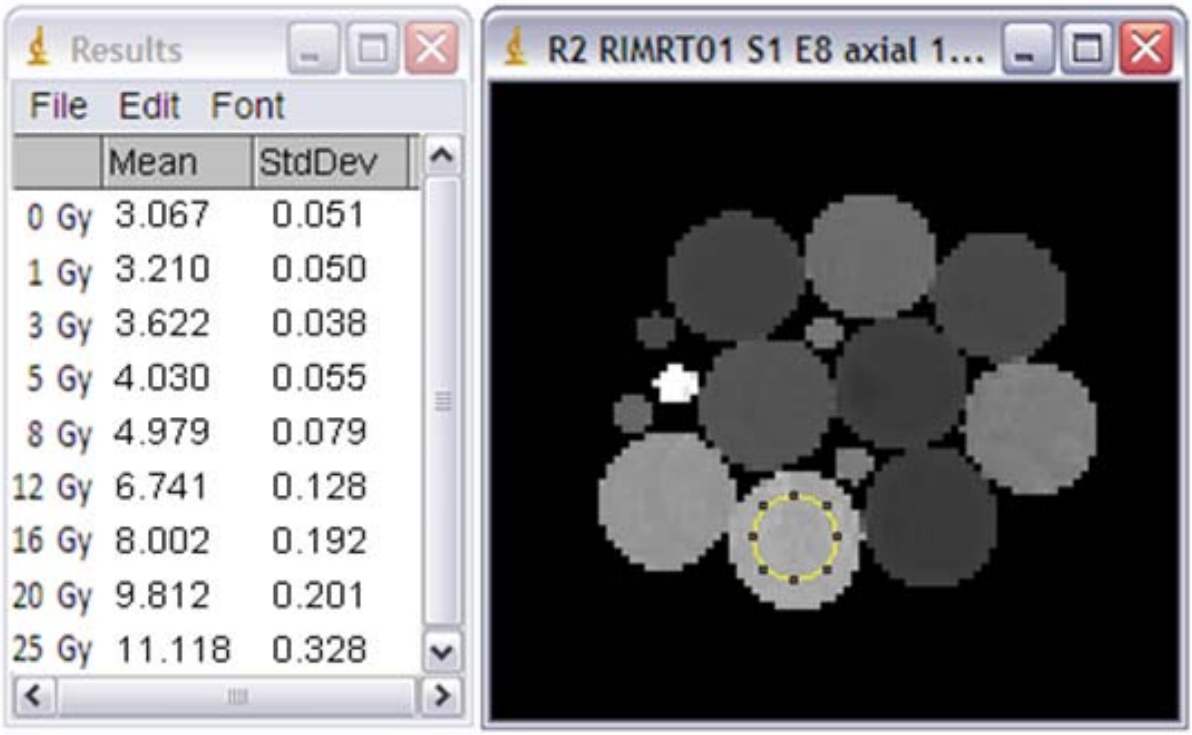

Figure 4.21 **Right:** T2-image for a slice through calibration vials at depth of reference measurements using a calibrated ionization chamber. **Left:** mean R2 values and their standard deviations.

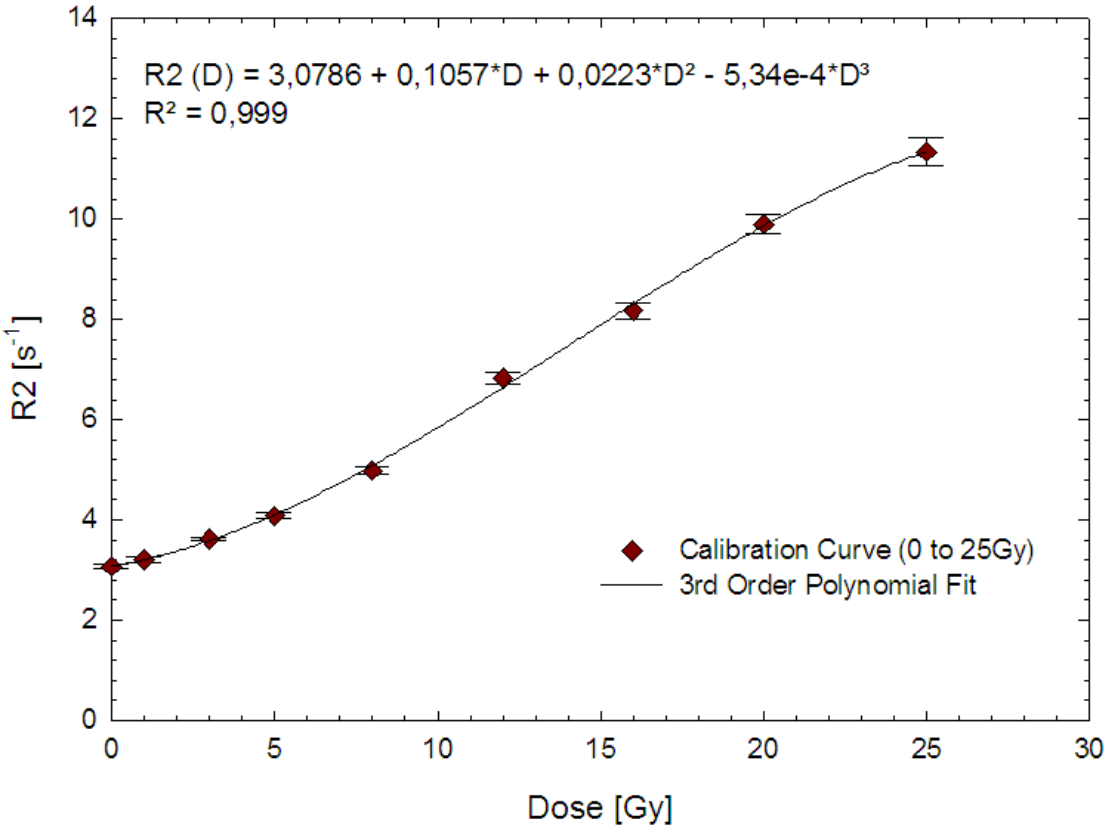

Figure 4.22: Calibration curves for the IMRT experiment.
Third order polynomial fit over the whole dose range

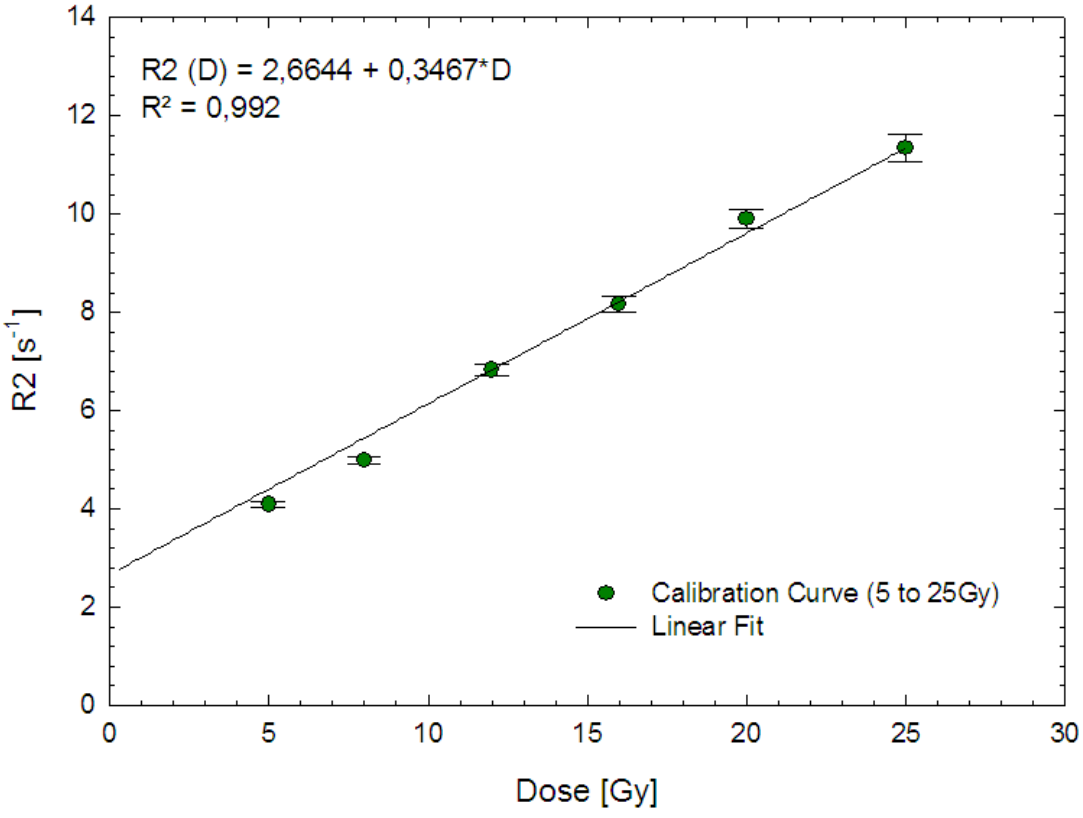

Figure 4.23: Calibration curves for the IMRT experiment. Linear fit from 5 to 25Gy.

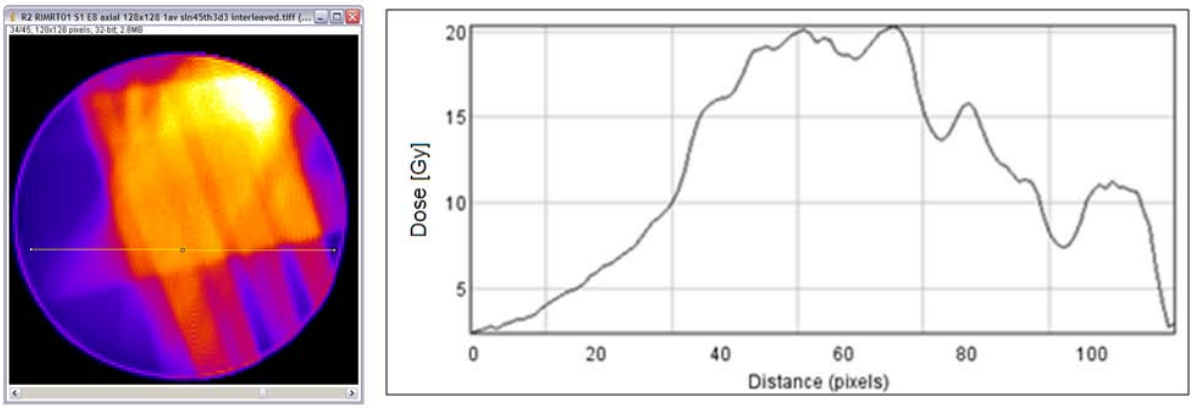

Figure 4.24: Exemplary slice through the IMRT-phantom (in false colors) with line profile (1 pixel corresponds to 1.56mm).

The comparison of dose maps generated with MR-based polymer gel dosimetry and the planned dose distribution was performed with Verisoft™3.2 (PTW, Freiburg, Germany). The software is designed to compare radiotherapy plan images with x-ray-film images. In x-ray images areas of strong blackening are equal to high dose regions, but in digital grey value images the highest grey value is shown as white. Therefore Verisoft™ shows inverted Look Up Tables (LUT) to have high dose values with strong blackening represented as high grey values. As a consequence dose images have to be inverted before imported to Verisoft.

Unfortunately image import to Verisoft™ was limited to 8-bit images offering only 256 different grey values. Therefore the 32-bit MR-dose-maps generated with the linear calibration curve (figure 4.23) had to be modified to prevent severe information loss at transformation from 32-bit to 8-bit images. The stack of dose-maps used for the IMRT-analysis is compromised of pixels with relevant grey values in the range from 0 to approximately 25.00000 ($<2^{22}$) representing dose-values from 0Gy to 32Gy (see figure 4.25). The maximum grey value is set to 31.875 and then multiplied with 8 to fill the interval from 0 to 255. Later, the values were rounded to integers and dose maps were converted to 8 bit images. If two pixels are differing by one grey value the difference in dose after conversion is 0.125Gy instead of 1Gy before conversion. Hence the multiplication before converting to integer values increases the resolution by a factor of 8.

The modified images were imported to Verisoft™. The software itself offers the possibility to manually set the maximum dose value in a dose map. In each slice of the MR-dose maps the maximum dose value was identified with ImageJ. The scaled and to Verisoft™ imported images could then be rescaled to the correct dose values.

Dose maps generated by the planning system were also exported. The grey scale LUT had to be inverted too before images could be imported into Verisoft™. An exemplary comparison of planning system and MR-T2-map images of the same slice of the IMRT phantom is shown in 4.24.

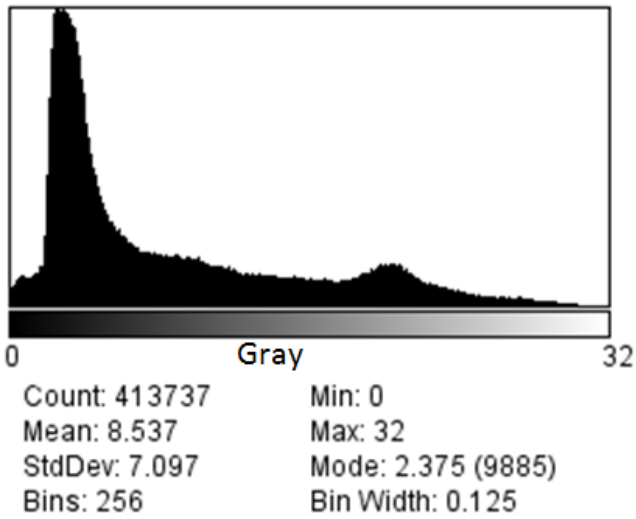

Figure 4.25: Dose-value-histogramm of the entire stack (calibration vials and IMRT-phantom).

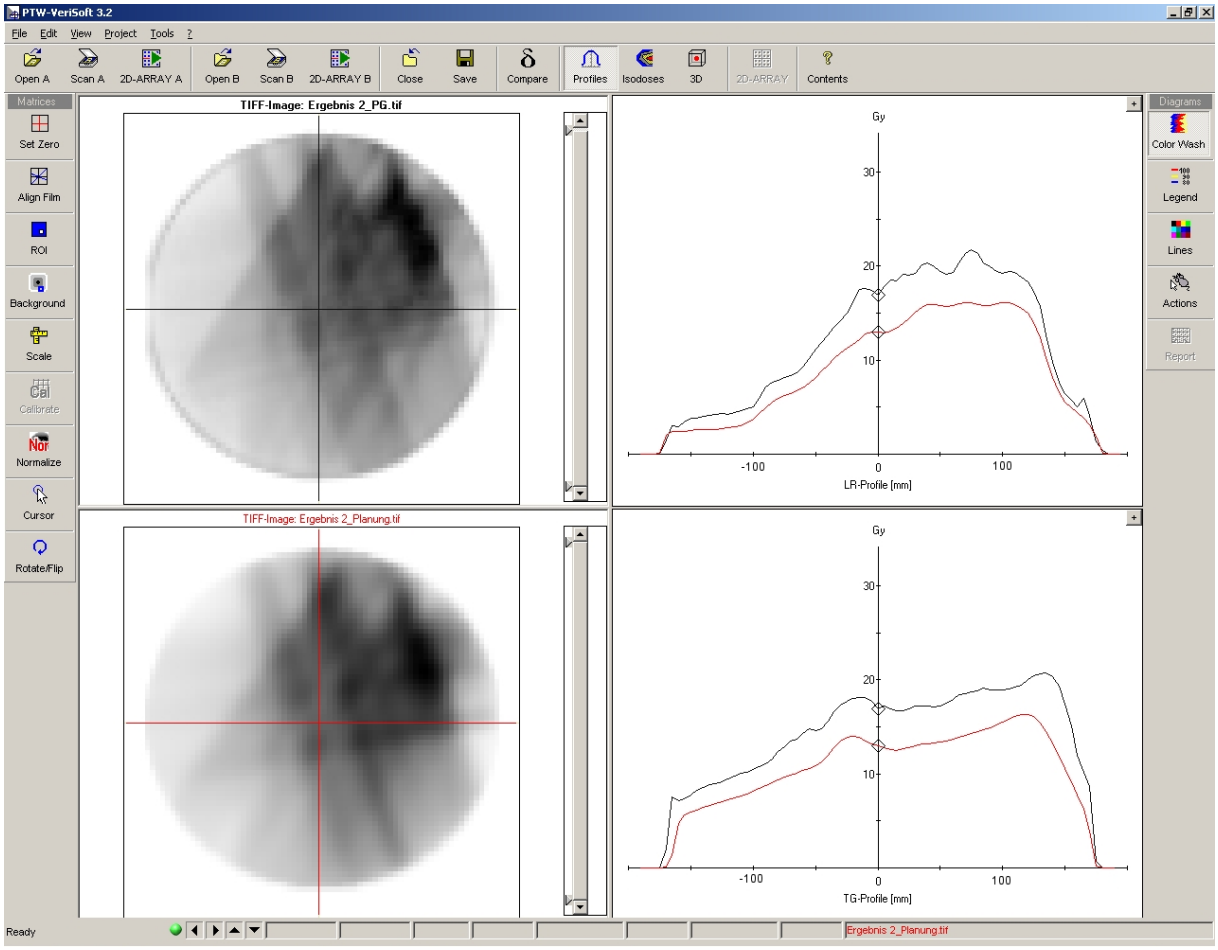

Figure 4.26: Comparison of the same slice through the phantom. **Left side top**: T2-dose-map. **Left side bottom**: Planning system dose map. On the right side comparisons of the line profiles of MR-image (black line) and planning system (red line) are shown. **Right side top**: left-right profile. **Right side bottom**: Anterior-posterior profile.

The values in the MR-dose map are about 25% higher than in the planning system throughout the whole slice. The reason for this strong overestimation of dose in the calibrated MR-dose maps should be a topic of further investigation. A possible reason would be erroneous irradiation of the calibration vials. A misplacement of the ionization chamber or the gels in depth of the water tank during absolute dose calibration, could be responsible. A difference of about 5cm would yield a 25% difference in absorbed dose. Another possible reason could be volume dependent heating up of the gels during irradiation, due to the exothermic nature of the polymerization process. For MAGAT gels Sedaghat et al (2009) observed a temperature increase of ~2°C in 18ml vials and ~10°C in 275ml vials when irradiated with 10Gy (figure 4.27). DeDeene et al (2006) reported reduced relaxation rates for increased temperatures during irradiation (figure 4.28). If both effects are also occurring in MAGIC gels with the same magnitude they could explain an overestimation of dose of 25% in the large IMRT volume. Further investigations are necessary to verify this hypothesis.

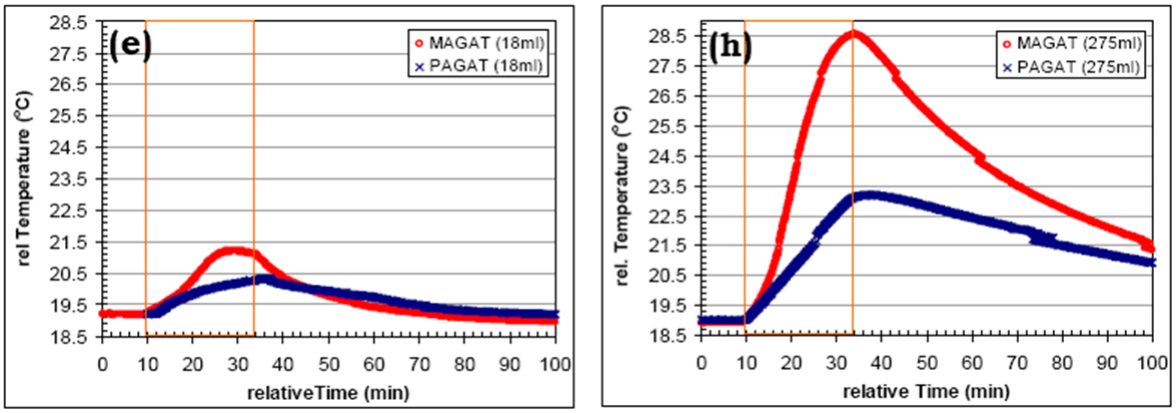

Figure 4.27 (Sedaghat et al 2009): Volume dependent temperature increase in MAGAT gels irradiated with 10Gy. 18ml gel vial on the left side and 275ml gel vial on the right side.

If the values in the MR-dose map are corrected with a multiplicative factor of 0.767, the agreement of MR images and planning system images is highly improved. The correction factor was estimated as average value of several values over the whole dose map (including high and low dose areas). An exemplary line profile comparison in Verisoft™ after correction is given in figure 4.30.

Possible reasons for the remaining differences are:

- Deviations between planned and applied doses
- Miss-positioning of the phantom during irradiation or in the MR-scanner (translation along the central axis, rotation around the central axis, miss-alignment of the central axis by several degrees)
- Inexact matching of the MR and planning system slices

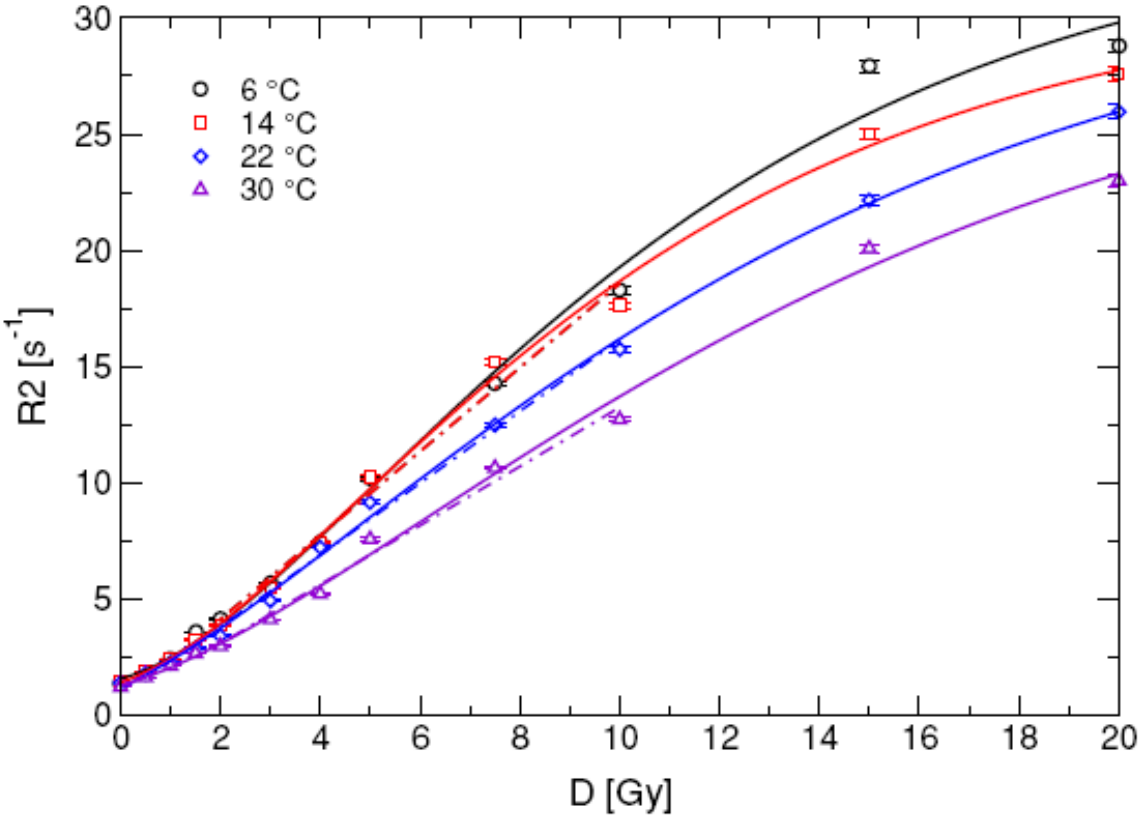

Figure 4.28 (DeDeene, Vergote et al 2006): Reduced polymerization rate in MAGAT gels for increasing temperature during irradiation.

An alternative to the comparison of line profiles is the gamma index method (Low et al 1998). The gamma index is a quality assurance method to compare calculated and measured doses for complex dose distributions. The graphic representation of the gamma index for each point allows a rapid evaluation of whole areas rather than lines. It incorporates the two criteria dose difference and distance-to-agreement. The dose difference criterion ΔD_M sets a tolerance for the maximum allowed deviation of planned and measured dose values (e.g. 3%). In regions of steep dose gradients a small spatial error can result in large differences of planned and measured doses, that are relatively unimportant. Therefore the distance-to-agreement (DTA) Δd_M (e.g. 3mm) is applied as second criterion. It is the distance between a point in the planned dose distribution and the nearest point in the measured dose distribution with the same dose. Each point of the measured dose distribution that fails both criteria is attributed a gamma index larger than 1. A gamma index evaluation of the exemplary slice of the IMRT phantom with the passing criteria ΔD_M = 3% and Δd_M = 3mm is shown in figure 4.31. The agreement of the corrected measured dose with planned dose, according to the chosen gamma index criteria, is almost 97%.

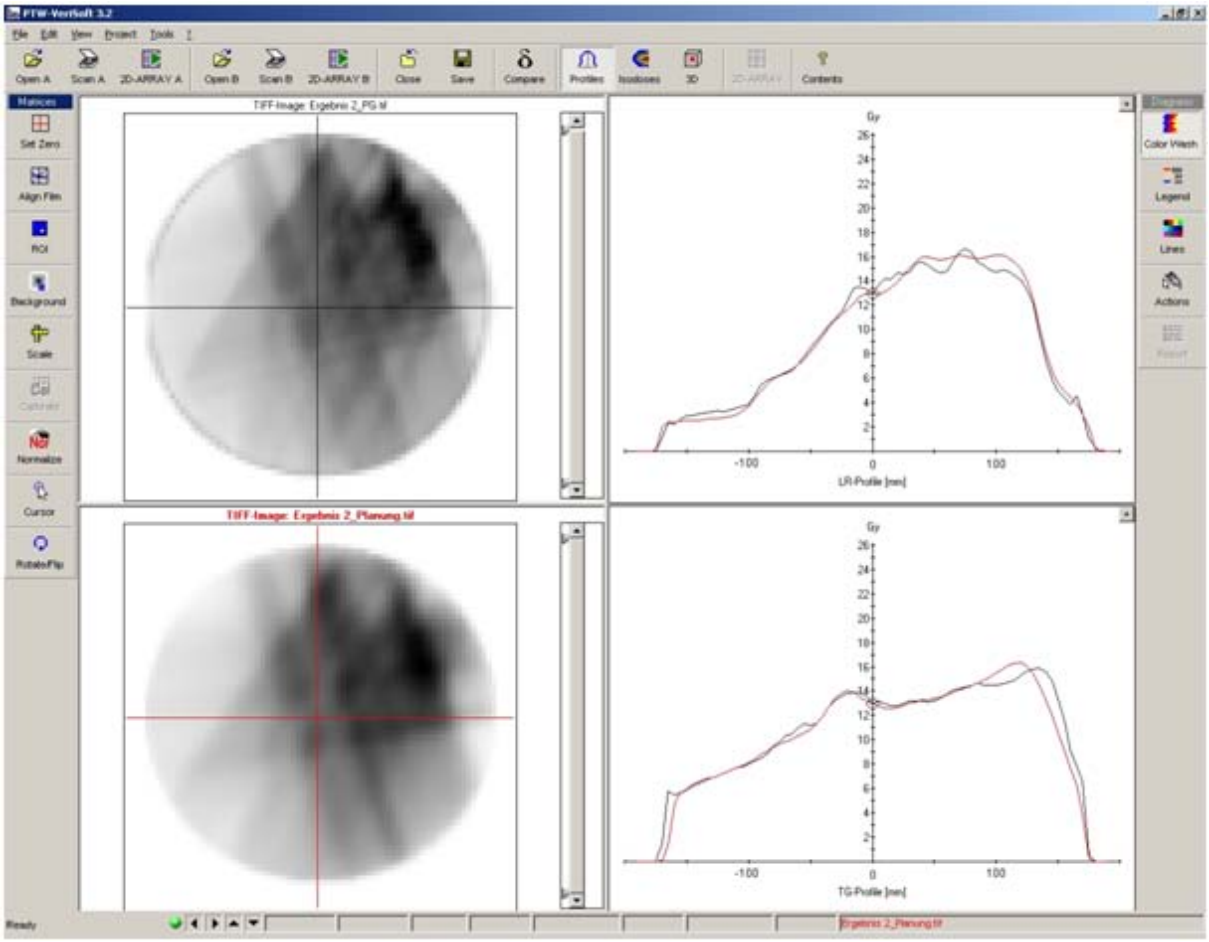

Figure 4.30: MR-dose map (image on top and left, black line profile) corrected with a multiplicative factor of 0.767 compared to the unaltered planning system dose maps (red line profile).

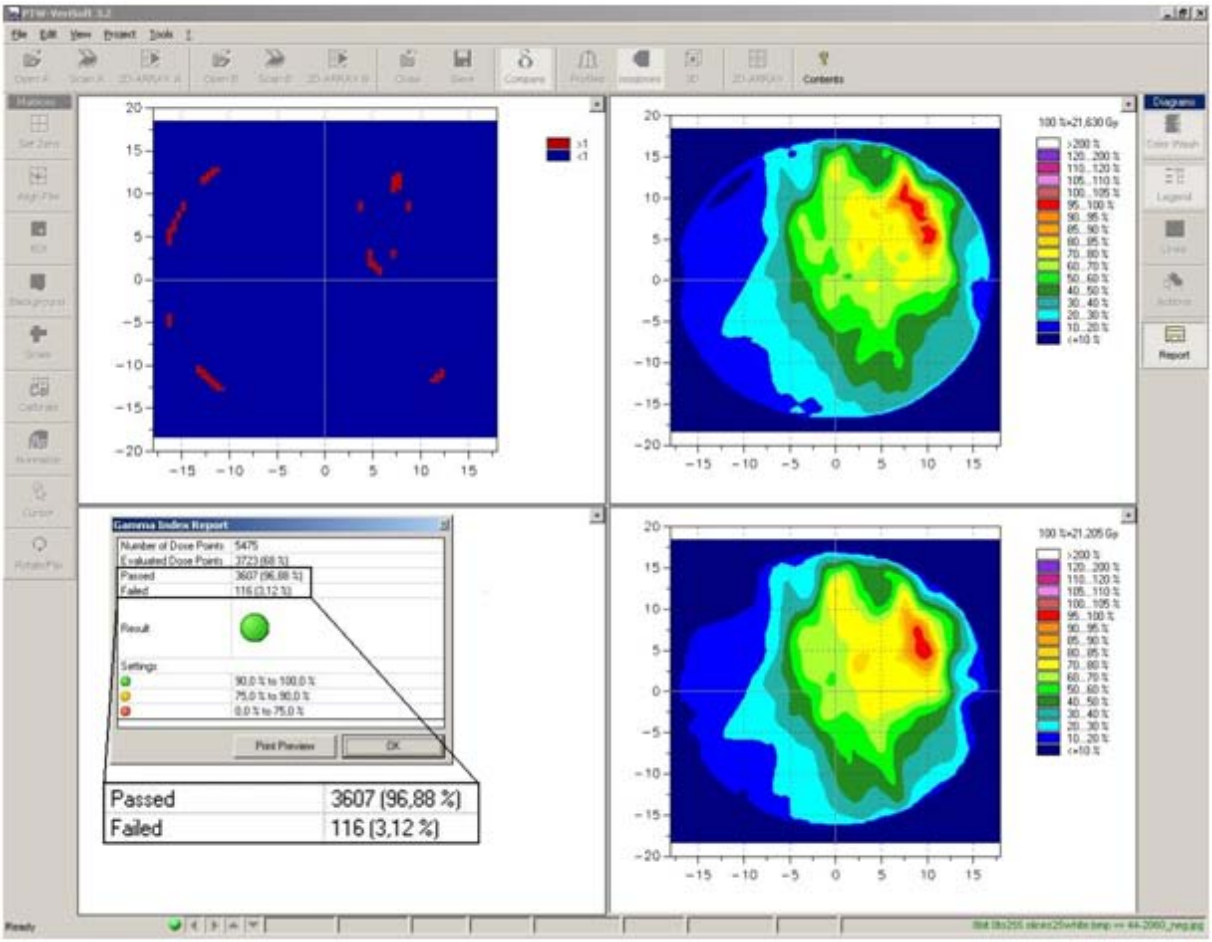

Figure 4.31: Gamma index report for an exemplary slice through the IMRT phantom. The windows on the right side represent the isodose regions of the MR-dose maps (top) and the planned dose distribution (bottom). The upper left window displays data points failing the gamma index criteria ΔD_M = 3% and Δd_M = 3mm as red dots. Almost 97% of data points pass the chosen gamma index criteria.

5 References

Abramoff M D, Magelhaes P J, Ram S J, 2004, Image Processing with ImageJ, Biophot. Int. 11/7 36-42

Andrews H L, Murphy R E, LeBrun E J, 1957, Gel dosimeter for depth dose measurements, Rev. Sci. Instrum. 28 329-32

Attix F H, 1986, Introduction to radiological physics and radiation dosimetry, Wiley, New York

Baldock C, Murry P, Kron T, 1999, Uncertainty analysis in polymer gel dosimetry, Phys. Med. Biol. 44 N243-6

Baldock C, Lepage M, Bäck S A, Murry P J, Jayasekera P M, Porter D, Kron T, 2001, Dose resolution in radiotherapy polymer gel dosimetry: effect of echo spacing in MRI pulse sequence, Phys. Med. Biol. 46 449-60

Bayreder C, Schön R, Wieland M, Georg D, Moser E, Berg A, 2008, The spatial resolution in dosimetry with normoxic polymer-gels investigated with the dose modulation transfer approach, Med. Phys. 35 1756-69

Bayreder C, 2009, High resolution resonance based dosimetry using normoxic polymer gels, PhD Thesis, Medical University of Vienna, Austria

Berg A., Ertl A, Moser E, 2001, High resolution polymer gel dosimetry by parameter selective MR-micorimaging on a whole body scanner at 3 T, Med. Phys. 28 833-43

Berg A, Pernkopf M, Waldhäusl C, Schmid W, Moser E, 2004, High resolution MR based polymer dosimetry versus film densitomertry: a systematic study based on the modulation transfer function approach, Phys. Med. Biol. 49 4087-108

Berg A, Bayreder C, Naumann I, Heufelder J, 2005, 3D-High-Resolution Dosimetry of a 12mm proton-beam in normoxic polymer gels, 14th International Conference of Medical Physics, Nurnberg, Germany, Sept. 14-17, 2005

Berg A, Bayreder C, Georg D, Bankamp A, Wolber G, 2009, Aspects of radiation beam quality and their effect on the dose response of polymer gels: photons, electrons and fast neutrons, J. Phys. Conf. Ser. 164

Bortfeld T, 2006, IMRT: A review and preview, Phys. Med. Biol. 51 R363-79

Brahme A, 1984, Dosimetric precision requirements in radiation therapy, Acta Radiol. Oncol. 23 379-91

Crescenti R A, Scheib S G, Schneider U, Gianolini S, 2007, Introducing gel dosimetry in a clinical environment: Costumization of polymer gel composition and magnetic resonance imaging parameters used for 3D dose verifications in radiosurgery and intensity modulated radiotherapy, Med. Phys. 34 1286-97

DeDeene Y, Van de Walle R, Achten E, DeWagter C, 1998, Mathematical analysis and experimental investigation of noise in quantitative magnetic resonance imaging applied in polymer gel dosimetry, Sign. Proces. 70 85-101

DeDeene Y, Hanselaer P, DeWagter C, Achten E, DeNeve W, 2000, An investigation of the chemical stabililty of a monomer/polymer gel dosimeter, Phys. Med. Biol. 45 859-78

DeDeene Y, Hurley C, Venning A, Vergote K, Mather M, Healy B J, Baldock C, 2002, A basic study of some normoxic polymer gel dosimeters, Phys. Med. Biol. 47 3441-63
DeDeene Y, Venning A, Hurley C, Healy B J, Baldock C, 2002b, Dose-response stability and integrity of the dose distribution of various polymer gel dosimeters, Phys Med. Biol. 47 2459-70
DeDeene Y, 2004, Fundamentals of MRI measurements in gel dosimetry, J. Phys. Conf. Ser. 3 87-114
DeDeene Y, 2004b, Essential characteristics of polymer gel dosimeters, J. Phys. Conf. Ser. 3 34-57
DeDeene Y, 2006, On the accuracy and precision of gel dosimetry, J. Phys. Conf. Ser. 56 72-85
DeDeene Y, Vergote K, Claeys C, DeWagter C, 2006, The fundamentals of normoxic polymer gel dosimeters: a comparison between a methacrylic acid based gel and acrylamide based gels, Phys. Med. Biol. 51 653-73
DeDeene Y, Pittomvils G, Visalatchi S, 2007, The influence of cooling rate on the accuracy of normoxic polymer gel dosimeters, Phys. Med. Biol. 52 2719-28
DeWagter C, 2004, The ideal dosimeter for intensity modulated radiation therapy (IMRT): What is required?, J. Phys. Conf. Ser. 3 4-8
Dogan N, Leybovich L B, Sethi A, 2002, Comparative evaluation of Kodak EDR2 and XV2 films for verification of intensity modulated radiation therapy, Phys. Med. Biol. 47: 4121-30
Doran S J and Krstajic N, 2006, The history and principles of optical computed tomography for scanning 3-D radiation dosimeters, J. Phys. Conf. Ser. 56 45-57
Evans A (editor), 1987, The evaluation of medical images, Hilger, Bristol, UK
Fong P M, Keil D C, Does M D, Gore J C, 2001, Polymer gels for magnetic resonance imaging of radiation dose distribution at normal room atmosphere, Phys. Med. Biol. 46 3105-13
Fricke H and Morse S, 1927, The chemical action of roentgen rays on dilute ferrous sulfate solutions as a measure of radiation dose, Am. J. Roent. Radium Ther. Nucl. Med. 18 430-2
Gore J C, Kang Y S, Schulz R J, 1984, Measurment of radiation dose distribution by nuclear magnetic resonance (NMR) imaging, Phys. Med. Biol. 29 1189-97
Gustavsson H, Karlsson A, Bäck S A J, Olsson L E, Haraldsson P, Engström P, Nyström H, 2003, MAGIC-type polymer gel for three-dimensional dosimetry: Intensity-modulated radiation therapy verification, Med. Phys. 30 1264-71
Gustavsson H, Bäck S A J, Medin Joakim, Grusell E, Olsson L E, 2004, Linear energy transfer dependence of normoxic polymer gel dosimeter investigated using proton beam absorbed dose measurements, Phys. Med. Biol. 49 3847-55
Haacke E M, Brown R W, Thompson M R, Venkatesan R (editors), 1999, Magnetic Resonance Imaging: Physical Principles and Sequence Design, Wiley, New York
Hayashi S, Yoshioka M, Usui S, Haneda K, Tominaga T, 2009, The role of gelatin in methacrylic acid based gel dosimeter, J. Phys. Conf. Ser. 164
Hendee W R, Ibbott G S, Hendee E G, 2005, Radiation Therapy Physics, Wiley, New York
Hepworth S J, Leach M O, Doran S J, 1999, Dynamics of polymerization in polyacrylamide gel (PAG) dosimeters: II. Modelling oxygen diffusion, Phys. Med. Biol. 44 1875-84

Hilts M, 2006, X-Ray computed tomography imaging of polymer gel dosimeters, J. Phys. Conf. Ser. 56 95-107

Hurley C, Venning A, Baldock C, 2005, A study of normoxic polymer gel dosimeter comprising methacrylic acid, gelatin and tetrakis (hydroxymethyl) phosphonium chloride (MAGAT), App. Rad. Isot. 63 443-56

Ibbott G, Beach M, Maryanski M, 2002, An anthropomorphic head phantom with BANG ® polymer gel insert for dosimetric evaluation of IMRT treatment delivery, International Atomic Energy Agency, November 2002

IAEA (International Atomic Energy Agency), 2000, Technical Reports Series No.398: Absorbed dose determination in external beam radiotherapy, IAEA, Vienna

ICRU (International Commission on Radiation Units and Measurement), 1980, Report 33: Radiation Quantities and Units, ICRU, Bethesda, MD

ICRU (International Commission on Radiation Units and Measurement), 1987, Report 42: Use of Computers in External Beam Radiotherapy Procedures with High-Energy Photons and Electrons, ICRU, Bethesda, MD

ICRU (International Commission on Radiation Units and Measurement), 1998, Report 60: Fundamental Quantities and Units for ionizing radiation, ICRU, Bethesda, MD

Jirasek A, 2006, Experimental investigations of polymer gel dosimeters, J. Phys. Conf. Ser. 56 23-34

Lepage M, McMahon K, Galloway G J, DeDeene Y, Back S A J, Baldock C, 2002, Magnetization transfer imaging for polymer gel dosimetry, Phys. Med. Biol. 47 1881-90

Liney G P, Bodber M J, Wilson A D, Goodby J W, Turnbull L W, 2009, Relaxometry changes in a gel dosimetry phantom due to continued RF exposure, J. Phys. Conf. Ser. 164

Low D A, Harms W B, Mutic S, Purdy J A, 1998, A technique for the quantitative evaluation of dose distributions, Med. Phys. 25 656-61

Luci J J, Whitney H M, Gore J C, 2007, Optimization of MAGIC gel formulation for three-dimensional radiation therapy dosimetry, Phys. Med. Biol. 52 N241-8

MacDougall N D, Pitchford W G, Smith M A, 2002, A systematic review of the precision and accuracy of dose measurements in photon radiotherapy using polymer and Fricke MRI gel dosimeters, Phys. Med. Biol. 47 R107-21

Maryanski M J, Gore J C, Keenan R P, Schulz R J, 1993, NMR relaxation enhancement in gels polymerized and cross-linked by ionizing radiation: a new approach in 3D dosimetry by MRI, Magn. Reson. Imaging 11 253-8

Maryanski M J, Schulz R J, Ibbott G S, Gatenby J C, Xie J, Horton D, Gore J C, 1994, Magnetic resonance imaging of radiation dose distributions using a polymer-gel dosimeter, Phys. Med. Biol. 39 1437-55

Mayles P, Nahum A, Rosenwald J C, 2007, Handbook of radiotherapy physics, Taylor & Francis, New York

McAuley K B, 2006, Fundamentals of Polymer Gel Dosimeters, J. Phys. Conf. Ser. 56 35-44

Murakami Y, Nakashima T, Wanatabe Y, Akimitsu T, Matsuura K, Kenjo M, Kaneyasu Y, Wadasaki K, Hirokawa Y, Ito K, 2007, Evaluation of the basic properties of the BANGkitTM gel dosimeter, Phys. Med. Biol. 52 2301-11

Murphy P S, Cosgrove V P, Schwarz A, Webb S, Leach M O, 2000, Proton spectroscopic imaging of polyacrylamide gel dosimeters for absolute radiation dosimetry, Phys. Med. Biol. 45 835-45

Pappas E, 2009, On the role of polymer gels in the dosimetry of small photon fields used in radiotherapy, J. Phys. Conf. Ser. 164

Podgorsak E B (editor), 2003, Review of Radiation Oncology Physics: A Handbook for Teachers and Students, Educational Reports Series, IAEA, Vienna

Ramm U, Moog J, Spielberger B, Bankamp A, Böttcher H D, Kraft G, 2004, Investigations of dose response of BANG® Polymer-Gels to Carbon Ion Irradiation

Reddy G G, Nagabhushanam T, Santappa M, 1982, Oxygen-ascorbic acid-copper(II) Initiating system. A kinetic study of the polymerization of methyl acrylate in aqueous medium, Makromol. Chem. 183 905-13

Salomons G J, Park S, McAuley K B, Schreiner L J, 2002, Temperature increases associated with polymerization of irradiated PAG dosimeters, Phys. Med. Biol. 47 1435-48

Scheib S G, Vogelsanger W, Gianolini S, Crescento R, 2004, Normoxic polymer gel – basic characterization and clinical use, J. Phys. Conf. Ser. 3184-7

Schreiner L J, 2009, Where does gel dosimetry fit in the clinic?, J. Phys. Conf. Ser. 164

Schulz R J, Gore J C, 1990, Reported in Imaging of 3D Dose Distributions by NMR, National Cancer Institute Grant Application 2R01CA46605-04

Schulz R J, de Guzman A F, Nguyen D B, Gore J C, 1990, Dose-response curves for Fricke-infused agarose gels as obtained by nuclear magnetic resonance, Phys. Med. Biol. 35 1611-22

Sedaghat M, Tremblay V H, Tremblay L, Bujold R, Lepage M, 2009, Volume-dependent internal temperature increase within polymer gel dosimeters during irradiation, J. Phys. Conf. Ser. 164

Sellakumar P, Samuel E J J, Supe S S, 2007, Water equivalence of polymer gel dosimeters, Radiat. Phys. Chem. 76 1108-15

Suchowerska N, Hoban P, Butson M, Davison A, Metcalfe P, 2001, Directional dependence in film dosimetry: radiographic and radiochromic film, Phys. Med. Biol. 46, 1391-7

Taqui Khan M M, Martell A E, 1967, Metal ion and chalate catalyzed oxidation of ascorbic acid by molecular oxygen: I. Cupric and ferric ion catalyzed oxidation, J. Am. Chem. Soc. 89 4176-84

Ting J Y and Davis L W, 2001, Dose verification for patients undergoing IMRT, Med. Dosim. 26 205-13

Venning A J, Nitschke K N, Keall P J, Baldock C, 2005, Radiological properties of normoxic polymer gel dosimeters, Med. Phys. 32 1047-53

Vergote K, DeDeene Y, Vanden Bussche E, DeWagter C, 2004, On the relation between the spatial dose integrity and the temporal instability of polymer gel dosimeters, Phys. Med. Biol. 49 1437-55

Wanatabe Y, 2005, Variable transformation of calibration equations for radiation dosimetry, Phys. Med. Biol. 50 1221-34